FRIEND VIRUS-INDUCED ERYTHROLEUKEMIA: RELATIONSHIP TO VIRAL *env* EXPRESSION, CELLULAR ONCOGENE EXPRESSION, AND PROVIRAL INTEGRATION

by

Brian C. Gliniak

A DISSERTATION

Presented to the Department of Biochemistry
and the Oregon Health Sciences University
School of Medicine
in partial fulfillment of
the requirements for the degree of

Doctor of Philosophy

May 1988

APPROVED: [redacted]

.....

(Professor in Charge of Thesis)

[redacted]

.....

(Chairman, Graduate Council)

LIST OF FIGURES

ACKNOWLEDGEMENTS

Obtaining a graduate degree is a long process and many people deserve acknowledgement for their contributions over the years. Unfortunately, it is impossible to mention everyone and I hope they felt my appreciation along way. I would like to thank the Department of Biochemistry for allowing me to work towards my Ph. D. degree. I would also like to thank Dr. David Kabat for giving me the opportunity to work in his laboratory and for constantly challenging me to do the best work possible. Through his guidance and encouragement I feel that I have grown tremendously as a scientist and I greatly appreciate how much he has taught me. I am grateful to Jennifer Au, Susan Kozak, Richard Bestwick, and Craig Spiro for making the laboratory a very friendly place to work. And probably most of all, I would like to thank my wife Cameron for providing endless support and encouragement over a very long five years. Obtaining this degree was only possible through her sacrifices and I hope that one day I can repay the favor.

Abstract

The Friend virus complex causes a progressive murine erythroleukemia. The early phase of the disease is considered premalignant because the infected erythroblasts have a limited proliferative capacity and continue to differentiate. In contrast, 3-8 weeks post-infection malignant Friend cells emerge that can be maintained in culture, are transplantable, and appear to be blocked at the proerythroblast stage of differentiation. Thus, the Friend cells have escaped the commitment to differentiate and now have the capacity for unlimited self-renewal and are considered immortal.

Expression of gp55 at the cell's surface provides the mitogenic signal for the initial erythroblastosis. Previous work had demonstrated that the SFFV gp55 was inefficiently processed to the surface and the majority remained within the rough endoplasmic reticulum. We have shown that the majority of gp55 is still present as an intracellular monomer, but a portion of the intracellular molecules are dimerized by disulfide bonds and all of the cell surface molecules are dimerized. We have demonstrated that the intracellular dimers are the precursors to the cell surface dimers, however not all of the dimers formed reach the cell surface. Instead, it appears that several different forms of the dimer can be detected intracellularly, while only one dimer form is found at the cell surface. We have proposed that the initial folding and dimerization of gp55 generates a structurally heterogeneous population of molecules. Only those dimers that are "correctly folded" can escape the rough endoplasmic reticulum and are transported to the cell surface where they generate a mitogenic signal. This would imply that the transported molecules would be conformationally unique from the intracellular dimers. Those molecules that are incompetent for transport remain trapped in the RER.

We have shown that the erythroleukemic progression is associated with an increase in the relative expression levels of the cellular oncogenes c-*myc*, c-*myb*, and p53 in the erythroleukemia cell lines. In addition, our genomic structural studies demonstrated amplifications of c-*myc* copy numbers and p53 rearrangements. Such results imply that changes in expression of these cellular oncogenes were selected during progression and may contribute to the proliferation and tumorigenicity of these cells. Progression is associated with a decreased tendency in cellular differentiation and an increased capacity for self-renewal. This has led to the hypothesis that leukemias represent a block in differentiation. Friend cells can still be induced to differentiate with compounds such as DMSO. This induction results in a rapid decrease in c-*myc*, c-*myb*, and p53 transcript levels. These results are consistent with the belief that increased expression of cellular oncogenes may contribute to leukemic progression by interfering with erythropoiesis.

Proviral integration studies using a "tagged" virus has demonstrated that a single clonal population eventually emerges to form the advanced leukemia. Moreover, common integration sites are suggested by the clustering of the proviruses in only a few areas of the genome. This implies that the "stages" of erythroleukemia may only involve a single critical proviral integration event. The continued expression of gp55 may contribute to the progression by providing a constitutive mitogenic stimulus, whereas the proviral integration may allow the erythroblasts to escape from its commitment to erythroid differentiation and become immortalized. Thus, the SFFV proviral integration may represent a primary genetic alteration to the infected erythroblast that eventually culminates in a transformed cell. Cloning and characterizing these proviral integration sites should provide a significant new insight into Friend erythroleukemia.

I. Introduction

A. Discovery

The Friend virus complex causes a progressive erythroleukemia in susceptible mice. The original isolate of Friend virus was obtained as a cell-free extract from a Swiss mouse that had developed erythroleukemia following inoculation with Ehrlich mouse carcinoma cells (1, reviewed 2, 3). The disease could be serially transmitted by injecting filtrates prepared from spleen extracts. The pathology of this disease was characterized by rapid enlargement of the spleen (splenomegaly) and anemia. In addition, the peripheral blood contained elevated levels of hyperbasophilic cells that morphologically resembled proerythroblast progenitor cells. These cells are referred to as Friend cells. Because of the resulting anemia, the original isolate has been termed Friend virus-anemia strain (FV-A).

Two groups independently obtained derivatives of the original Friend virus preparation that induced a disease characterized by polycythemia (increased levels of erythrocytes in the peripheral blood), rather than anemia (4, 5, 6). The polycythemia inducing strain has been designated FV-P.

B. Rauscher Isolate

In 1962, Rauscher isolated a virus from a transplantable ascites tumor that induced an erythroproliferative disease very similar to the disease induced by the anemic strain of Friend virus (7). Recent molecular cloning and DNA sequence studies have demonstrated that Rauscher and Friend virses are closely related to

each other and that they probably have a common ancestor (8, 9). A polycythemia variant of Rauscher virus has not been isolated.

C. Hematopoiesis

The Friend virus has a rapid and dramatic effect on erythroid cells in the infected mouse. Proliferation of proerythroblasts (Friend cells) in the spleens of infected mice can be detected as early as 30 hours following virus inoculation (1, 10, 11). Distinct macroscopic splenic foci can be seen by 9 days post-infection (6, 12, 13). By three weeks post-infection, the spleen and liver become greatly enlarged and many infected mice die due to splenic rupture between 2-6 weeks. To fully understand the effect of the Friend virus on murine erythroid cells, a brief review of normal hematopoiesis is necessary.

The circulating red and white blood cells have finite life-spans and must constantly be replenished. This process is termed hematopoiesis and has been thoroughly reviewed (14-16). Hematopoiesis involves a hierarchy of stem cells with different developmental and proliferative capacities (see Fig. 1). The most primitive stem cells, residing mostly in the bone marrow, are pluripotent and have a substantial capacity for self-renewal, although this capacity is not unlimited. The rate of stem cell replication and differentiation is regulated by a complex set of humoral and microenvironmental factors. The transition from a pluripotent stem cell to a progenitor capable of only differentiation along a single developmental pathway is termed determination or commitment. The committed progenitor cells form a series of stem cell pools that have a limited self-renewal capability and that are replenished from their precursors. Thus, cells in each stem cell pool can

Figure 1. Summary of the hematopoietic cell lineages. Abbreviations used in the erythroid differentiation pathway include: CFU-S (coloney-forming unit, spleen), BFU-E (burst-forming units, erythroid), and CFU-E (coloney-forming units, erythroid).

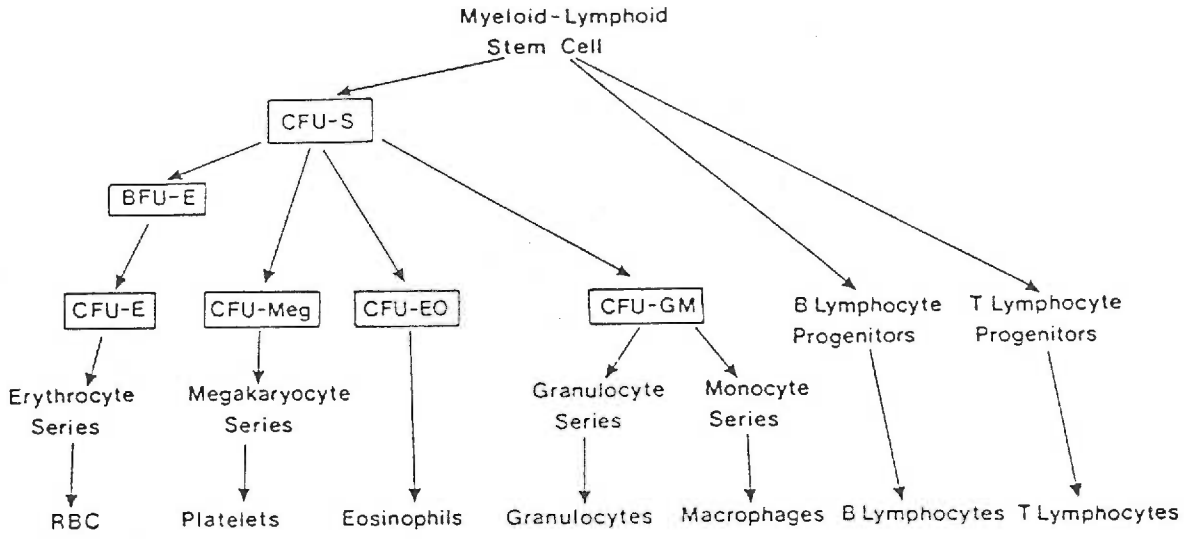
Myeloid-Lymphoid
Stem Cell
CFU-S
BFU-E
CFU-E
CFU-Meg
CFU-EO
CFU-GM
B Lymphocyte
Progenitors
T Lymphocyte
Progenitors
Erythrocyte
Series
Megakaryocyte
Series
Granulocyte
Series
Monocyte
Series
RBC
Platelets
Eosinophils
Granulocytes
Macrophages
B Lymphocytes
T Lymphocytes

proliferate for a limited time before progressing along the developmental pathway. As cells progress along the pathway, their ability to proliferate becomes more restricted as they become more differentiated.

The erythroid lineage includes several distinct precursor cells that are derived from a pluripotent precursor stem cell called the CFU-S (coloney-forming unit, spleen) (see Fig. 1). At least two distinct classes of erythroid precursor cells have been identified by their ability to form hemoglobinized colonies in semisolid medium. Primitive erythroid precursors, referred to as BFU-E (burst-forming units, erythroid), form large clusters of colonies (called bursts) that become hemoglobinized 4-6 days in culture with the addition of erythropoietin (Epo). The cells in these bursts are mature erythroid cells that have no self-renewal capacity. The relatively more mature erythroid precursor cells are termed CFU-E (coloney-forming unit, erythroid) and can form small hemoglobinized colonies when cultured for 48 hours in the presence of Epo. Thus, the BFU-E undergo a limited number of divisions and then differentiate to form the CFU-E stem cell pool. Similarly, the CFU-E divide briefly and then differentiate to form mature erythrocytes.

D. Viral Host Range

The murine leukemia viruses (MuLV) can be distinguished by their abilities to penetrate into cells of different mammalian species, and they are classified accordingly as ecotropic, xenotropic, amphotropic, and dualtropic (also called polytropic). These differences in host range are determined by the abilities of the MuLV envelope glycoproteins to bind to different receptors on the surfaces of the

appropriate target cells (reviewed 17). Consequently, the expression of a given MuLV envelope glycoprotein on the surface of the infected cell will interfere with subsequent infection by another member of the same virus group.

The efficient infection of ecotropic MuLVs, including the Friend and Rauscher MuLVs that are helpers to their SFFVs, is restricted to mouse cells, although some strains can also infect rat cells. Xenotropic MuLVs are endogenous to mouse cells but can only infect non-murine cells such as rat, mink and human. The amphotropic MuLVs are inherited in certain strains of wild mice and it is believed they have a broad host range and can infect all mammalian species. Finally, the dualtropic MuLVs are recombinants between ecotropic MuLVs and endogenously inherited DNAs that are related, but not identical to xenotropic MuLVs. These highly leukemogenic viruses can cause foci on mink cells and are designated mink cell focus-inducing (MCF) viruses. They have a dualtropic host range in that they can infect mouse and non-mouse cells.

E. Viral Life Cycle

The MuLV infection cycle is a multi-step process (reviewed 18, 19). Infection begins with the binding of a virion envelope glycoprotein to a specific cell surface receptor . As discussed above, this binding helps define the viral host range. After binding, the virion core penetrates into the cytoplasm of the host cell and the viral RNA genome is reverse transcribed by a RNA-directed DNA polymerase called reverse transcriptase. The double stranded DNA intermediate is called a provirus and this integrates into the host's genome. A transcriptional promoter located in the long terminal repeat (LTR) of the provirus directs the transcription of full length

viral RNA. This genomic RNA is spliced to form subgenomic mRNAs that encode the viral proteins. The core proteins are synthesized as polyprotein precursors in the cytoplasm while the envelope precursor is synthesized on endoplasmic reticulum bound ribosomes. The envelope glycoproteins are processed from the rough endoplasmic reticulum, through the Golgi apparatus and to the plasma membranes. The viral nucleocapsids form and bud from the plasma membrane. Consequently, the viral lipid bilayer is acquired from the host cell's membrane.

F. Friend Viral Complex

The Friend virus is a complex of two distinct viral components: a replication-competent Friend murine leukemia virus (F-MuLV) and a replication-defective spleen focus-forming virus (SFFV) (12, 20). As will be described in detail, considerable evidence has shown that the SFFV is responsible for the rapidly developing erythroleukemia, while the role of F-MuLV is to provide the replicative functions that the defective SFFV lacks (13, 21). The difference between the anemia and polycythemia-inducing virus isolates is also determined by their SFFV components (13). Therefore, viral stocks which differ by their ability to induce polycythemia or anemia are designated $SFFV_P$ or $SFFV_A$, respectively.

1. MuLV Genome

The replication-competent F-MuLV contains a 38S, positive sense messenger RNA (22-24, reviewed 25). The MuLV genome encodes three genes called *gag*, *pol*, and *env* which are arranged 5'-*gag-pol-env*-3'. The *gag, pol,* and *env* genes encode the viral core proteins, reverse transcriptase, and the viral envelope proteins, respectively (reviewed 25). The primary *gag* gene translation products are synthesized from the 38S mRNA to produce three

polyproteins at 65,000, 80,000, and 180,000-daltons. These have been termed Pr65^{gag}, gPr80^{gag}, and Pr180$^{gag\text{-}pol}$, respectively. Translation of the larger polyproteins is believed to be the result of a translational read-through at the 3' end of the *gag* sequences (26). The Pr65^{gag} is cleaved to generate the internal structural *gag* proteins of the viral particles (27). The gPr80^{gag} is the precursor to the glycosylated *gag* polyprotein found at the cell surface (28) and the Pr180$^{gag\text{-}pol}$ is incorporated into budding virions and is eventually proteolytically cleaved to form the mature reverse transcriptase (29). This cleavage is believed to activate the reverse transcriptase (29).

The *env* gene encodes a polyprotein that is translated from a spliced, 22S subgenomic mRNA on ribosome bound to the endoplasmic reticulum (19, 30). The glycosylated form of this polyprotein, gPr90, is then proteolytically cleaved to form the viral envelope glycoprotein, gp70, and its membrane anchor, p15E (19, 31, 32). The gp70 and p15E remain associated by disulfide bridges and/or noncovalent bonds (33-35) and become incorporated into budding virus particles. In addition, due to the fact that much of the gp70 is only noncovalently associated to p15E, gp70 molecules are readily lost from infected cells and budded virions (36).

2. The SFFV genome

Once the SFFV was isolated free of its helper MuLV by cloning at a limiting dilution into fibroblasts (37, 38), it was possible to compare its genome with that of its helper MuLV and with xenotropic and dualtropic MuLVs. Molecular cloning and sequencing of several strains of Friend SFFV and Rauscher SFFV have indicated that they all have similar structures and presumed origins (8, 9).

The SFFV appears to have arisen by recombination between its natural helper virus and endogenous mouse, dualtropic-specific genetic sequences (39, 40). Using liquid hybridization techniques (39, 40), it was shown that the SFFV is an *env*-gene recombinant virus that contains both F-MuLV and MCF sequences. The SFFV *env* gene is in fact highly related to the recombinant-type *env* genes of MCF viruses. The MCFs have also arisen by recombination of ecotropic MuLVs with endogenous dualtropic-specific *env* gene sequences (for review see 41). Friend MCF virus has been implicated in an F-MuLV-induced erythroproliferative disease that is quite similar, yet distinct, from that induced by SFFV (42)

Consistent with its replication defectiveness, $SFFV_P$ genome contains a 32S RNA (38, 43-45), in contrast to the 38S RNA for MuLV. This size difference is due to partial deletions in the *gag*, *pol* and *env* genes. Thus, $SFFV_P$ does not encode a functional reverse transcriptase and only encodes a 15,000- to 45,000-dalton *gag* protein rather than the 65,000-dalton F-MuLV *gag* precursor (38, 43, 45). A 21S subgenomic RNA has been shown to code for the SFFV *env* protein (45-47). The envelope protein is a 52-55,000 dalton glycoprotein (gp55) (45, 48-50) that is immunologically and structurally related to the larger gp70-p15E glycoproteins of MCF viruses (48, 51). The gp55 is inefficiently processed from the rough endoplasmic reticulum to the plasma membrane and is not incorporated into budding virions (49, 50). However, recent work has shown that gp55 is slowly shed into the medium (52).

G. Effect of the Friend Virus Complex on Hematopoiesis

1. FV-P effect on erythroid cells

Infection of mice with the $SFFV_P$ viral complex causes a multi-staged erythroleukemia (reviewed 2, 3). The early stage of the disease begins within 1-2 days of infection and is characterized by extensive erythroblast proliferation in the spleen and marrow. This erythroid hyperplasia causes distinct splenic foci within 6-10 days post-infection (6, 12, 13, 53). By three weeks post-infection, the spleen and liver become greatly enlarged and polycythemia develops due to continuing preprogrammed differentiation of the infected proliferating erythroblasts (54-57). In the later stages, between 4-6 weeks, transplantable tumorigenic cells can be isolated from the host animal and death usually occurs due rupture of the spleen.

In vitro analysis has helped characterize some of the cellular changes that occur during the disease. Whereas the Friend virus can infect a variety of hematopoietic cells, the pathogenic targets appear to be the Epo-responsive erythroid precursor cell (58, 59). Proliferation and preprogrammed differentiation of CFU-E and BFU-E is normally dependent on the hormone Epo (see Fig. 1). However, viral infection of the erythroid precursor cells dramatically reduces this requirement for Epo and mice infected with $SFFV_P$ continue to produce red blood cells under conditions where Epo levels would be insufficient to support normal erythropoiesis (11, 55, 57, 60).

Hankins et al. (60) described the appearance of large erythroid bursts in semisolid medium 5 days after infecting bone marrow cells with FV-P *in vitro*. While normal erythroid bursts (BFU-Es) require the addition of Epo for coloney formation *in vitro*, the FV-P infected cells can form bursts without the the addition of exogenous Epo. Biological and physical characterization of these bursts indicate that they are formed from erythroid progenitor cells that are more

primitive than CFU-Es (57, 60). These BFU-E erythroid progenitor cells are believed to be the precursor cells responsible for the increase in number of CFU-E seen in the mouse within 3 days post-infection. These bursts form regardless of which helper virus is used to rescue the SFFV and they do not form with helper virus alone (57). This work clearly demonstrated that the SFFV component was responsible for the Epo independent burst transformation. Using a similar approach, Kost et al. (58, 59) demonstrated that the major target cells for the Friend virus are erythroid precursor cells that have matured beyond the day 8 BFU-E.

In summary, both the BFU-E and CFU-E progenitors are committed to the erythroid lineage and their proliferative capacity becomes restricted as they differentiate. Both the differentiation and proliferation of these cells normally require Epo. Infection by FV-P causes mitogenesis independent of Epo, but the commitment to terminal differentiation is not eliminated. Consequently, infected mice develop polycythemia.

2. FV-A effect on erythroid cells

The initial viral isolate described by Friend induced an erythroleukemia characterized by the development of anemia (1, 10). Infection of mice with FV-A causes an erythroleukemia that is very similar to that caused by the FV-P strain. Foci can be detected on the surface of the spleen 9-10 days post-infection (13, 53), however these foci are not as distinct as those induced by FV-P. FV-A infected mice develop splenomegaly, an increase in Epo-dependent erythroid colony-forming cells (CFU-E), and anemia (13, 61).

In contrast with $SFFV_P$, CFU-E and BFU-E infected with $SFFV_A$ remain

partly sensitive to Epo (57, 62). Hankins et al. (57) demonstrated that infection of bone marrow cells *in vitro* results in an increase in the number of cells capable of forming BFU-E and CFU-E colonies in the absence of Epo. However, they contained significantly less hemoglobin than those induced by FV-P. To fully differentiate, these colonies required the addition of Epo, but at a level that would not induce differentiation of uninfected erythroid precursor cells.

In summary, FV-A can cause Epo-independent mitosis of BFU-Es and CFU-Es. The proliferative capacity of the infected cells remains limited because they are committed to differentiation and their self-renewal capability is not increased by infection, although terminal differentiation still requires the low level presence of Epo. Thus, FV-A infection stimulates limited erythroblastosis without complete differentiation and the ineffective erythropoiesis results in anemia. Therefore, the major difference between FV-P and FV-A seems to be that the erythroblastosis caused by FV-P is associated with Epo-independent terminal differentiation.

H. Multiple Stages of Erythroleukemia Development

The progressive nature of the erythroleukemia has been demonstrated by several experimental studies. Fragments of enlarged spleens from mice infected with either complex cannot be successfully transplanted subcutaneously to syngeneic hosts within the first two weeks of infection. Only after three weeks post-infection has it been possible to obtain tumor cell lines from the spleen (63-65). These cells resemble proerythroblasts but they are blocked in their ability to differentiate (66). However, they have the ability to be induced to undergo terminal erythroid differentiation by the addition of such chemicals as dimethylsulfoxide (DMSO) (66).

Further evidence for distinct stages in the development of the erythroleukemia was obtained using the *in vitro* cell culture in semisolid medium (methylcellulose). Culturing spleen cells of mice infected 1-2 weeks previously with FV-P results in the development of only small erythroid colonies (65). These colonies have undergone erythroid development as judged by hemoglobin production and only have a limited capacity to divide. In contrast, large erythroid colonies (10^4-10^5 cells) can be grown in methylcellulose after 3 weeks post-infection (65). Only a small portion (1-5%) of these cells undergo spontaneous erythroid differentiation. These cells can form spleen colonies in irradiated hosts and produce tumors when injected subcutaneously into unirradiated hosts.

Use of *in vitro* colony-forming assay has revealed some important differences between the FV-P and FV-A strains. Methylcellulose colonies are detected as early as 3 weeks post-infection with FV-P, whereas FV-A infection requires greater than 8 weeks for colony formation (65). Using an assay that detects tumor formation in the omentum of secondary irradiated recipients, a similar kinetic difference is seen in the appearance of tumorigenic cells after injection with FV-P and FV-A (64). Cell lines derived from colony-forming units also differ in their differentiation characteristics. Clonal cell lines derived from FV-A infected cells have a low level of hemoglobin positive cells, will accumulate the erythroid specific membrane protein spectrin after exposure to Epo, and are generally unresponsive to DMSO. In contrast, FV-P derived cell lines exhibit a higher level (25%) of cells with detectable hemoglobin, are unaffected by Epo, and respond to low levels of DMSO (1%) by differentiating. The ability to undergo terminal erythroid differentiation is one characteristic Friend virus-transformed

cells have in common with normal hematopoietic cells.

The final stage of Friend erythroleukemia is characterized by the emergence of immortalized tumorigenic cells with a high self-renewal capacity. These cells appear to be autonomous of both humoral and cellular factors that regulate the behavior of normal hematopoietic cells. This is further supported by the evidence that FV-P derived colony-forming cells can proliferate to form macroscopic spleen colonies in genetically anemic SL/SL^d mice (67). These mice contain two mutations that result in a defective cellular microenvironment that prevents spleen colony formation by normal hematopoietic cells. Thus, the malignant cells have escaped the commitment to differentiate and have gained the capacity for unlimited self-renewal.

I. Genetic Elements Required for SFFV Pathogenesis

1. Role of SFFV in pathogenesis

Because of the difficulty of propagating the replication-defective SFFV *in vitro*, early attempts to define the role of each viral component in disease development centered on analysis of the F-MuLV helper virus. A replication-competent virus was first isolated free of SFFV by passage of the viral complex through mice or rats resistant to SFFV (68, 69). The virus recovered from these animals induced a T cell lymphatic leukemia. However, using T cell-depleted mice or newborn mice, the Friend MuLV was able to induce erythroleukemia, rather than a lymphoid leukemia, after a long latent period of 25 to 45 days (70). This erythroleukemia was restricted to newborn mice. In contrast, the full Friend complex can induce a rapid erythroleukemia in both newborn and adult mice.

The generation of Epo-independent erythroid cells, both *in vivo* and *in vitro*, was found to be independent of the helper-virus used in the infection. Rescue of SFFV nonproducer cell lines with a variety of helper viruses, including F-MuLV, Moloney MuLV, and amphotropic MuLV, induced a disease characterized by the appearance of a large number of Epo-independent CFU-Es (13). In addition, the formation of erythroid bursts following *in vitro* infection of bone marrow cells was independent of which helper MuLVs were pseudotyped with SFFV (57).

This earlier work strongly suggested that the SFFV was needed for the induction of the erythroleukemia. However, it still was not clear if the role of the helper virus was to provide its replicative functions and spread the disease or to cooperate in some additional critical way to induce the disease. Several recent reports have addressed this issue by using *in vitro* packaging cell lines to produce helper-free stocks of SFFV (70-73). In all reports it was shown that helper-free SFFV is able to induce extensive erythroid hyperplasia *in vitro* and *in vivo*. However, the ability of helper-free $SFFV_P$ to generate advance stages of the erythroleukemia was not consistently observed (70). Further work by Ruscetti et al (72, 73) and our studies (thesis results) have shown that helper-free $SFFV_P$ is capable of inducing a progressive multi-stage erythroleukemia. This work has conclusively shown that the SFFV component is responsible for the observed erythroleukemia *in vivo*.

2. Role of SFFV *env* gene in pathogenesis

Early studies suggested that the envelope protein encoded by the SFFV was critical in the development of the erythroleukemia. For example, while the ability of SFFV to produce their *gag* proteins vary with strain and infected cell, all

SFFVs encode a gp55 envelope glycoprotein (75). Oligonucleotide fingerprinting comparisons between SFFV and its ecotropic MuLV helper have shown that only sequences at the 3' end of the genome (those encoding the envelope protein) are unique to SFFV (24, 44). Moreover, as previously described, the SFFV *env* gene is closely related to the *env* genes of MCF viruses (8, 39, 40, 76). These MCF viruses have been implicated as causes in a variety of progressive hematopoietic neoplasms, including the erythroleukemia caused in new borns by F-MuLV (reviewed 41).

3. Studies with subgenomic fragments of SFFV DNA and spontaneous mutants

Molecular cloning of the SFFV genome provided further evidence for the importance of the envelope gene. When a subgenomic fragment derived from the 3' end of an SFFV clone was co-transfected with helper virus DNA into fibroblast cultures, biologically active SFFV recombinants were recovered (77). In addition, deletions introduced into the *env* gene within this subgenomic fragment could eliminate the biological activity of the SFFV recovered from the co-transfection assay (78). These experiments were consistent with the hypothesis that the *env* gene mediates the pathogenicity of SFFV. However, the co-transfection assay used in these experiments required the biologically active virus to form after the recombination of the SFFV sequences with those of the helper. It is possible that a negative result in the co-transfection assay represents a failure in this recombination rather than an absence of the leukemogenic sequences. The resulting inactive viruses were not isolated and characterized.

More direct genetic evidence was obtained from the isolation of

transmissible spontaneous SFFV mutants. Ruta et al. (79) from this laboratory showed that non-pathogenic or weakly pathogenic SFFVs contained non-overlapping mutations in their *env* genes. These mutants encoded envelope glycoproteins that had abnormal electrophoretic mobilities and were defective in their processing to the plasma membranes. Similar mutants have also been isolated for R-SFFV (80). However, when these SFFV mutants were injected into newborn mice, revertants formed that were fully leukemogenic in mice of all ages (81). Sequence analysis of these revertants showed that they contained secondary *env* mutations that restored pathogenic function to the SFFV (82). Site-directed SFFV *env* mutants are also nonpathogenic (83).

J. Structural Characteristics of the SFFV *env* Gene

1. Sequence analysis

The complete nucleotide sequence of the $SFFV_P$ *env* gene has been determined (76, 84, 85) (summarized, Fig. 2). The open reading frame predicts that the primary translation product has a total of 409 amino acids with a M_r ~44,752. The sequence reveals that there are five potential N-linked glycosylation sites and twelve cysteines available for disulfide bonding.

As previously described, it is believed that the SFFV genome was generated by genetic recombination. A comparison of SFFV *env* sequences with related MuLV*env* sequences demonstrates that the recombination has resulted in a SFFV envelope glycoprotein with several unique characteristics (Fig. 3) (8). The amino-terminal portion of the molecule has a high degree (>90%) of sequence homology with the amino-terminal portion of the gp70 of MCF virses. This portion

of the MCF gp70 is known to be coded for by the acquired endogenous dualtropic-specific *env*-like sequences (reviewed 82). These are referred to in Fig. 3 as xeno-related sequences. The fact that the amino-terminal domain is so highly conserved between the SFFV and MCF envelope glycoproteins suggests that this portion of the molecule contains a functionally active site for this group of pathogenic viruses. Indeed, all MCFs contain this closely related amino-terminal region and they all bind to a receptor different from that used by ecotropic MuLVs (87). Consequently, it is believed this amino terminal region must involve the receptor-binding domain of the MCF envelope glycoprotein. The carboxyl-terminus is highly homologous to ecotropic gp70 and p15E sequences. However, due to a single base pair insertion, the p15E-related domain of gp55 is shortened and contains a unique set of amino acids at its carboxyl-terminus.

2. Fusion glycoprotein

The primary translation product of the MuLV prototype envelope gene is a polyprotein containing gp70 and Pr15E that is eventually cleaved to form the mature envelope protein. In contrast, the SFFV env gene product is synthesized as a 55,000-dalton glycoprotein and is inefficiently processed to the cell surface. Sequencing analysis of the SFFV *env* gene reveals a large deletion (585 base pair) that eliminates the cleavage site between gp70 and Pr15E. This results in a gene product where the amino-terminal gp70 and carboxy-terminal p15E sequences are joined and remain covalently linked (see Fig. 4). In addition, the sequences coding for the membrane anchoring region of gp55, as compared to the similar domain in MuLV p15E, contain the insertion of a 6 base-pair tandem repeat insertion in this domain causes a frameshift mutation that results in

Figure 2. Nucleotide sequence and deduced amino acid sequence of the SFFV gp55 gene and its flanking regions as determined by Amanuma et al. (76). Nucleotide sequence is presented as the same (+) strand in the DNA form of the SFFV genome. The CHO designation represents the consensus sequence for N-linked glycosylation.

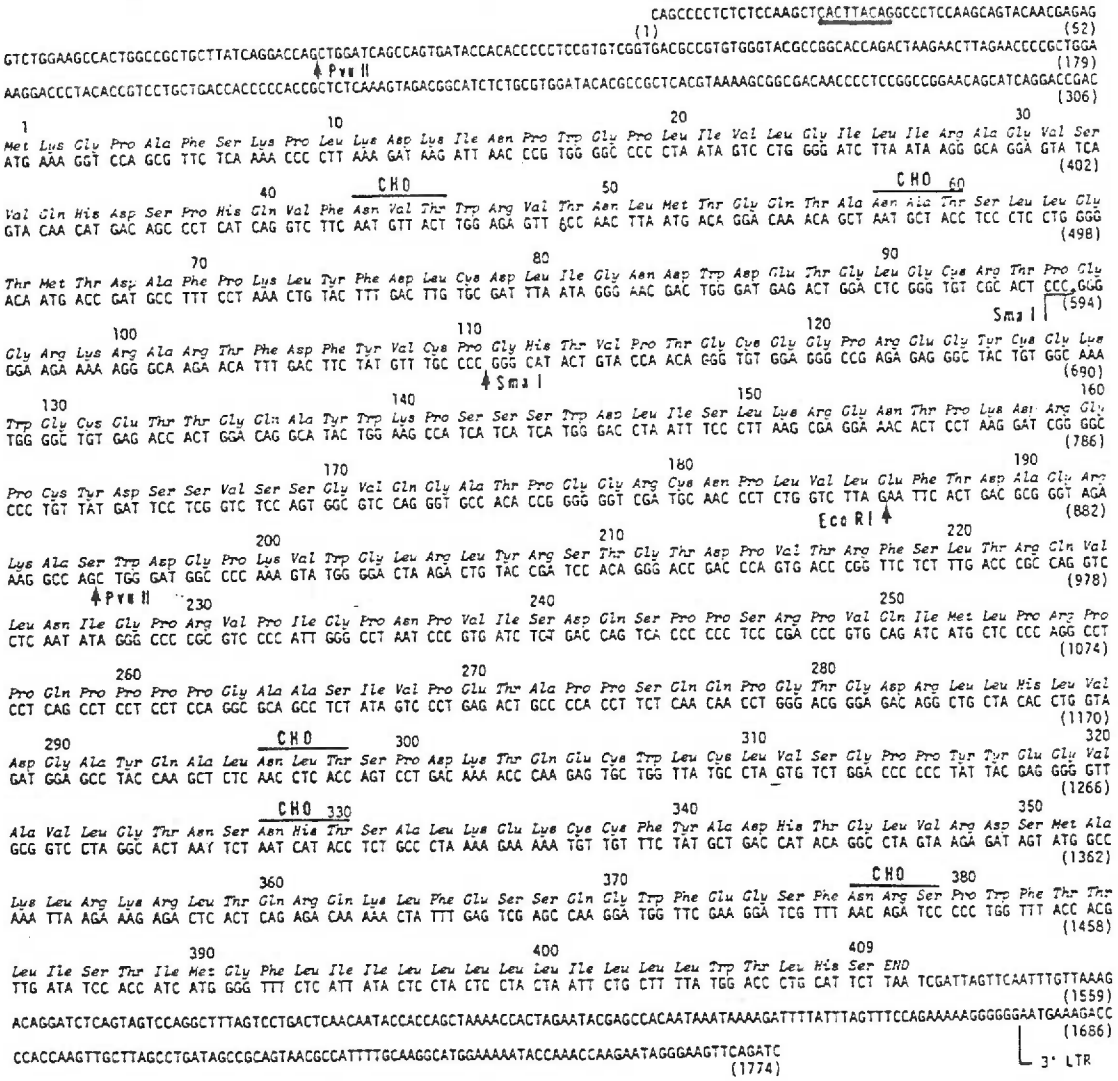
CAGCCCCTCTCTCCAAGCTCACTTACAGGCCCTCCAAGCAGTACAACGAGAG
(1)
(52)
GTCTGGAAGCCACTGGCCGCTGCTTATCAGGACCAGCTGGATCAGCCAGTGATACCACACCCCCTCCGTGTCGGTGACGCCGTGTGGGTACGCCGGCACCAGACTAAGAACTTAGAACCCCGCTGGA
Pvu II
(179)
AAGGACCCTACACCGTCCTGCTGACCACCCCCACCGCTCTCAAAGTAGACGGCATCTCTGCGTGGATACACGCCGCTCACGTAAAAGCGGCGACAACCCCTCCGGCCGGAACAGCATCAGGACCGAC
(306)
1
10
20
30
Met Lys Gly Pro Ala Phe Ser Lys Pro Leu Lys Asp Lys Ile Asn Pro Trp Gly Pro Leu Ile Val Leu Gly Ile Leu Ile Arg Ala Glu Val Ser
ATG AAA GGT CCA GCG TTC TCA AAA CCC CTT AAA GAT AAG ATT AAC CCG TGG GGC CCC CTA ATA GTC CTG GGG ATC TTA ATA AGG GCA GGA GTA TCA
(402)
CHO
CHO
40
50
60
Val Gln His Asp Ser Pro His Gln Val Phe Asn Val Thr Trp Arg Val Thr Asn Leu Met Thr Gly Gln Thr Ala Asn Ala Thr Ser Leu Leu Glu
GTA CAA CAT GAC AGC CCT CAT CAG GTC TTC AAT GTT ACT TGG AGA GTT ACC AAC TTA ATG ACA GGA CAA ACA GCT AAT GCT ACC TCC CTC CTG GGG
(498)
70
80
90
Thr Met Thr Asp Ala Phe Pro Lys Leu Tyr Phe Asp Leu Cys Asp Leu Ile Gly Asn Asp Trp Asp Glu Thr Gly Leu Gly Cys Arg Thr Pro Glu
ACA ATG ACC GAT GCC TTT CCT AAA CTG TAC TTT GAC TTG TGC GAT TTA ATA GGG AAC GAC TGG GAT GAG ACT GGA CTC GGG TGT CGC ACT CCC GGG
(594)
Sma I
100
110
120
Gly Arg Lys Arg Ala Arg Thr Phe Asp Phe Tyr Val Cys Pro Gly His Thr Val Pro Thr Gly Cys Gly Gly Pro Arg Glu Gly Tyr Cys Gly Lys
GGA AGA AAA AGG GCA AGA ACA TTT GAC TTC TAT GTT TGC CCC GGG CAT ACT GTA CCA ACA GGG TGT GGA GGG CCG AGA GAG GGC TAC TGT GGC AAA
Sma I
(690)
130
140
150
160
Trp Gly Cys Glu Thr Thr Gly Gln Ala Tyr Trp Lys Pro Ser Ser Ser Trp Asp Leu Ile Ser Leu Lys Arg Gly Asn Thr Pro Lys Asn Arg Gly
TGG GGC TGT GAG ACC ACT GGA CAG GCA TAC TGG AAG CCA TCA TCA TCA TGG GAC CTA ATT TCC CTT AAG CGA GGA AAC ACT CCT AAG AAT CGG GGC
(786)
170
180
190
Pro Cys Tyr Asp Ser Ser Val Ser Ser Gly Val Gln Gly Ala Thr Pro Glu Gly Arg Cys Asn Pro Leu Val Leu Glu Phe Thr Asp Ala Gly Arg
CCC TGT TAT GAT TCC TCG GTC TCC AGT GGC GTC CAG GGT GCC ACA CCG GGG GGT CGA TGC AAC CCT CTG GTC TTA GAA TTC ACT GAC GCG GGT AGA
Eco RI
(882)
200
210
220
Lys Ala Ser Trp Asp Gly Pro Lys Val Trp Gly Leu Arg Leu Tyr Arg Ser Thr Gly Thr Asp Pro Val Thr Arg Phe Ser Leu Thr Arg Gln Val
AAG GCC AGC TGG GAT GGC CCC AAA GTA TGG GGA CTA AGA CTG TAC CGA TCC ACA GGG ACC GAC CCA GTG ACC CGG TTC TCT TTG ACC CGC CAG GTC
Pvu II
(978)
230
240
250
Leu Asn Ile Gly Pro Arg Val Pro Ile Gly Pro Asn Pro Val Ile Ser Asp Gln Ser Pro Pro Ser Arg Pro Val Gln Ile Met Leu Pro Arg Pro
CTC AAT ATA GGG CCC CGC GTC CCC ATT GGG CCT AAT CCC GTG ATC TCT GAC CAG TCA CCC CCC TCC CGA CCC GTG CAG ATC ATG CTC CCC AGG CCT
(1074)
260
270
280
Pro Gln Pro Pro Pro Pro Gly Ala Ala Ser Ile Val Pro Glu Thr Ala Pro Pro Ser Gln Gln Pro Gly Thr Gly Asp Arg Leu Leu His Leu Val
CCT CAG CCT CCT CCT CCA GGC GCA GCC TCT ATA GTC CCT GAG ACT GCC CCA CCT TCT CAA CAA CCT GGG ACG GGA GAC AGG CTG CTA CAC CTG GTA
(1170)
CHO
290
300
310
320
Asp Gly Ala Tyr Gln Ala Leu Asn Leu Thr Ser Pro Asp Lys Thr Gln Glu Cys Trp Leu Cys Leu Val Ser Gly Pro Pro Tyr Tyr Glu Gly Val
GAT GGA GCC TAC CAA GCT CTC AAC CTC ACC AGT CCT GAC AAA ACC CAA GAG TGC TGG TTA TGC CTA GTG TCT GGA CCC CCC TAT TAC GAG GGG GTT
(1266)
CHO
330
340
350
Ala Val Leu Gly Thr Asn Ser Asn His Thr Ser Ala Leu Lys Glu Lys Cys Cys Phe Tyr Ala Asp His Thr Gly Leu Val Arg Asp Ser Met Ala
GCG GTC CTA GGC ACT AAY TCT AAT CAT ACC TCT GCC CTA AAA GAA AAA TGT TGT TTC TAT GCT GAC CAT ACA GGC CTA GTA AGA GAT AGT ATG GCC
(1362)
CHO
360
370
380
Lys Leu Arg Lys Arg Leu Thr Gln Arg Gln Lys Leu Phe Glu Ser Ser Gln Gly Trp Phe Glu Gly Ser Phe Asn Arg Ser Pro Trp Phe Thr Thr
AAA TTA AGA AAG AGA CTC ACT CAG AGA CAA AAA CTA TTT GAG TCG AGC CAA GGA TGG TTC GAA GGA TCG TTT AAC AGA TCC CCC TGG TTT ACC ACG
(1458)
390
400
409
Leu Ile Ser Thr Ile Met Gly Phe Leu Ile Ile Leu Leu Leu Leu Leu Ile Leu Leu Leu Trp Thr Leu His Ser END
TTG ATA TCC ACC ATC ATG GGG TTT CTC ATT ATA CTC CTA CTC CTA CTA ATT CTG CTT TTA TGG ACC CTG CAT TCT TAA TCGATTAGTTCAATTTGTTAAAG
(1559)
ACAGGATCTCAGTAGTCCAGGCTTTAGTCCTGACTCAACAATACCACCAGCTAAAACCACTAGAATACGAGCCACAATAAATAAAAGATTTTATTTAGTTTCCAGAAAAAGGGGGGAATGAAAGACC
(1686)
CCACCAAGTTGCTTAGCCTGATAGCCGCAGTAACGCCATTTTGCAAGGCATGGAAAAATACCAAACCAAGAATAGGGAAGTTCAGATC
(1774)
3' LTR

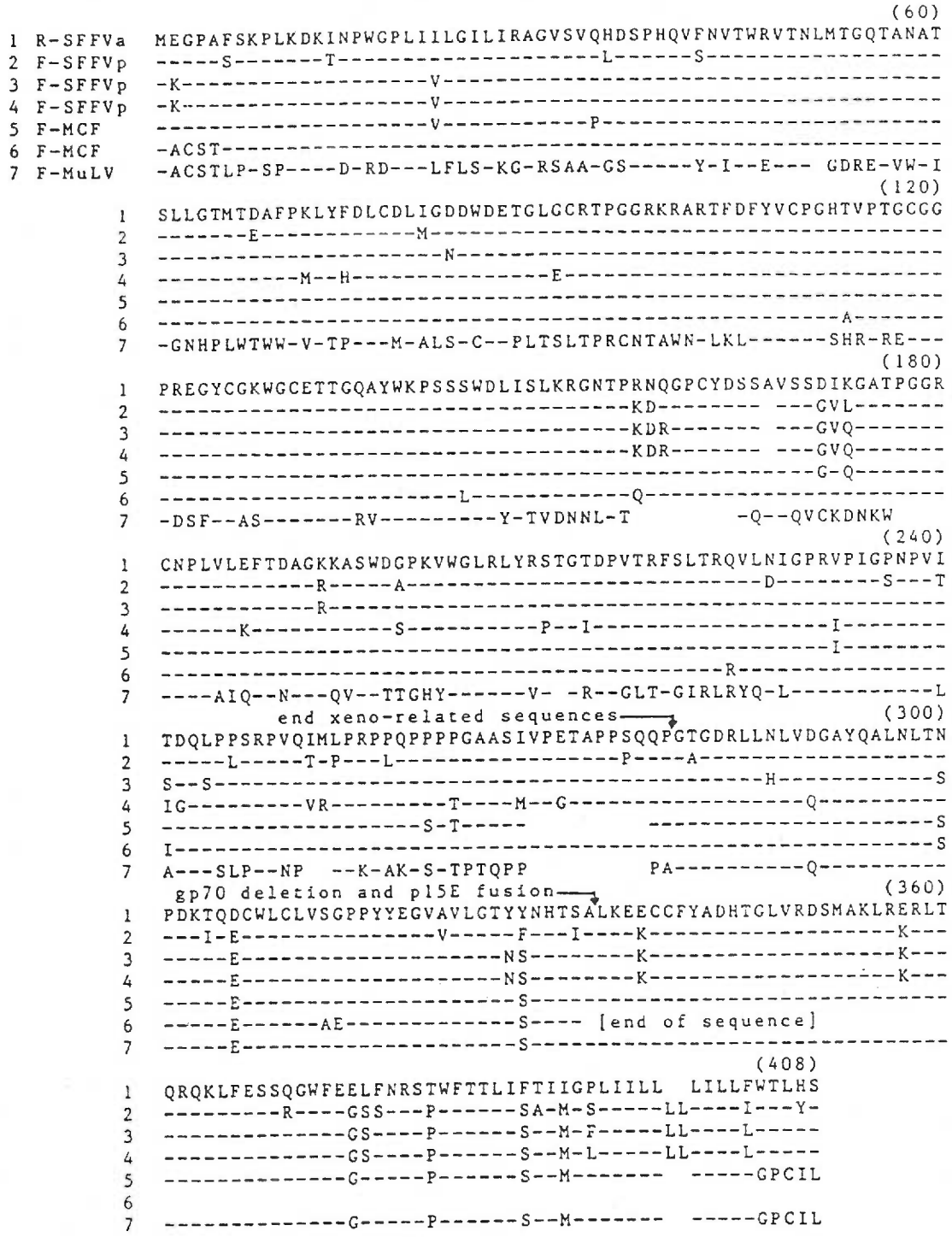
(60)
1 R-SFFVa MEGPAFSKPLKDKINPWGPLIILGILIRAGVSVQHDSPHQVFNVTWRVTNLMTGQTANAT
2 F-SFFVp -----S-------T----------L------S----------
3 F-SFFVp -K----------V----------
4 F-SFFVp -K----------V----------
5 F-MCF ----------V----------P----------
6 F-MCF -ACST----------
7 F-MuLV -ACSTLP-SP----D-RD---LFLS-KG-RSAA-GS-----Y-I--E--- GDRE-VW-I
(120)
1 SLLGTMTDAFPKLYFDLCDLIGDDWDETGLGCRTPGGRKRARTFDFYVCPGHTVPTGCGG
2 -------E----------M----------
3 ----------N----------
4 ----------M--H----------E----------
5 ----------
6 ----------A-------
7 -GNHPLWTWW-V-TP---M-ALS-C--PLTSLTPRCNTAWN-LKL------SHR-RE---
(180)
1 PREGYCGKWGCETTGQAYWKPSSSWDLISLKRGNTPRNQGPCYDSSAVSSDIKGATPGGR
2 ----------KD-------- ---GVL-------
3 ----------KDR------- ---GVQ-------
4 ----------KDR------- ---GVQ-------
5 ----------G-Q-------
6 ----------L----------Q----------
7 -DSF--AS-------RV---------Y-TVDNNL-T -Q--QVCKDNKW
(240)
1 CNPLVLEFTDAGKKASWDGPKVWGLRLYRSTGTDPVTRFSLTRQVLNIGPRVPIGPNPVI
2 ----------R-----A----------D--------S---T
3 ----------R----------
4 ------K----------S----------P--I----------I--------
5 ----------I--------
6 ----------R----------
7 ----AIQ--N---QV--TTGHY------V- -R--GLT-GIRLRYQ-L----------L
end xeno-related sequences
(300)
1 TDQLPPSRPVQIMLPRPPQPPPPGAASIVPETAPPSQQPGTGDRLLNLVDGAYQALNLTN
2 -----L-----T-P---L----------P----A----------
3 S--S----------H----------S
4 IG---------VR---------T----M--G----------Q----------
5 ----------S-T----- ----------S
6 I----------S
7 A---SLP--NP --K-AK-S-TPTQPP PA----------Q----------
gp70 deletion and p15E fusion
(360)
1 PDKTQDCWLCLVSGPPYYEGVAVLGTYYNHTSALKEECCFYADHTGLVRDSMAKLRERLT
2 ---I-E----------V-----F---I----K----------K---
3 -----E----------NS--------K----------K---
4 -----E----------NS--------K----------K---
5 -----E----------S----------
6 -----E------AE----------S---- [end of sequence]
7 -----E----------S----------
(408)
1 QRQKLFESSQGWFEELFNRSTWFTTLIFTIIGPLIILL LILLFWTLHS
2 ---------R----GSS---P------SA-M-S-----LL----I---Y-
3 ----------GS----P------S--M-F-----LL----L-----
4 ----------GS----P------S--M-L-----LL----L-----
5 ----------G-----P------S--M------- -----GPCIL
6
7 ----------G-----P------S--M------- -----GPCIL

premature termination of the molecule 34 codons before the termination codon in MuLV p15E (76, 84, 85). These changes result in a hydrophobic carboxyl terminus which appears buried in the membrane with no portion of the molecule exposed on the cytoplasmic side of the membrane (88).

Protease digestion analysis of the SFFV envelope glycoprotein has provided additional structural information about the molecule. The gp55 encoded by wild-type F-SFFV can be cleaved by *S. aureus* V8 protease to form primary fragments V-1 (M_r32,500) and V-2 (M_r 21,500) (79, 80). The larger fragment V-1 is derived from the amino-terminal region of gp55 and contains the antigenic sites specifically related to the gp70s of dual-tropic MuLVs (48, 51). Increasing V8 protease digestion results in further cleavage of V-1 to produce secondary fragments V-3 (M_r 20,000) and V-4 (M_r 12,400).

Extensive V8 proteolytic fragmentation analysis of the related R-SFFV gp54 protein suggested that the dualtropic- and ecotropic-related regions fold into separate globular domains that are connected by a flexible proline-rich hinge (80, 81). The glutamyl peptide bond found within this hinge appears to be highly susceptible to cleavage with V8 protease to generate the primary proteolytic fragments. Moreover, disulfide bonds occur within the dualtropic- and ecotropic-related domains, but not between the globular domains (80, 81).

3. Post-translational processing

The SFFV *env* gene product is synthesized on ribosomes associated with the rough endoplasmic reticulum (RER). The predominate form of gp55 accumulates within the RER and retains its high mannose-containing oligosaccharide composition (45, 48-50). Whereas the MuLV envelope precursor

Figure 4. Comparison of a typical MuLV envelope precursor polyprotein with the SFFV envelope glycoprotein. The open areas of the gp55 are homologous to the ecotropic F-MuLV envelope glycoprotein. The shaded areas represent nonecotropic regions that are highly homologous to dualtropic MCF virus envelope glycoproteins. The solid region at the C-terminus of gp55 represents sequences unique to this glycoprotein.

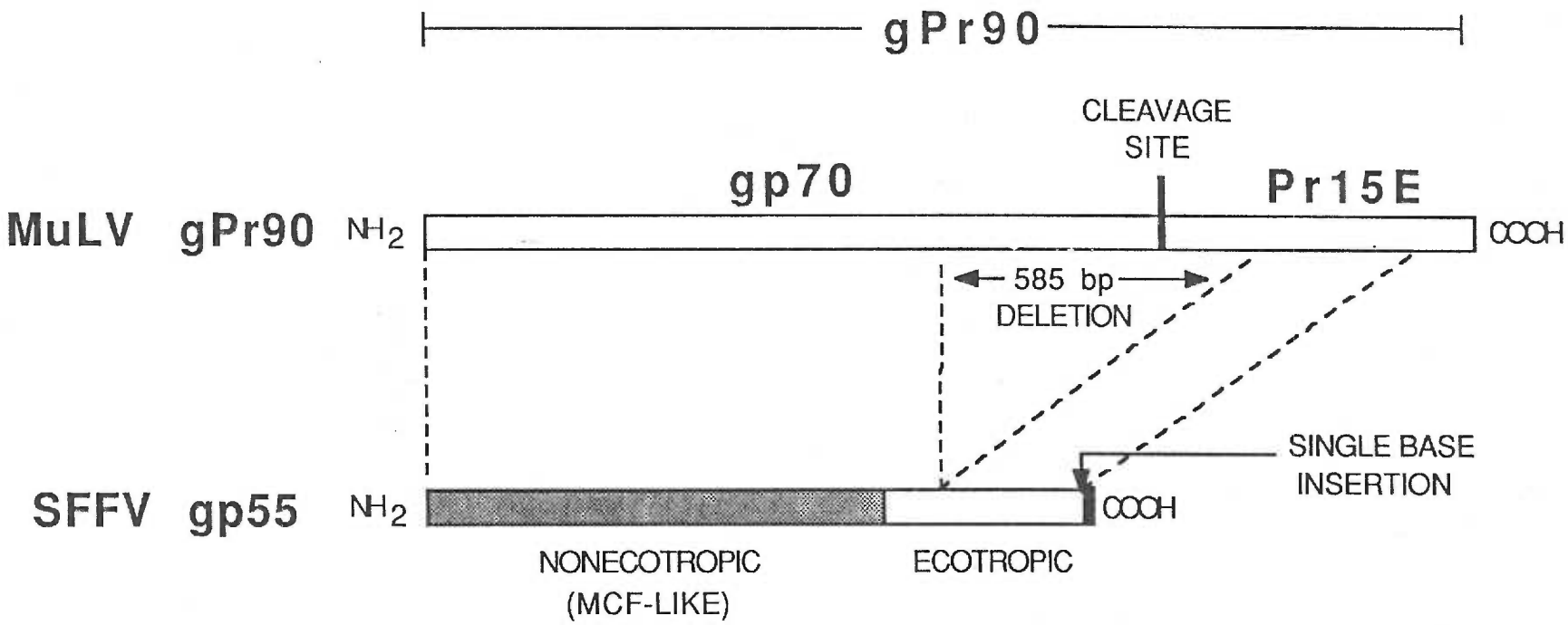
gPr90
CLEAVAGE SITE
gp70
Pr15E
MuLV gPr90
NH2
COOH
585 bp DELETION
SINGLE BASE INSERTION
SFFV gp55
NH2
COOH
NONECOTROPIC (MCF-LIKE)
ECOTROPIC

has seven attached N-linked oligosaccharide chains, gp55 has only four (89). A small portion (~5%) of gp55 is processed to the cell surface and gains a complex carbohydrate motif as it passes through the Golgi apparatus (90). The processed protein, which incorporates a variety of sugars such as galactose, fucose, and glucosamine, has a molecular weight of 65,000-daltons (under denaturing and reducing SDS-PAGE conditions) and can be detected on the cell surface (49, 50). The additional oligosaccharide processing probably contributes to the substantial size increase of the more highly processed cell surface component.

The reason for the inefficient processing of gp55 has never been resolved. Earlier work by Ruta et al. (90) from this laboratory suggested that the unique structure of gp55 allowed for the heterogeneous cessation of gp55 processing because of spontaneous, random denaturation. In contrast, Srinvas and Compans (88) suggested that the *env* deletions in SFFV may have removed critical "signals" believed to be involved in the transport of glycoproteins. A major portion of my thesis project involves the re-evaluation of gp55 processing and the characterization of several critical post-translational modifications.

K. Model of gp55 Action

Previous analysis of nonpathogenic, spontaneous viral mutants and pathogenic revertants suggested a critical role for the cell surface form of gp55. Recent work using *in vitro* mutagenesis has confirmed the importance of cell surface expression of gp55 (83). The nonpathogenic mutants contained lesions in dualtropic-specific sequences that are highly conserved among all strains of SFFV. All pathogenic SFFVs encoded glycoproteins that were expressed on the cell surface, whereas the nonpathogenic glycoproteins were exclusively

intracellular. In addition, the pathogenic SFFVs specifically caused a weak interference to superinfection by dualtropic MuLVs. These results are compatible with the multidomain model for the structure of gp55 and suggest that the processing of gp55 to the plasma membranes is required for pathogenesis. Once at the cell surface, the carboxyl-terminal region anchors the molecule to the plasma membrane while the amino-terminal domain of gp55 binds to dualtropic murine leukemia virus receptors. Interaction with this receptor is believed to stimulate erythroblastosis.

L. Thesis Objectives

The expression of the SFFV envelope glycoprotein at the cell surface is essential to initiate erythroblastosis (79, 80, 83). However, this glycoprotein is very inefficiently processed to the plasma membranes and the vast majority remains in the RER. During the course of my thesis work, I observed that a portion of the intracellular molecules and all of the cell surface gp55 exists as a disulfide-linked dimer. Because all of these processing intermediates exist naturally in the Friend erythroleukemia cells, we have thoroughly characterized the biosynthesis, assembly, and post-translational processing of this newly discovered dimer component to gain more insight into the mechanism of protein folding and intracellular transport. We have used this data to derive a new model for the inefficient processing of gp55 to the cell surface.

The Friend virus is known to induce a multi-staged erythroleukemia (reviewed 2, 3). However, very little is known concerning the progression of the erythroleukemia at the molecular level. We have analyzed the expression levels

of thirteen cellular oncogenes during both the leukemic progression and differentiation of Friend cells to determine if any oncogene was expressed preferentially in a particular stage of the disease. Genomic analysis was performed to identify the potential mechanism of activation for those oncogenes found to be active. Expression of gp55 is required for the initiation of the erythroleukemia, but little is known about its role in the progression and maintenance of the malignant state. Therefore, the expression of the SFFV *env* gene and levels of cell surface gp55 were analyzed during progression and differentiation. We relate these results to the hypothesis that the malignant leukemic state represents a block in differentiation.

The recombinant nature of the SFFV genome has made the unambiguous identification of the proviral integration sites impossible. To overcome this problem, we have constructed a helper-free "tagged" virus that is capable of inducing a fatal erythroleukemia. Using this tagged virus we have been able to address the clonality of the advanced leukemias and map the SFFV proviral integration sites.

II. MATERIALS AND METHODS

A. Animals, Cells, and Viruses.

Female DBA/2J mice between 4-6 weeks of age were used for the oncogene expression analysis described in Chapter VI. Female NIH/Swiss mice between 4-6 weeks of age were used for the "tagged" virus analysis described in Chapter VII. The F745 and F4.6 cell lines have been previously described (91). The FVT/A cell line was originally designated HFL/d cl. A and described by Anand et al. (75). The uninfected normal rat kidney (NRK) cells and SFFV infected NRK Cl 1 cells were originally provided by D. Troxler (NIH) and characterized by Ruta et al. (90). All cell lines were grown in Dulbecco modified Eagle medium (Gibco Diagnostics) supplemented with 10% fetal calf serum and antibiotics. Anemia was induced by subcutance injects of 40 ug phenylhydrazine per gram body weight at -96,-72, and -48 h in a volume of 0.2 ml PBS.

Stocks of the Friend erythroleukemia viral complex were prepared from the infected F4.6 cell line. All viral preparations were isolated from actively growing, subconfluent cell cultures 24 h after addition of fresh growth medium. Culture fluids were collected, filtered through 0.45μm-pore filters and stored at -70°C til use. Viral infection was by tail vein injection using 0.5 ml virus stock (51,000 PFU/ml by the S^+L^- assay) and enlarged spleens were isolated two weeks later.

B. Gel Electrophoresis.

Polyacrylamide (10 to 20%) gels containing sodium dodecyl sulfate were prepared as described by Laemmli (92). Straight 15% and 20% acrylamide gels were also used as indicated in Fig. legends. Electrophoresis was at 20 mA with a voltage ceiling set at 200 v. Immune precipitates were prepared for

electrophoresis by boiling for 10 mins in Laemmli modified sample buffer (0.0625 M tris-HCl, pH 6.8, 2.3% SDS, 20% glycerol, and 5% mercaptoethanol). The mercaptoethanol was omitted where indicated in Fig. legends.

C. Immunoblotting.

Cells were lysed in immunoprecipitation buffer (IPB) (20 mM Tris-HCl, pH 7.5, 1 mM EDTA, 0.1% SDS, 0.5% sodium deoxycholate, 1% triton X-100, and 0.02% sodium azide) at approximately $1x10^6$ cells per 100ul. Samples were fractionated on 10-20% SDS-polyacrylamide gradient gels. Proteins were electroblotted for 1.5 h at 100 volts onto nitrocellulose paper in electroblotting buffer (25 mM Tris, 190 mM glycine, and 20% methanol, pH 8.3) with a Hoefer Transphor system. Blots were allowed to dry at room temperature and stored at -20°C til use. Filters were preincubated in 25 mM Tris-HCl, pH 8.0, 144 mM NaCl, and 0.5% Tween 20 (TTBS) with 3% gelatin (J.T. Baker Chem Co.) at room temperature for 30 mins, and then incubated in TTBS with 1% gelatin containing the desired antiserum for 1 h at room temperature. The antiserum used includes the monospecific goat antibody to F-MuLV gp70 that was generously provided by D. Bolognesi (Duke University, Durham, N.C.). A rat monoclonal antiserum specific to SFFV gp55 as described by Ruscetti et al. (93). This serum reacts with both gp55 and dual tropic MCF gp70s, but not with ecotropic virus gp70s. A second rabbit anti-rat antibody (Bionetics, Kensigton, Md.) was added after the gp55 monoclonal antibody incubation. The blots were then incubated for 1 h with [^{125}I]-protein A (NEN, Boston, Ma., 20 uCi/ug) at 50 ul per ml buffer. Filters were washed thoroughly with TTBS, dried, and exposed to X-ray film at -70°C with intensifer screen.

D. Immunoprecipitation.

All samples were precipitated by secondary immune precipitations. Viral proteins were precipitated directly from IPB lysate or culture medium. Approximately 15 ul of F-MuLV gp70 antibody was used per 1 ml of lysate or medium. Adsorption was allowed to continue for 2 h at $4^{o}C$. Immunoprecipitations were performed by using a variation of the fixed *Staphylococcus aureus* (Pansorbin, Calbiochem). The pansorbin was washed and suspended (10% v/v) in IPB. Pansorbin at 50 ul per ml of lysate was added and allowed to react for 1 h at $4^{o}C$. Precipitation of the antigen-antibody complex was accomplished by microfuge centrifugation. Lysates and medium were first preabsorbed with normal goat serum for 1 h at $4^{o}C$ then followed by pansorbin adsorption.

E. Metabolic Labelling of Cells.

F745 erythroleukemia suspension cells were incubated at $1x10^{6}$ cells/ml in methionine- and cysteine-free minimal essential medium (Gibco) plus 10% FBS for 10 minutes prior to labelling. L-[^{35}S]-methionine and L-[^{35}S]-cysteine (New England Nuclear) were added at 50uCi/ml and incubated for the indicated period of time. Cells were spun down and resuspended in an equal volume of complete medium for "chase" analysis. Aliquots of 1 ml were removed at the times indicated in the Fig. legends and cells were lysed in 1 ml immunoprecipitation buffer after centrifugation from the medium. Lysis buffer contained 20 mM iodoacetamide if indicated in Fig. legend. Viral proteins were analyzed by immunoprecipitation from cell lysates or directly from the medium.

For [^{35}S]-pulse analysis, cells were preincubated and labelled exactly as described for the pulse-chase analysis. Aliquotes of 1 ml (~$1x10^{6}$ cells/ml) were removed at the indicated times and added directly into an equal volume of 2x

immunoprecipitation buffer. Lysis buffer contained 20 mM iodoacetamide if indicated in Fig. legend. Viral proteins were analyzed by immunoprecipitation.

F. [^{125}I] Cell Surface Labelling.

Lactoperoxidase-catalysed cell surface iodination was performed on $1x10^7$ F745 cells in 1 ml phosphate buffered saline (PBS) w/Ca and Mg. Approximately 75 ug lactoperoxidase and 0.75 mCi NaI^{125} (NEN) were added to the cells in PBS followed by 30 ul of 0.03% H_2O_2 at 0, 3, 6, and 9 min. Reaction was carried out at room temperature. Cells were washed 3x in PBS and lysed in IPB or cultured for 18 h in complete medium. Viral proteins were analyzed by immunoprecipitation and gel electrophoresis.

G. Autoradiography and Molecular Weight Determination.

Gels for autoradiographic analysis were fixed in 12.5% TCA overnight and processed with Enhance (New England Nuclear) according to the manufacture's instructions. Gels were dried and exposed to Kodak X-ray film with an intensifer screen at -70^{o}C. The ^{14}C-labelled molecular weight markers (Amersham) correspond to the following sizes: 200,000 (myosin); 92,500 (phosphorylase b); 69,000 (BSA); 46,000 (ovalbumin); 30,000 (carbonic anhydrase); 21,500 (trypsin inhibitor); and 14,300 (lysozyme).

H. Two-Dimensional Gel Electrophoresis.

Two-dimensional gel analysis of the viral proteins was performed as originally described by Brenner et al. (94). The nonreduced immunoprecipitates were separated in the first dimension through a 12.5% acrylamide tube gel. These gels were run a 30 mA and 200 v for 4 hrs. Prior to second-dimension

analysis, the tube gels were reduced by soaking in 0.1 M Tris-HCL, pH 6.8, 2.0% SDS, and 5.0% mercaptoethanol for 1 h at 37°C. Tube gels were placed horizontally on top of a standard 10-20% acrylamide slab gel for analysis in the second-dimension and held down with 1% agarose. Second-dimension electrophoresis was carried out at 30 mA, 200 v, for 7 hrs. Gels were transferred to nitrocellulose for immunoblotting or processed for autaradiography.

I. N-Glycanase Digestion.

Nonreduced [^{35}S]-labelled gp55 was isolated from dried acrylamide gels exactly as described for the V8 digestion. The glycoprotein was eluted in 100 ul 0.55 M $NaPO_4$, pH 7.5, 0.5% SDS overnight at room temperature. Samples were boiled for 3 mins prior to digestion. Eluted gp55 was divided into three equal aliquotes and the NP-40 concentration was adjusted to 1.25% from a 7.5% stock. N-glycanase (Genezyme) at 250 units/ml was added to a final concentration of 0, 0.25, and 2.5 units. Digestion was performed overnight at 37°C. The reaction was stopped by adding an equal volume of Laemmli sample buffer and boiling for 5 mins. Samples were re-electrophoresed in the presence or absence of mercaptoethanol and gels were processed for autoradiography.

J. V8 Protease Digestion.

F745 cells were labelled with [^{35}S]-methionine and [^{35}S]-cysteine, immunoprecipitated, and electrophoresed. The gel was dried down without prior fixation in 12.5% TCA. Areas of the dried acrylamide gel corresponding to the gp55 components were cut out and eluted overnight at room temperature in ~100 ul 0.125 M Tris-HCl, pH 7.5, 0.5% SDS. Eluted samples were dived into four equal aliquotes and S. aureus V8 protease (1 mg/ml elution buffer) was added to a final concentration of 0, 0.1, 1.0, and 10 ug. Samples were incubated for 30

mins at 37^{o}C. The reaction was stopped by adding an equal volume of Laemmli sample buffer and boiling for 5 mins. Samples were re-electrophoresed and processed for autoradiography.

K. Free Sulfhydryl Analysis.

Approximately 1x10^{6} F745 cells were lysed in 100 ul IPB, pH 7.5, with and without 20 mM iodoacetamide. The cell lysate was reacted with IPB equilibrated organomercurial agarose (Affi-gel 501, Biorad) for 30 mins at 4 ^{o}C. The organomercurial agarose was pelleted and the supernatant was saved for analysis. The resin was washed 3x with IPB and the absorbed proteins were eluted with 2x 100 ul IPB + 5% mercaptoethanol washes. Equivalent amounts of control lysate, unabsorbed lysate, and eluted washes were mixed with Laemmli sample buffer, electrophoresed, and analyzed by immunoblotting.

L. Sucrose Velocity Gradient Sedimentation.

Sucrose gradient analysis was carried out as previously described by Copeland et al. (95). Approximately 2.5x10^{6} F745 PC4 cells were lysed in 500 ul 50 mM Tris-HCl, pH 7.5, 150 mM NaCl, and 1% Triton X-100. The lysate was layered onto a 5-30% continuous sucrose gradient that overlaid a .5 ml 60% sucrose cushion. The sucrose was dissolved in the above lysis solution. Centrifugation was carried out at 45,000 rpm in a SW55Ti rotor for 15 hrs at 4^{o}C. The gradient was fractionated into fifteen 400 ul samples. An equal volume of 2x IPB was added to each sample and immunoprecipitation with F-MuLV gp70 serum was carried out. Viral proteins were visualized by immunoblotting.

M. Northern Blot Analysis.

Total cellular RNA was extracted by the guanidine thiocynate-CsCl method (96). Poly A+ RNA was isolated by the oligo dt procedure and quantified by measuring the $O.D._{260}$ (97). Glyoxal denatured Poly A+ RNA was analyzed by electrophoresis through 1.2% agarose gels followed by Northern blot transfer to nitrocellulose (98). Blots were probed with nick translated plasmids to specific radioactiviteis of ~$1x10^8$ cpm/ug DNA (97). Filters were prehybrized at 42°C for 4 h in a solution consisting of 50% formamide, 5X SSPE, 5X Denhardt's, 0.1% SDS, and 200ug/ml salmon sperm DNA. Hybridization was carried out for 20 h at 42°C with ~10^6 cpm nick-translated probe per ml hybridization buffer (same as prehybridization buffer except with 1X Denhardt's and 100 ug/ml salmon sperm DNA). Blots were washed twice in 1X SSC, 0.1% SDS at room temperature for 5 mins and then washed twice in 0.1X SSC, 0.1% SDS at 42°C for 1 h. The blots were then exposed to X-ray film with an intensifying screen at -70°C.

N. Southern Blot Analysis.

High molecular weight DNA was isolated from cells by detergent lysis and phenol:chloroform extractions (97). Tissue samples were first frozen at -70°C and pulverized to a fine powder before extraction. DNA was incubated with various restriction endonucleases according to manufacturer specifications, electrophoresed overnight through a 0.8% agarose gel (15ug DNA per lane), denatured, neutralized, and transferred to nitrocellulose (99). Blots were hybridized to ^{32}P-labeled probes under the exact conditions used for Northern blots. After hybridization, blots were washed twice in 1X SSC, 0.1% SDS at room temperature for 5 mins and then washed twice in 0.1X SSC, 0.1% SDS at 62°C for 1 h.

O. DMSO Induced Differentiation.

The cell line F745 PC4 D2 was originally obtained from Dr. David Housman of MIT (100). Erythroid differentiation was induced by the addition of dimethyl sulfoxide (DMSO, J.T. Baker Chem. Co.) to a final concentration of 1.8% as previously described (91).

P. Analysis of DMSO Induced gp55 Shedding.

F745 PC4 D2 cells were resuspended in fresh medium at a density of $2.5x10^5$ cells/ml. DMSO was added to a final concentration of 1.8%. At the indicated times, 2 mls of medium was removed from the culture, immunoprecipitated with antiserum to F-MuLV gp70, and analyzed by Western Immunoblot. A control culture without DMSO was analyzed in parallel. Blots were quantified by densitometry.

Q. Preparation of Helper-free SFFV-related Virus.

The plasmid pSVSF was derived from the Lilly-Steeves polycythemia strain of SFFV that was molecularly cloned in a circular permuted form by Linemeyer et al (77). To prepare the plasmid pSVSF (Fig. 1), the 215-base pair Hind III fragment of SV40 DNA (101) was inserted into the unique Hind III (77) site of a colinear SFFV plasmid (82) prepared from the clone of Linemeyer et al (77). Helper-free SVSF virus was harvested from a cell line derived from a population of psi-2 (102) cells that had been co-transfected with pSVSF and pSV2neo (103). Stable transformants were isolated by selection in G418 (Gibco), and individual clones were checked for expression of the SFFV-specific envelope glycoprotein, gp55, by immunoblotting. One cell line, designated psi-2/SVSF 4-4, was used as the source of virus for these experiments.

R. Analysis of Pathogenic Activity

Friend virus causes a complex disease of which the most prominent lesion is the enlarged spleen (1, 10). For analysis of the *in vivo* effects of helper-free virus, undiluted culture medium (0.75 ml) from psi-2/SVSF 4-4 cells was injected via tail vein into 4-6 week old female NIH Swiss mice on two successive days after pre-treatment of the nice with subcutaneous injections of phenylhydrazine at -18, -42, and -66 h. For analysis of *in vivo* activity of SVSF virus in the presence of helper virus, culture medium from psi-2/SVSF 4-4 cells (0.4 ml) was mixed with 0.1 ml of medium from R-NIH cells, which produce Rauscher murine leukemia helper virus (R-MuLV). Alternatively NIH cells were infected with 1 ml of R-NIH medium. The infected cells were passaged for several weeks and medium (0.5 ml) from confluent cultures were used to infect mice. There was no pretreatment before the single 0.5 ml tail vein injection when helper virus was present.

S. Assay for Malignancy

Spleen tissue form advanced stages of Friend disease can cause tumors on the omenta of isogenic recipient mice (64). Recipients were 4- to 6-week old female NIH/Swiss mice, sublethally irradiated with a single dose of 500 R from a ^{137}Cs source. Transplanted tissue was injected interperitoneally within 24 h of irradiation. Omenta were removed three weeks of injection and examined for tumors.

III. Identification and Characterization of Novel Disulfide-linked SFFV Envelope Glycoprotein Oligomers.

A. Abstract

The spleen focus-forming virus (SFFV) envelope glycoprotein (gp55) is inefficiently processed to the cell surface. The majority remains in the rough endoplasmic reticulum and only a small percentage (~5%) is processed through the Golgi apparatus to the plasma membrane. The expression of gp55 at the plasma membranes has been shown to be essential for the stimulation of erythroblastosis. We have demonstrated that the SFFV envelope glycoproteins can be found as several distinct complexes associated with the cells. These include an intracellular monomer, an intracellular disulfide-linked dimer, and a cell surface disulfide-linked dimer. The cell surface dimer is eventually shed into the extracellular medium where it can be found in both the dimeric and monomeric forms. This shedding appears to be associated with the removal of ~2,500-daltons from each subunit and may be caused by the proteolytic removal of gp55's putative membrane anchor. Moreover, two-dimensional gel electrophoresis suggests that disulfide bond mediated heterogenity exists within both the intracellular monomers and dimers. The intracellular dimers can be separated into a cluster of distinct components while only a single dimer can be found at the cell surface. This suggests that only a unique homodimer is competent for cell surface expression and that this minor component is responsible for the pathogenesis caused by SFFV.

B. General Introduction

Previous work has demonstrated the necessity for cell surface expression of SFFV gp55 in the development of erythroleukemia. Nonpathogenic *env* mutants, whether spontaneous or site-directed, lack the cell surface form of gp55 (79, 83). Moreover, pathogenic revertant viruses contain second site *env* mutations that restore synthesis of the plasma membrane form of the glycoprotein (82). From this and other evidence, our laboratory has proposed a model of gp55 action in which the cell surface form binds to a critical membrane receptor to stimulate erythroblast mitosis (83).

The SFFV envelope glycoprotein is synthesized on endoplasmic reticulum bound ribosomes as a 55,000-dalton glycoprotein (45, 48-50). Initial characterization of this glycoprotein demonstrated that the vast majority remains within the endoplasmic reticulum and that only a small percentage (2-5%) reaches the cell surface (90, 104). In denaturing and reducing gel electrophoresis conditions it was shown that the cell surface glycoprotein has an apparent MW of 65,000-daltons (49, 90, 104). The increased size is caused at least partly by processing of its Asn-linked oligosaccharides in the Golgi apparatus during transport to the plasma membranes (90). The cell surface glycoprotein is then shed into the extracellular medium (52).

We have recently made the observation that in denaturing and nonreducing gel electrophoresis conditions several high molecular weight disulfide-linked envelope components appear. More significantly, the 65,000-dalton cell surface form of gp55 is not observed when the envelope glycoproteins are analyzed in the absence of reducing agent. In this chapter I describe the characterization of

C. Results

1. One dimensional gel electrophoresis analysis

One dimensional gel electrophoresis analysis of Friend erythroleukemia cell lines and SFFV infected NRK fibroblasts in the presence and absence of reducing agent is shown in Fig. 5. Cell lysates were analyzed by the Western blot technique using either a polyclonal F-MuLV anti-gp70 serum or a monoclonal antibody against gp55 (93). In denaturing and reducing conditions, envelope glycoproteins specific to both the MuLV and SFFV can be detected in two independently derived erythroleukemia cell lines using the polyclonal anti-gp70 serum (lanes 1 and 2). The F-MuLV envelope glycoproteins include the glycosylated precursor gPr90 and the processed derivative gp70. In comparison, the SFFV envelope glycoproteins are detected primarily as the intracellular gp55, and to a lesser extent, as the processed M_r 65,000-dalton cell surface form called $gp55^p$. In nonreducing conditions (lanes 3 and 4), the primary gp55 band has a slightly faster electrophoretic mobility than the reduced gp55 band. This is consistent with intrachain disulfide bonding within these molecules. Moreover, bands corresponding to $gp55^p$ are no longer detectable. Instead, two new bands are detected with apparent MW of 105,000- and 120,000-daltons. Several very high molecular weight bands (in excess of 200,000-daltons) can also be seen near the top of the gel.

Immunoblotting using the monoclonal antibody against gp55 detects the same SFFV envelope proteins under reducing conditions (lanes 5 and 6) as seen with polyclonal anti-gp70 serum (lanes 1 and 2). This monoclonal antibody also crossreacts with MCF-related envelope proteins and detects a band at ~70,000-

Figure 5. Immunoblot analysis of reduced and nonreduced Friend viral envelope glycoproteins. (A) Erythroleukemia cells ($1x10^6$ cells) were lysed in immunoprecipitation buffer (100 ul) and an equivalent amount of protein was electrophoresed, transferred to nitrocellulose, and immunoblotted with either F-MuLV anti-gp70 serum (lanes 1-4) or gp55 monoclonal 7C10 (lanes 5-8). Both F745 (lanes 1, 3, 5 and 7) and F4-6 (lanes 2, 4, 6 and 8) erythroleukemia cell lines were analyzed in the presence (lanes 1, 2, 5 and 6) or absence (lanes 3, 4, 7 and 8) of reducing agent. In addition to the viral envelope glycoproteins, the position of the novel 105 kd and 120 kd nonreduced bands are indicated to the left of the figure. (B). Uninfected NRK cells ($1x10^7$ cells) (lanes 1, 2, 5 and 6) and SFFV infected NRK CL 1 ($1x10^7$ cells) (lanes 3, 4, 7 and 8) were immunoprecipitated with normal goat serum (lanes 1, 3, 5, and 7) followed by anti-gp70 serum (lanes 2, 4, 6, and 8). Immunoprecipitates were electrophoresed in the presence (lanes 1-4) or absence (lanes 5-8) reducing agent. Glycoproteins were transferred to nitrocellulose and immunoblotted with anti-gp70 serum.

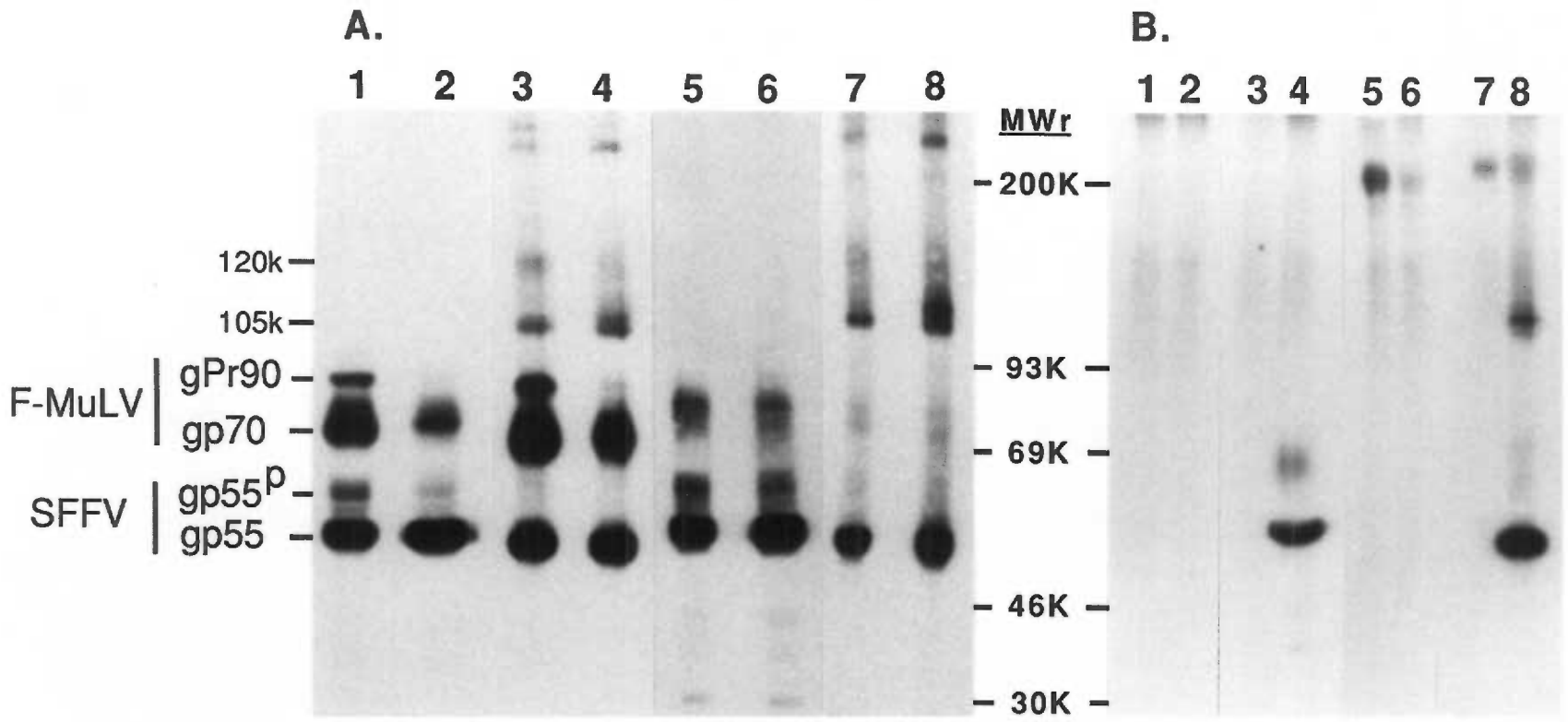
A.
1 2 3 4 5 6 7 8
120k
105k
F-MuLV
gPr90
gp70
SFFV
gp55^p
gp55
MWr
200K
93K
69K
46K
30K
B.
1 2 3 4 5 6 7 8

daltons. In nonreducing conditions (lanes 7 and 8), the monoclonal antibody detects several high molecular weight bands with the same apparent mobilities as detected by the polyclonal anti-gp70 antiserum (lanes 3 and 4).

Analysis of SFFV infected NRK (normal rat kidney) fibroblasts show a similar appearance of high molecular weight bands in nonreducing conditions (Fig. 5B). This cell line is only infected with SFFV and no helper virus proteins are detected. In reducing conditions, only the intracellular gp55 and $gp55^{p}$ forms are seen after immunoprecipitation and immunoblot analysis (Fig. 5B, lane 4). Analysis of these glycoproteins in the absence of reducing agent (lane 8) results in a faster migrating gp55 and the appearance of high molecular weight bands similar to the erythroleukemia cells (Fig. 5A). The lack of any corresponding bands in the normal goat serum precipitation (lanes 1, 3, 5, and 7) or in uninfected NRK cells (lanes 2 and 6) confirms the SFFV specificity of these components.

One dimensional gel analysis of immunoprecipitated [^{35}S]-labelled erythroleukemia cell lysates reveals a similar pattern (Fig. 6) to that obtained by the immunoblotting procedure. Analysis of the envelope components found in the medium 8 h after [^{35}S]-labelling is shown in lanes 5-8. Previous reports have shown that both gp70 and gp55 are shed from the cells into the medium (36, 52). Immunoprecipitation of the medium (lane 6) supports this conclusion. Hereafter, we will refer to the shed gp55 component as $gp55^{s}$ to distinguish it from the intracellular gp55 and the cell surface $gp55^{p}$. The $gp55^{s}$ component is smaller in apparent M_r by ~2.5 kd than the cell associated $gp55^{p}$ (lane 2 vs. 6) when these components are analyzed with reduction. Under nonreducing conditions, an additional band appears in the medium (lane 8) that is slightly smaller than the

Figure 6. Electrophoretic analysis of reduced and nonreduced [^{35}S]-labelled Friend viral glycoproteins. F745 (1x10^{6} cells) were labelled with [^{35}S]-methionine and [^{35}S]-cysteine (50uCi/ml) for 2 h in met- and cys-free EMEM. Cells (lanes 1-4) were lysed in immunoprecipitation buffer and immunoprecipitated with normal goat serum (lanes 1 and 3) followed by F-MuLV anti-gp70 (lanes 2 and 4). Immunoprecipitates were analyzed with (lanes 1 and 2) and without (lanes 3 and 4) reduction. An equivalent amount of [^{35}S]-labelled cells were cultured for 8 h in complete medium (lanes 5-8). Medium samples were precipitated with normal goat serum (lanes 5 and 7) followed by anti-gp70 serum (lanes 6 and 8). Immunoprecipitates were analyzed with (lanes 5 and 6) and without (lanes 7 and 8) reduction. In addition to the viral glycoproteins, the 105 kd and 120 kd bands are marked to the left of the gel.

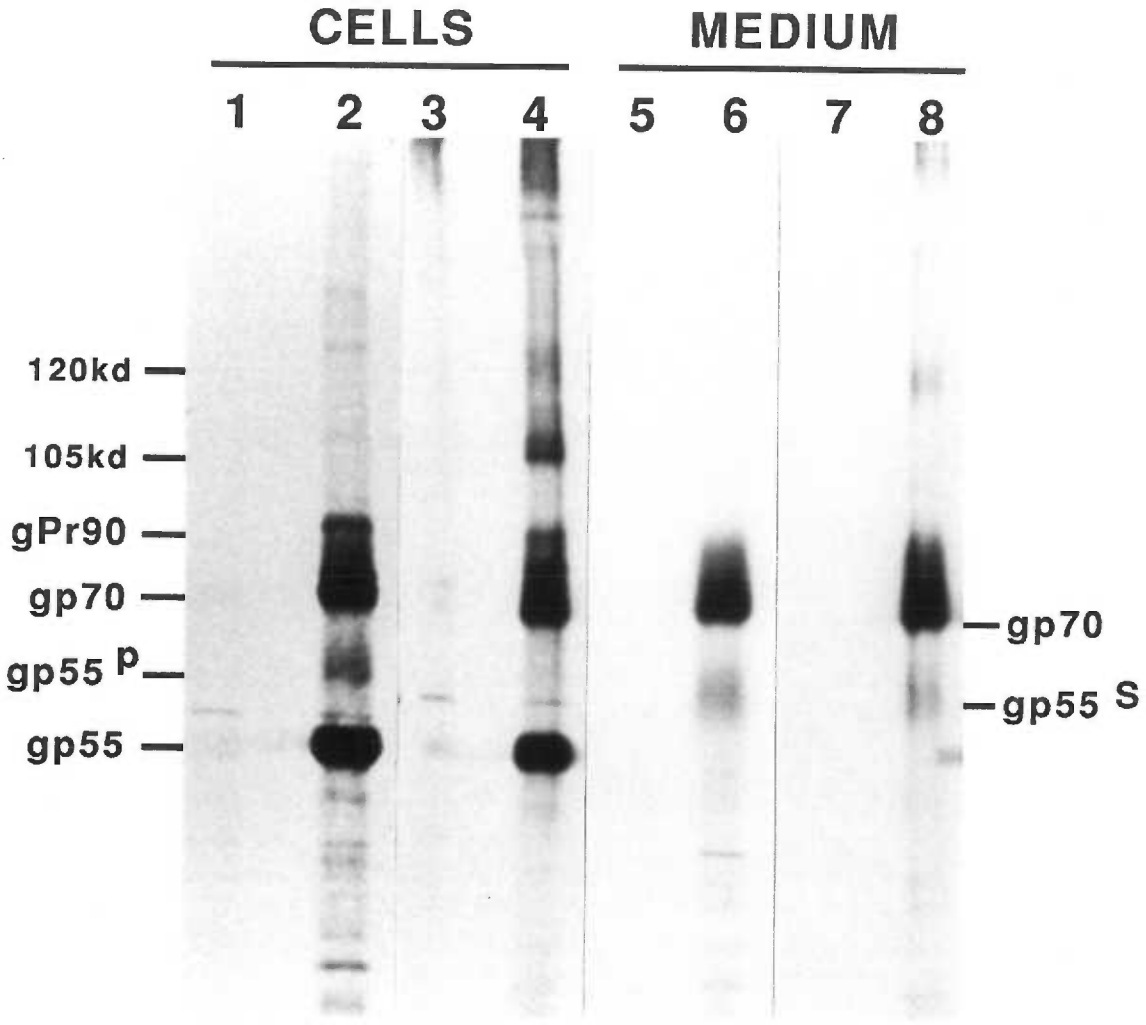
CELLS
MEDIUM
1
2
3
4
5
6
7
8
120kd
105kd
gPr90
gp70
gp55 P
gp55
gp70
gp55 S

120,000-dalton cell associated band (lane 4) .

2. Two-dimensional gel analysis

To identify the viral envelope proteins in each higher molecular weight nonreduced component, immunoprecipitates were analyzed by two-dimensional SDS-PAGE using nonreducing conditions in the first-dimension and either reducing or nonreducing conditions in the second-dimension. This technique has been successfully utilized by Brenner et al. (94) to analyze cross-linked proteins in the human T cell receptor complex.

Two-dimensional electrophoretic analysis of F745 erythroleukemia cell lysates is shown in Fig. 7. Unlabelled lysates were first precipitated with anti-gp70 serum, then separated by electrophoresis in nonreducing conditions in the first-dimension, and in nonreducing (Fig. 7A) or reducing (Fig. 7B) conditions in the second-dimension. Viral envelope protein samples were then transferred to nitrocellulose and detected by immunoblotting. As seen in Fig. 7A, second-dimension electrophoresis in nonreducing conditions results in a vertical line of viral proteins within the slab gel. This is the expected pattern if the disulfide bonds are not broken prior to second dimension analysis. In contrast, Fig. 7B reveals the mobilities of these viral proteins when reducing conditions were used in the second-dimension.

The F745 erythroleukemia cells express both F-MuLV and SFFV envelope glycoproteins. The prominent F-MuLV gp70 and gPr90 components are separated with their expected mobilities in this two-dimensional analysis (Figs. 7A and 7B) and are not present in any oligomerized forms. This is in agreement with previously published reports (31, 32, 105). Therefore, our discussion will

Figure 7. Two-dimensional gel electrophoresis of Friend viral envelope glycoproteins. Exact conditions for this procedure are described in Materials and Methods. F745 erythroleukemia cells were immunoprecipitated with anti-gp70 serum, electrophoresed in the first dimension under nonreducing conditions, and electrophoresis in the second dimension without (panel A) and with (panel B) reduction. On the top of each gel is a representative nonreduced separation in the first dimension. Both the gp70 and gp55 mobilities are marked in this dimension (panel A and B) in addition to the 105 kd and 120 kd bands (panel B). The positions of the viral proteins in the second dimension (panel B) were determined by running a reduced F745 lysate on the side of the 10-20% acrylamide slab gel.

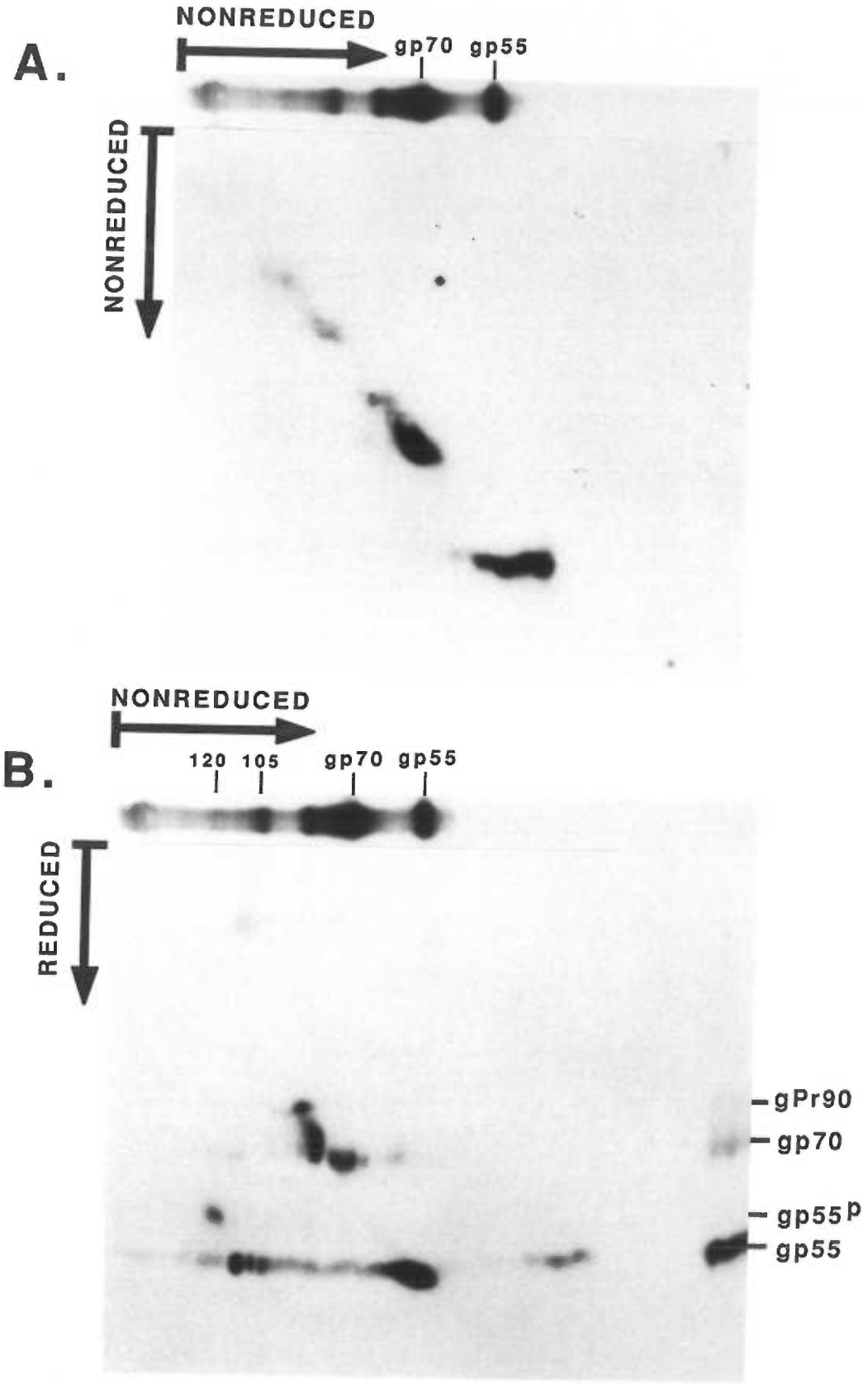
A.
NONREDUCED
gp70
gp55
NONREDUCED
B.
NONREDUCED
120
105
gp70
gp55
REDUCED
gPr90
gp70
gp55p
gp55

focus primarily on the SFFV envelope glycoproteins.

The primary intracellular SFFV gp55 band is resolved as a very broad component with second-dimension reduction (Fig. 7B). This would imply that disulfide bond mediated heterogenity may have existed in the nonreduced gp55. In addition, it can be seen that the105,000-dalton band is resolved into a cluster of distinct components that migrate in parallel with the major gp55 band in the reduced dimension. In contrast, the 120,000-dalton band migrates in the reduced dimension as a single component with the mobility of $gp55^{p}$. The mobilities of these components in the second dimension were confirmed by running a reduced cell lysate on the side of the slab gel (bands on the extreme right of the gel). These results suggested that gp55 can form a variety of disulfide-bonded components. The components at M_r 55,000 and M_r 105,000 appear to be heterogeneously disulfide bonded, whereas the $gp55^{p}$ 120,000-dalton component is homogeneous in its electrophoretic separation.

The existence of gp55 in disulfide-linked complexes could represent oligomerization of the envelope glycoproteins or disulfide bonding to other proteins. To address this issue, the same two-dimensional gel procedure was repeated using [^{35}S]-methionine and [^{35}S]-cysteine labelled immunoprecipitates (Fig.8). If the gp55 proteins were disulfide-linked to a cellular protein, second-dimension analysis in reducing conditions would cleave these bonds and allow the labelled proteins to migrate with their individual mobilities. If the cellular protein has a different molecular weight than gp55, this would be observed electrophoretically as two distinct components migrating in a vertical line as the proteins separated. Analysis of [S^{35}]-labelled cell lysates (Fig. 8A) generates the

Figure 8. Two-dimensional gel electrophoresis of [^{35}S]-labelled Friend viral glycoproteins. F745 cells were labelled with [^{35}S]-methionine and [^{35}S]-cysteine (50uCi/ml) for 2 h in met- and cys-free EMEM. Half of the labelled cells ($2.5x10^6$ cells) were lysed and half were incubated in complete medium for 18 h. Both the cell lysate and medium were immunoprecipitated with anti-gp70 serum and analyzed by two-dimensional electrophoresis. Two-dimensional separation of [^{35}S]-labelled viral glycoproteins associated with the cells is shown in panel (A) and the medium in panel (B). A representative nonreduced one dimensional separation is shown at the top of each gel. A standard 10-20% SDS-PAGE seperation of reduced [^{35}S]-labelled viral glycoproteins is shown at the right.

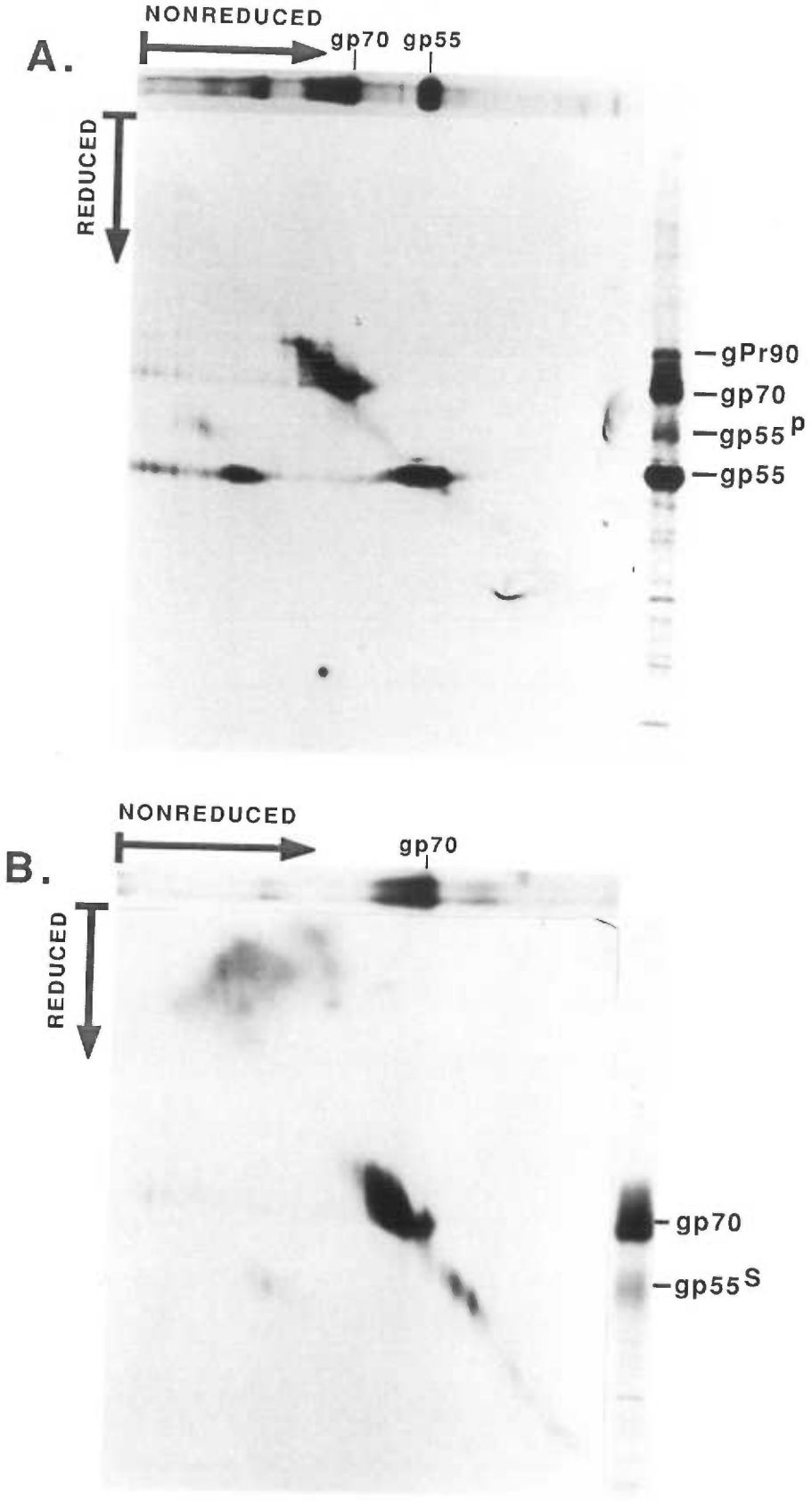
A.
NONREDUCED
gp70 gp55
REDUCED
gPr90
gp70
gp55 p
gp55
B.
NONREDUCED
gp70
REDUCED
gp70
gp55 S

same pattern that was seen by immunoblotting (Fig. 7B). This suggests that the disulfide-linked complexes contain only gp55 specific glycoproteins. Therefore, gp55 exists in cell lysates as an intracellular monomer, as an 105,000-dalton intracellular gp55 oligomer, and as an 120,000-dalton cell surface $gp55^p$ oligomer. Because the intracellular oligomer appears to contain only gp55 glycoproteins and has an apparent M_r approximately twice that of the intracellular monomer, we infer that it is a dimer. Similarly, the cell surface oligomer has an apparent M_r twice that of the $gp55^p$, and we propose that it is a dimer.

A similar analysis was performed on the shed viral components that occur in the medium (Fig. 8B). The high molecular weight component migrates after reduction with a mobility similar to shed monomeric $gp55^s$. This suggests that $gp55^s$ is present in the extracellular medium as both a dimer and monomer.

3. ^{125}I-Labelling of membrane glycoproteins

Cell surface iodination provides a sensitive and selective procedure to label and analyze plasma membrane proteins. Previous analysis has already demonstrated that the $gp55^p$ is exposed to the outside of the cell and could be iodinated (49) whereas gp55 is exclusively intracellular. We have used this technique to confirm the previously described results and to further study the critical $gp55^p$ component. After labelling the cell surface proteins, a cell lysate was analyzed by the two-dimensional electrophoresis method (Fig. 9). As expected, the most prominently labelled viral surface glycoprotein is gp70. However, in addition to gp70, a band with an apparent MW of 95,000-daltons is labelled (Fig. 9A, top of slab gel). With second-dimension analysis, this band

Figure 9. Two-dimensional gel electrophoresis of ^{125}I-labelled Friend viral envelope glycoproteins. Lactoperoxidase catalyzed cell surface iodination of F745 erythroleukemia cells was performed on $1x10^7$ cells as described in Materials and Methods. Half of the cells were lysed and half were cultured in DMEM for 18 h. Both the cells and medium were immunoprecipitated with anti-gp70 serum and analyzed by two-dimensional electrophoresis. Two-dimensional seperation of [^{125}I]-labelled viral glycoproteins found on the cell surface (panel A) or in the medium (panel B). A representative one dimensional seperation of nonreduced [^{125}I]-labelled viral glycoproteins is shown at the top of each gel with 95 kd and 120 kd bands marked in panel A. A standard 10-20% SDS-PAGE seperation of reduced [^{125}I]-labelled viral glycoproteins is shown at the right.

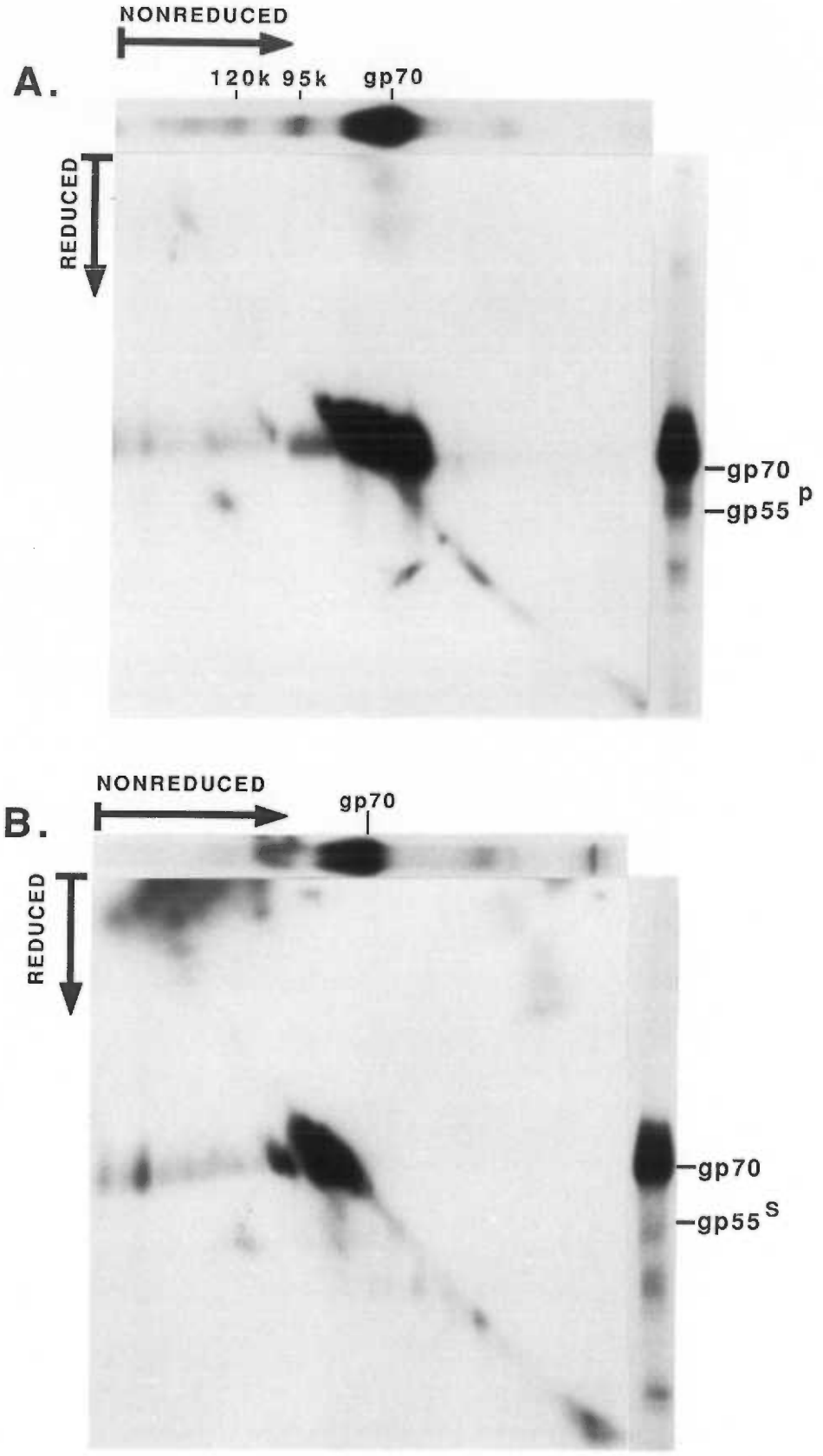
A.
NONREDUCED
120k
95k
gp70
REDUCED
gp70
gp55 p
B.
NONREDUCED
gp70
REDUCED
gp70
gp55 s

migrates in parallel with gp70 (Fig. 9A). We conclude that this band represents the disulfide-linked gp70-p15E MuLV component. Consistent with this identification, this component is also found in the extracellular medium (Fig. 9B) as would be expected because it is eventually incorporated into budding virions (34, 35, 106).

The labelled 120,000-dalton cell surface $gp55^{p}$ oligomer migrated as expected for a disulfide-linked dimer with second-dimension reduction (Fig. 9A). Consistent with previous results, only a single cell surface dimer can be electrophoretically resolved. After labelling, a portion of the cells were incubated in fresh medium for 18 h. During this culturing period the cells appeared to remain fully viable. The medium was recovered and analyzed for ^{125}I-labelled viral proteins by immunoprecipitation. As shown in Fig. 9B, a substantial amount of labelled viral proteins were shed into the medium. In agreement with the previous [^{35}S]-labelling analysis, the $gp55^{s}$ component is found in the medium in both the dimer and monomer form.

4. Lack of dimers in MuLV gp70s

Dimerization of gp55 was an unexpected modification of this glycoprotein because no previous work has reported oligomerization of MuLV envelope glycoproteins. However, sequence analysis has shown that gp55 is a unique fusion glycoprotein containing both MCF-like sequences and ecotropic MuLV envelope sequences that form independently folded domains. Which domain confers the ability of gp55 to dimerize represents an important structural aspect of the SFFV envelope glycoprotein.

Analysis of erythroleukemia cell lines that express MuLV envelope

glycoproteins have already shown that the ecotropic gp70 is not dimerized (for example, Figs. 5 and 6). This implied that the ecotropic sequences of gp55 may not be capable of forming interchain disulfide bonds and suggested that the MCF-related domain may mediate dimerization. To test this hypothesis, we analyzed the ability of wild-type MCF gp70 to form dimers under nonreducing conditions (Fig. 10). In MuLV-infected fibroblasts (Fig. 10A), precipitation with MuLV gp70 specific serum confirms that only bands corresponding to gPr90 and gp70 appear under both nonreducing (lane 2) and reducing (lane 4) conditions. Likewise, two MCF-infected fibroblast lines (Fig. 10B) express only the precursor and processed forms of the envelope glycoproteins in the absence (lanes 2 and 4) and presence (lanes 6 and 8) of reducing agent. The high molecular weight bands observed in nonreducing conditions (Fig. 10B, lanes 1-4) are in excess of 200,000-daltons and are present in both the normal goat serum (lanes 1 and 3) and MCF anti-gp70 precipitations (lanes 2 and 4). Similar bands were also observed in the analysis of both uninfected and infected NRK cell lines analyzed in nonreducing conditions (Fig. 5B, lanes 5-8). Therefore, we conclude that these bands do not represent viral glycoproteins. This demonstrates that dimerization of the dualtropic MCF and ecotropic MuLV gp70s is not a normal post-translational modification for these glycoproteins. Thus, the unique structure of the gp55 fusion glycoprotein allows it to be modified in a manner not common to the related MuLV gp70s.

Figure 10. Reduced and nonreduced analysis of MuLV and MCF envelope glycoproteins. Virus infected fibroblasts were grown to 2/3 confluency on 100 mm dishes (~10^7 cells) and lysed in immunoprecipitation buffer for immunoprecipitation analysis. (A) MuLV infected NIH 3T3 cells were immunoprecipitated with normal goat serum (lane 1 and 3) followed by F-MuLV anti-gp70 serum (lanes 2 and 4). Immunoprecipitates were electrophoresed with (lanes 1 and 2) and without (lane 3 and 4) reduction. (B) MCF infected NIH 3T3 cells were immunoprecipitated with normal goat serum (lanes 1, 3, 5, and 7) followed by MCF anti-gp70 serum (XBV2) (lanes 2, 4, 6, and 8). Immunoprecipites were electrophoresed with (lanes 1-4) and without (lanes 5-8) reduction. Following electrophoresis, proteins were immunoblotted with F-MuLV anti-gp70 serum (panel A) or with MCF anti-gp70 serum (panel B).

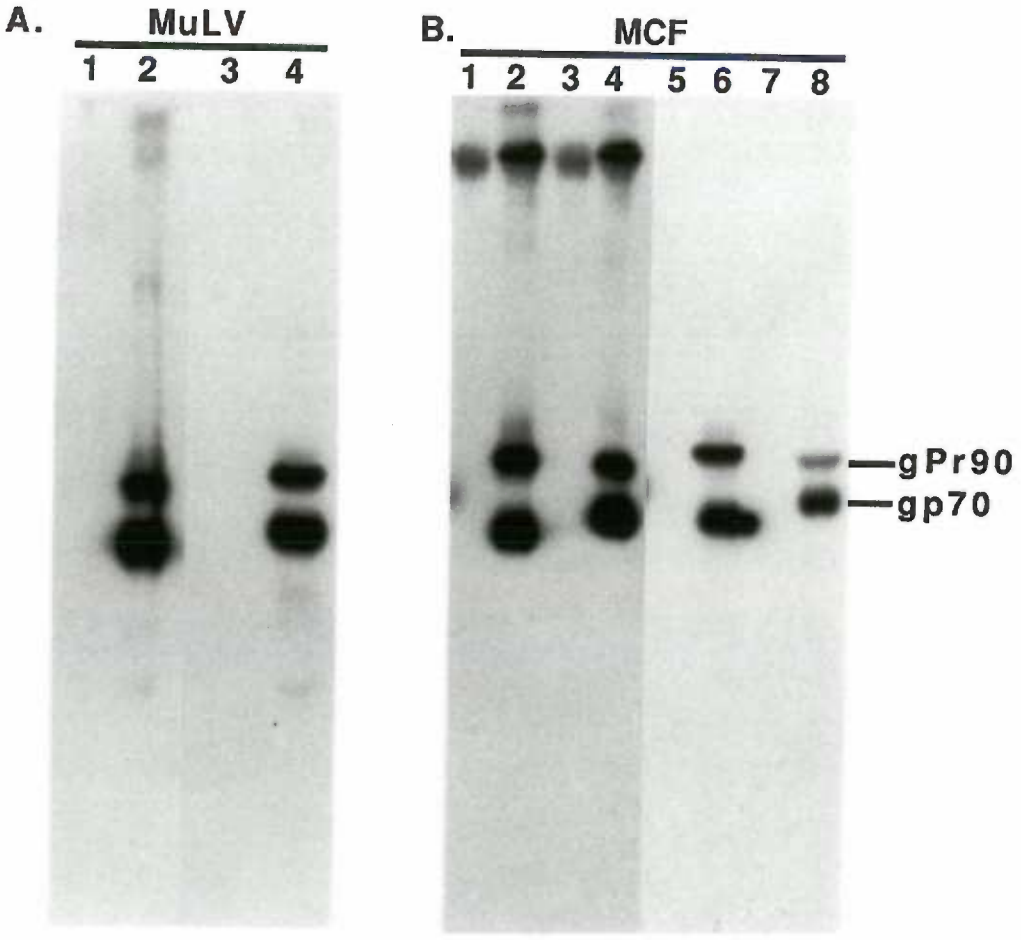
A.
MuLV
1 2 3 4
B.
MCF
1 2 3 4 5 6 7 8
gPr90
gp70

D. Discussion

The Friend virus envelope glycoproteins are found as several distinct complexes associated with both the cells and medium (summarized, Fig. 11). In denaturing and nonreducing gels the SFFV envelope glycoprotein electrophorese as an intracellular monomer, an intracellular dimer, and a cell surface dimer. These different components will be referred to as gp55, $(gp55)_2$, and $(gp55^p)_2$, respectively. The cell surface form is eventually shed into the medium where it can be detected both in the dimer and monomer configuration. To be consistent with the cell associated gp55 designations, the shed monomeric form will be referred to as $gp55^s$ and the dimeric form as $(gp55^s)_2$. Because the $gp55^p$ component is only observed as dimer, we infer that the cell surface dimers are shed into the culture medium and are reduced to the monomer form. In addition, these results demonstrate that the reduced $gp55^s$ is approximately 2.5 kd smaller than the reduced $gp55^p$ (Figs. 6 and 11). This may be caused by the proteolytic cleavage of the hydrophobic carboxy-terminus believed to anchor $gp55^p$ into the membrane (88). Removal of this anchor would presumably cause shedding of $gp55^p$ from the cell surface.

Analysis of F-MuLV and MCF envelope glycoproteins in nonreducing conditions demonstrate that they are not dimerized (Fig. 10). Instead, the glycosylated precursor gPr90 is proteolytically processed to form gp70-p15E complexes that are transported to the cell surface. In agreement with previous reports, the gp70 attachment to the p15E membrane anchor may be by both covalent and noncovalent bonding (34-36). Thus, neither ecotropic nor MCF-type envelope glycoproteins form disulfide-linked dimers during post-translational

Figure 11. Summary of the nonreduced and reduced Friend viral envelope glycoproteins associated with the cells and medium. (Top) Comparison of nonreduced cellular and extracellular viral glycoproteins. As indicated in the text, $(gp55)_2$ designates the intracellular dimer, $(gp55^{p})_2$ designates the cell surface dimer, and $(gp55^{s})_2$ designates the dimeric shed component. (Bottom) Comparison of reduced cellular and extracellular viral glycoproteins.

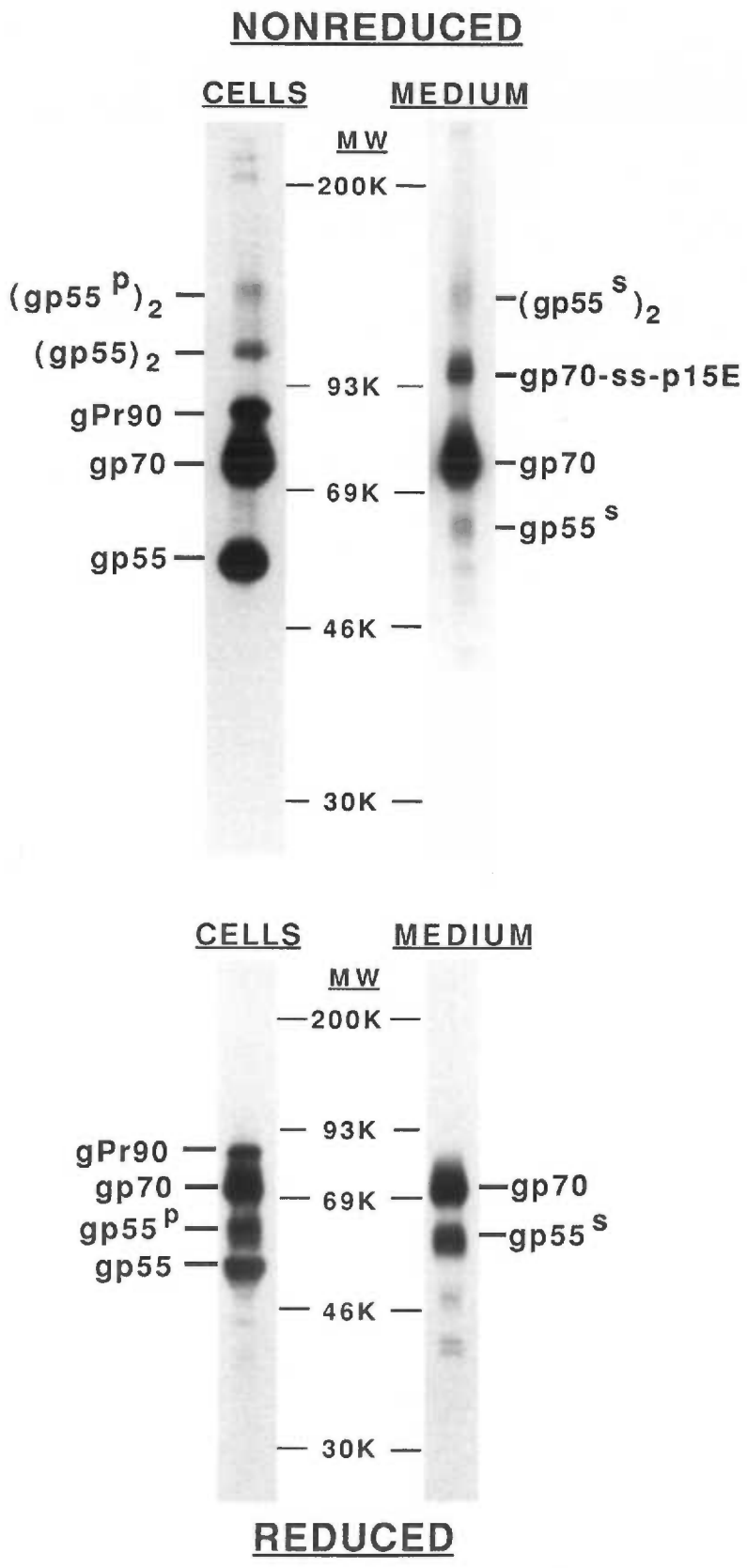
NONREDUCED
CELLS
MEDIUM
MW
200K
93K
69K
46K
30K
(gp55 p)2
(gp55)2
gPr90
gp70
gp55
(gp55 s)2
gp70-ss-p15E
gp70
gp55 s
CELLS
MEDIUM
MW
200K
93K
69K
46K
30K
gPr90
gp70
gp55 p
gp55
gp70
gp55 s
REDUCED

processing to the cell surface. In contrast, the recombinant gp55 is only processed to the cell surface as dimer. Therefore, the capacity to dimerize is not encoded in the parental-type *env* genes.

Both the SFFV and MCF viruses are capable of inducing a similar, yet distinct, erythroproliferative disease (107). For all isolates of $SFFV_P$, the amino acid homology between the amino-terminal region of gp55 and the same region of Moloney MCF (108), AKR MCF 247 (109), or Friend MCF (110) gp70s is between 90-95%. This includes a 67 amino acid region that is identical for all of these SFFV and MCF viral env genes. Moreover, recent mutagenesis studies from this laboratory (83) have shown that lesions in the dual tropic domain will eliminate SFFV's pathogenicity. This strongly suggests that both the MCF and SFFV envelope glycoproteins contain a conserved structure and/or active site necessary for disease induction. Thus, despite the processing differences between MCF and SFFV, this active site may be maintained after SFFV envelope biosynthesis and post-translational processing.

An important implication of this analysis is that specific post-translational processing appears to be necessary to generate the cell surface gp55 molecule. The prominent form of gp55 is the intracellular monomer, although two-dimensional electrophoresis would suggest that intrachain disulfide bond heterogenity exists within this population of molecules (Figs. 7 and 8). In addition, several distinct intracellular dimers can be electrophoretically resolved (Fig. 7), while only a single dimer component is found at the cell surface. We hypothesize that the inefficient intracellular transport of gp55 is caused by disulfide bond mediated structural heterogenity. The majority of gp55 remains trapped in the RER because of improper folding and lack of dimerization. Only a unique

homodimer is competent for cell surface expression and this minor component is responsible for the pathogenesis caused by SFFV. Therefore, it is of major importance to understand both the structural features and post-translational processing of gp55 that enable it to become exported to the cell surfaces.

IV. Additional Biochemical Studies of the Leukemogenic gp55 Glycoprotein Components.

A. Abstract

Post-translational modifications of gp55 generate structurally distinct components of this glycoprotein. Processing through the Golgi apparatus results in the acquisition of complex N-linked oligosaccharides that, in part, contribute to the significant size difference (~10,000-daltons) between the reduced intracellular and cell surface gp55 molecules. In addition, shedding of the cell surface dimer is associated with a 2,500-dalton reduction in size of each subunit. Proteolytic fragmentation analysis demonstrates that the amino-terminal portion of gp55, $gp55^{p}$, and $gp55^{s}$ are all similar in electrophoretic mobility. Therefore, these results suggest that the modifications that produce the size differences between the three components are localized to the carboxyl-terminal ends. Analysis of intracellular gp55 confirmed the existence of intrachain disulfide bonds within this molecule. Moreover, analysis of a deglycosylated gp55 suggested that structural microheterogenity mediated by disulfide bonds may occur within this molecule. No free sulfhydryls could be detected in any of the gp55 components. This would imply that all twelve cysteine residues found within envelope glycoprotein are involved in either intrachain or interchain disulfide bonds.

B. General Introduction

The results presented in chapter three suggest that gp55 is processed in a very heterogeneous fashion. A majority is retained in the RER as a monomer and only a small percentage of the gp55 molecules form disulfide-linked dimers. The dimers found in the RER form a structurally heterogeneous group and only one form of the intracellular dimers appears to be processed through the Golgi apparatus apparatus to the cell surface. This processed dimer, called $(gp55^{p})_2$, contains complex Asn-linked oligosaccharides and the reduced subunits have an apparent M_r of 65,000. This is considerably larger than the intracellular gp55 components. Subsequently, the cell surface dimers are shed into the culture medium. This shedding seems to be associated with a removal of ~2.5 kd from each subunit. Hence, the shed $(gp55^{s})_2$ molecules are slightly smaller than the cell surface $(gp55^{p})_2$ molecules. This complex processing raises many questions regarding the structural nature of the different gp55 components. Some of the structural differences between these different components will be addressed in this chapter.

C. Results

1. Structural differences between gp55, $gp55^P$, and $gp55^S$

The size differences of the three reduced gp55 components are shown electrophoretically in Fig. 12. The intracellular gp55 (lane 1) is substantially smaller than $gp55^P$ (lane 5) as seen by its faster electrophoretic mobility in this 20% acrylamide-SDS gel, and $gp55^S$ (lane 9) is slightly smaller than $gp55^P$ (by ~2.5 kd). Sequence analysis of the SFFV envelope glycoprotein has shown that the carboxyl-terminus contains the membrane anchoring portion of this molecule (76, 84, 85) (Fig. 2, Intro.). Within this membrane anchor region are approximately twenty amino acids that are buried in the plasma membrane bilayer, but do not extend through it (88). Therefore, shedding of $gp55^P$ would be expected to require removal of this hydrophobic anchor. If this were true, the size reduction observed in the shed molecule would occur in the carboxy-terminus.

To test this assumption, we compared the electrophoretic mobilities of the amino- and carboxy-termini generated by *S. aureus* V8 protease digestion of the reduced gp55 components (Fig. 12). Previous work has shown that gp55 can be cleaved by V8 protease to form the primary fragments V-1 (M_r~32,500) and V-2 (M_r~21,500). These correspond to the amino- and carboxy-termini of the gp55 molecule, respectively. With increasing amounts of V8 enzyme, V-1 is further cleaved to generate V-3 (M_r~20,000) and V-4 (M_r~12,400) (79-80).

A V8 proteolytic fragmentation analysis of gp55, $gp55^P$, and $gp55^S$ is shown in Fig. 12. The V-2 fragments (C-termini) are difficult to see because they contain fewer cysteine and methionine residues and because V-2 and V-3 often comigrate during electrophoresis. In addition, $gp55^P$ occurs only in trace amounts

Figure 12. Proteolytic fragmentation analysis of gp55, $gp55^{p}$, and $gp55^{s}$. F745 erythroleukemia cells (10^{7} cells) were labelled for 4 h with [^{35}S]-met and [^{35}S]-cys (50uCi/ml). Cells were lysed or incubated for 18 h in complete medium. Cell lysates and medium were immunoprecipitated with anti-gp70 serum and the gp55 components were eluted from dried acyrlamide gels. The glycoproteins were digested with increasing (0, 0.1, 1.0, 10 ug) amounts of V8 protease (lanes 1-4, 5-8, and 9-12, respectively). Samples were reelectrophoresed into a 20% acrylamide gel containing 0.1% SDS. Digestion of intracellular gp55 (lanes 1-4), $gp55^{p}$ (lanes 5-8), and $gp55^{s}$ (lanes 9-12). The gp55 samples (lanes 1-4) represent a 5 day exposure of the autoradiograph, whereas the $gp55^{p}$ and $gp55^{s}$ samples (lanes 5-12) represent a 60 day exposure of the same autoradiograph.

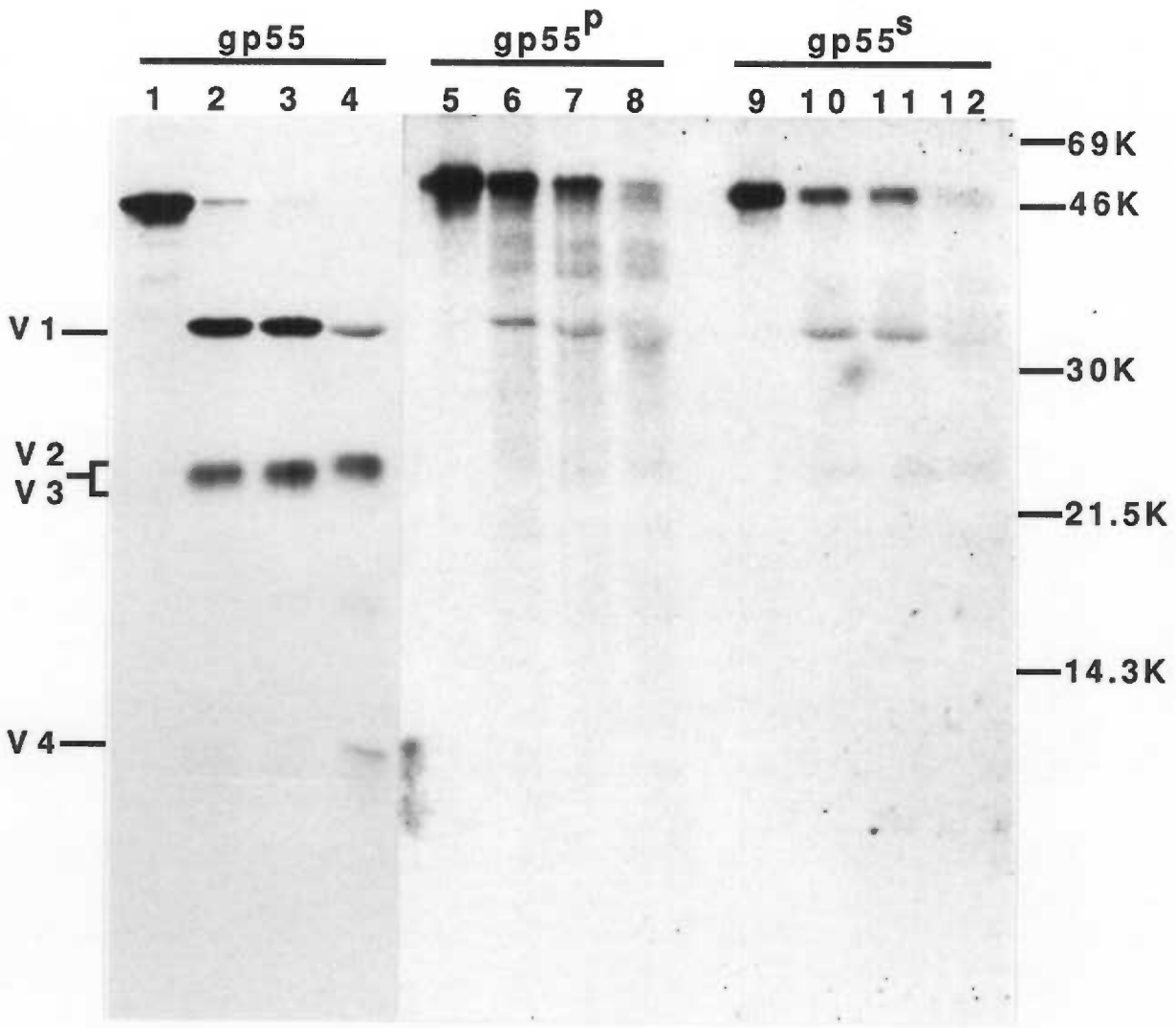
gp55
gp55p
gp55s
1 2 3 4
5 6 7 8
9 10 11 12
69K
46K
30K
21.5K
14.3K
V1
V2
V3
V4

on cells and obtaining sufficient quantities for proteolytic analysis is difficult. Despite these technical difficulties, the V-1 fragments (N-termini) of the intracellular gp55 (lanes 2-4), $gp55^{P}$ (lanes 6-8), and $gp55^{S}$ (lanes 10-12) are relatively clear and appear to have almost identical sizes. In addition, the secondary proteolytic V-3 fragments also have the same apparent size in all of the gp55 components. These results imply that the major size differences between these gp55 components must occur primarily in their carboxy-termini. Consistent with this assumption, bands that are larger in size than the V-1 fragments can be seen in the digested $gp55^{P}$ (lanes 6-8) and $gp55^{S}$ (lanes 10-12) samples that are not seen in the digested gp55 sample (lanes 2-4). These novel proteolytic fragments presumably represent the V-2 domain of the more extensively processed $gp55^{P}$ and $gp55^{S}$ components. Moreover, the presumptive V-2 fragment of $gp55^{S}$ is slightly smaller than the V-2 fragment of $gp55^{P}$. Thus, this carboxyl-terminal domain of the gp55 molecule must be post-translational modified to gain mass during cell surface transport and then undergo a lesser mass reduction during shedding.

Shedding of $(gp55^{P})_2$ would theoretically require the proteolysis of the membrane anchor from both subunits. If this hydrolysis were to occur randomly, approximately half the cell surface subunits would be heterodimers with only one remaining anchor. The fact that $gp55^{S}$ sized components are not observed in the $gp55^{P}$ preparations suggests that shedding involves the coordinated scission of both anchors in the dimeric $gp55^{P}$ molecules. Other evidence supporting this conclusion was obtained in experiments not shown.

The hypothesis that shedding involves the removal of a carboxy-terminal

Figure 13. Analysis of shed gp55 components. Culture medium from $1x10^7$ F745 cells were immunoprecipitated with normal goat serum (lane 1) followed by F-MuLV anti-gp70 serum (lane 2). To remove virions, medium was centrifuged at 50,000 rpm in an 80Ti rotor for 1 h at 4^oC. Centrifuged medium was then immunoprecipitated with normal goat serum (lane 3) and anti-gp70 (lane 4). The solubilized ultracentrifugation pellet is shown in lane 5. Medium from F745 cells cultured in DMEM lacking serum for 48 h were immunoprecipitated with normal goat serum (lane 6) and then anti-gp70 (lane 7). Immunoprecipitates were electrophoresed and viral proteins were analyzed by immunoblotting with anti-gp70 serum.

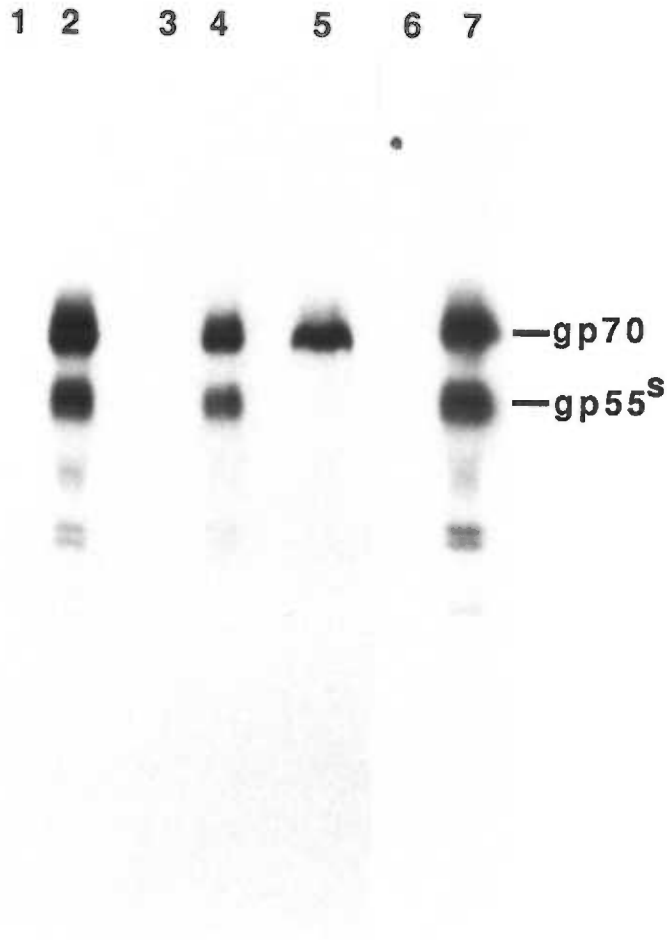
1 2 3 4 5 6 7
—gp70
—gp55^{s}

membrane anchor would predict that the gp55^{S} components would be found as soluble molecules in the culture medium. This would differ from MuLV gp70 which is lost from cell surfaces both as a soluble glycoprotein, and in membranous budded virions as gp70-p15E complexes (36). To test this, we analyzed the viral glycoproteins released from erythroleukemia cells into the culture medium (Fig. 13). Both the gp70 and gp55^{S} can easily be detected in the extracellular medium (lane 2). After centrifugation to remove the virions, the supernatant still contained both gp70 and gp55^{S} (lane 4). The virion pellet (lane 5) contained only gp70. This supports the idea that gp55^{S} is shed as soluble glycoprotein. The shedding of gp55^{S} could require hydrolysis of the membrane anchor by either a serum or cell associated protease. The results in lane 7 show that shedding occurred when cells were incubated in a serum-free medium for 48 hrs. Therefore, the shedding does not involve a serum protease.

2. Evidence that all of the cysteine residues in gp55 are involved in intrachain or interchain disulfide bonds.

Electrophoretic analysis of acrylamide gel eluted nonreduced and reduced intracellular gp55 demonstrates that intrachain disulfide bonds exist within this molecule (Fig. 14). Nonreduced gp55 (lane 1) migrates faster than reduced gp55 (lane 4). This is consistent with intrachain disulfide bonds maintaining a more compact polypeptide and increasing the electrophoretic mobility of the nonreduced molecule. Deglycosylation of gp55 with N-glycanase (Genzyme) yields a major band with a mobility of ~42,000-daltons under nonreducing conditions (lanes 2 and 3) and ~44,000-daltons under reducing conditions (lanes 5 and 6). The migration of the reduced deglycosylated gp55 is in agreement with

Figure 14. Reduced and nonreduced analysis of the deglycosylated intracellular gp55 molecule. Nonreduced [^{35}S]-methionine and [^{35}S]-cysteine labelled gp55 was eluted from dried polyacrylamid gels and digested with N-glycanase as described in the Materials and Methods. The nonreduced intracellular gp55 molecule was digested with 0, 0.25, and 2.5 units of N-glycanase (lanes 1-3 and 4-6, respectively) overnight at 37^{o} C. Digested samples were electrophoresed in the absence (lanes 1-3) or presence (lanes 4-6) of a reducing agent.

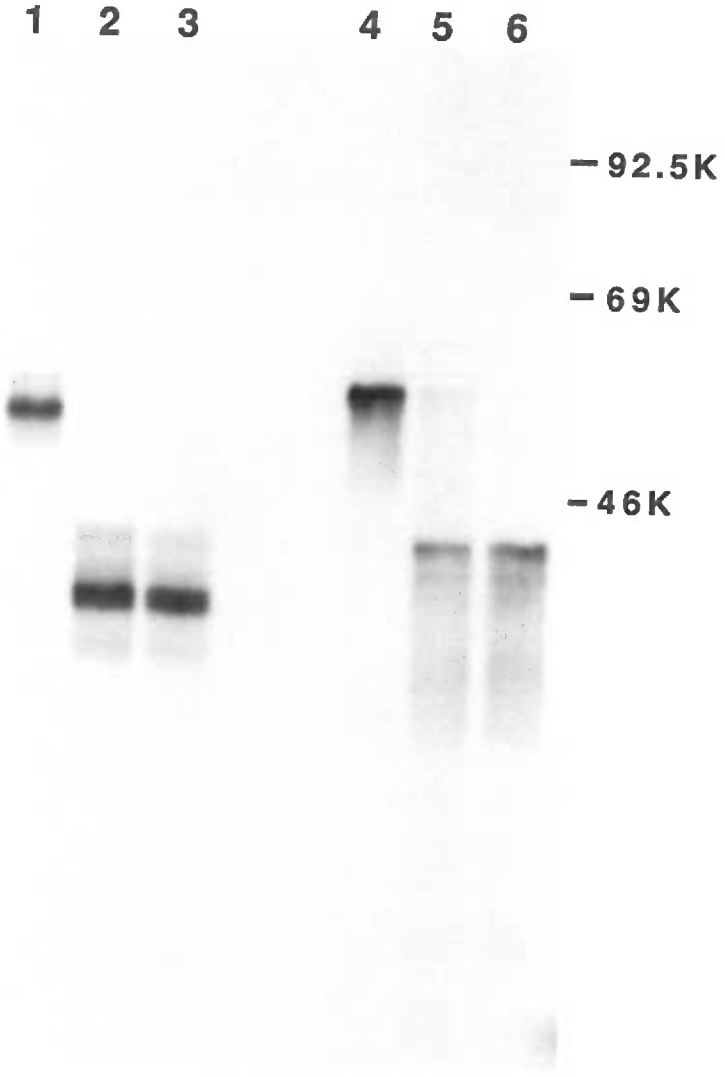
1
2
3
4
5
6
92.5K
69K
46K

Figure 15. Proteolytic fragmentation analysis of nonreduced and reduced intracellular gp55. The [^{35}S]-methionine and [^{35}S]-cysteine labelled protein was immunoprecipitated, eluted from dried polyacrylamide gels, and digested with increasing (0, 0.1, 1.0, 10 ug) amounts of *S. aureus* V8 protease (lanes 1-4, 5-8, and 9-12, respectively) as described in the Materials and Methods. The digested intracellular gp55 was reelectrophoresed in a 20% acrylamide gel containing 0.1% SDS. Lanes 1-4 correspond to digested nonreduced gp55 reelectrophoresed without reduction; lanes 5-8, digested nonreduced gp55 reelectrophoresed with reduction; and lanes 9-12, digested reduced gp55 reelectrophoresed with reduction.

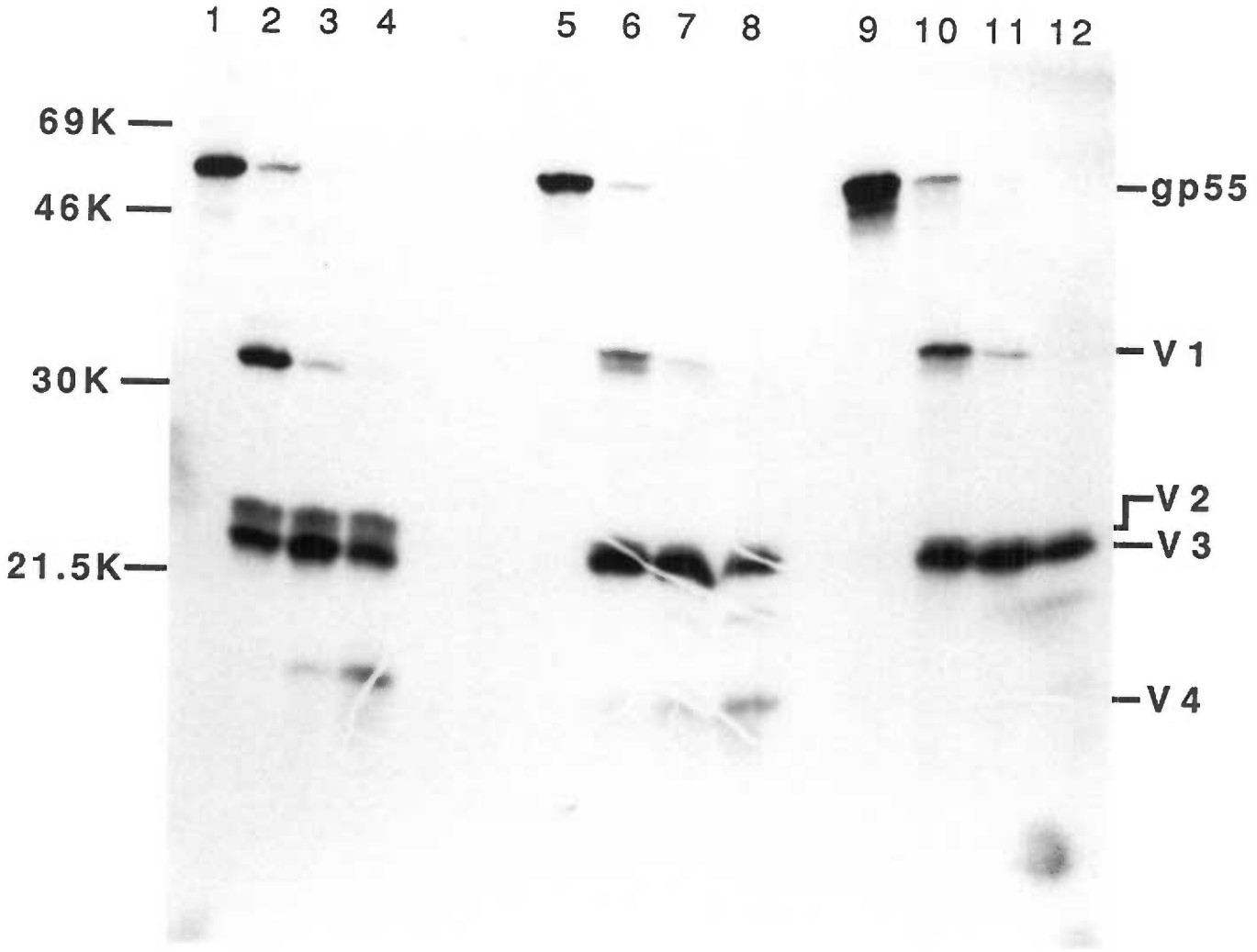
1 2 3 4
5 6 7 8
9 10 11 12
69K
46K
30K
21.5K
gp55
V1
V2
V3
V4

the size of the unglycosylated protein that is synthesized in the presence of the N-linked glycosylation inhibitor tunicamycin (89). Moreover, the results suggest that the nonreduced deglycosylated gp55 (lanes 2 and 3) may contain microheterogenity that is eliminated by reduction (lanes 5 and 6). This structural microheterogenity in the intracellular gp55 component is compatible with the heterogenity suggested in the two-dimensional gel separation of gp55 (Figs. 7 and 8).

Supportive evidence for intrachain disulfide bonding is shown by V8 proteolysis of intracellular gp55 (Fig. 15). The nonreduced gp55 V-1 domain (lanes 2-4) has a faster mobility than the reduced V-1 (lanes 6-8, 10-12). Furthermore, although V-2 and V-3 coelectrophorese when reduced (e.g. lanes 6-8, 10-12), they have different mobilities when nonreduced (lanes 2-4). Specifically, V-3 appears to electrophorese faster when these fragments are nonreduced. As can be seen in lanes 9-12, the V8 proteolytic pattern of a fully reduced gp55 is the same as the digestion of a nonreduced gp55 molecule (lanes 5-8). This demonstrates that the primary V8 cleavage sites remain highly susceptible regardless of disulfide bond reduction prior to digestion.

Evidence that the gp55 components lack free sulfhydryl groups was obtained by two methods. First, reaction of detergent-solubilized cell lysates with [^{14}C]-iodoacetamide did not result in the labelling of any gp55 components (data not shown). Secondly, as shown in Fig. 16, none of the gp55 molecules adsorbed onto an organomercurial resin (Biorad) which selectively binds to free sulfhydryls (111, 112). This binding involves the formation of a covalent mercaptide bond that can be cleaved by dilute reducing agents. Thus, when a denatured cell lysate

Figure 16. Free sulfhydryl analysis using an organomercurial resin. Approximately $1x10^6$ F745 cells were lysed in 100ul immunoprecipitation buffer in the absence (panel A) or presence (panel B) of 20 mM iodoacetamide. Cell lysates were reacted with organomercurial resin for 30 min at 4^oC. Absorbed proteins were eluted form the resin with 2 x 100ul immunoprecipitation buffer plus 5% mercaptoethanol washes. Equal volumes of lysates and elutions were combined with Laemmli sample buffer, electrophoresed, and analyzed by immunoblotting with anti-gp70 serum. (A) Analysis of organomercurial adsorption in the absence of iodoacetamide. Lane 1, control unreacted nonreduced lysate; lane 2, organomercurial reacted nonreduced lysate; lane 3, reduced unreacted control lysate; lane 4, reduced organomercurial reacted lysate; lane 5, first elution of lysate reacted organomercurial resin; and lane 6, second elution of lysate reacted organomercurial resin. (B) Lysis and organomercurial adsorption in the presence of 20 mM iodoacetamide. Lane 1, control unreacted nonreduced lysate; lane 2, organomercurial reacted nonreduced lysate; lane 3, reduced unreacted control lysate; lane 4, reduced organomercurial reacted lysate; lane 5, first elution of lysate reacted organomercurial resin; and lane 6, second elution of lysate reacted organomercurial resin.

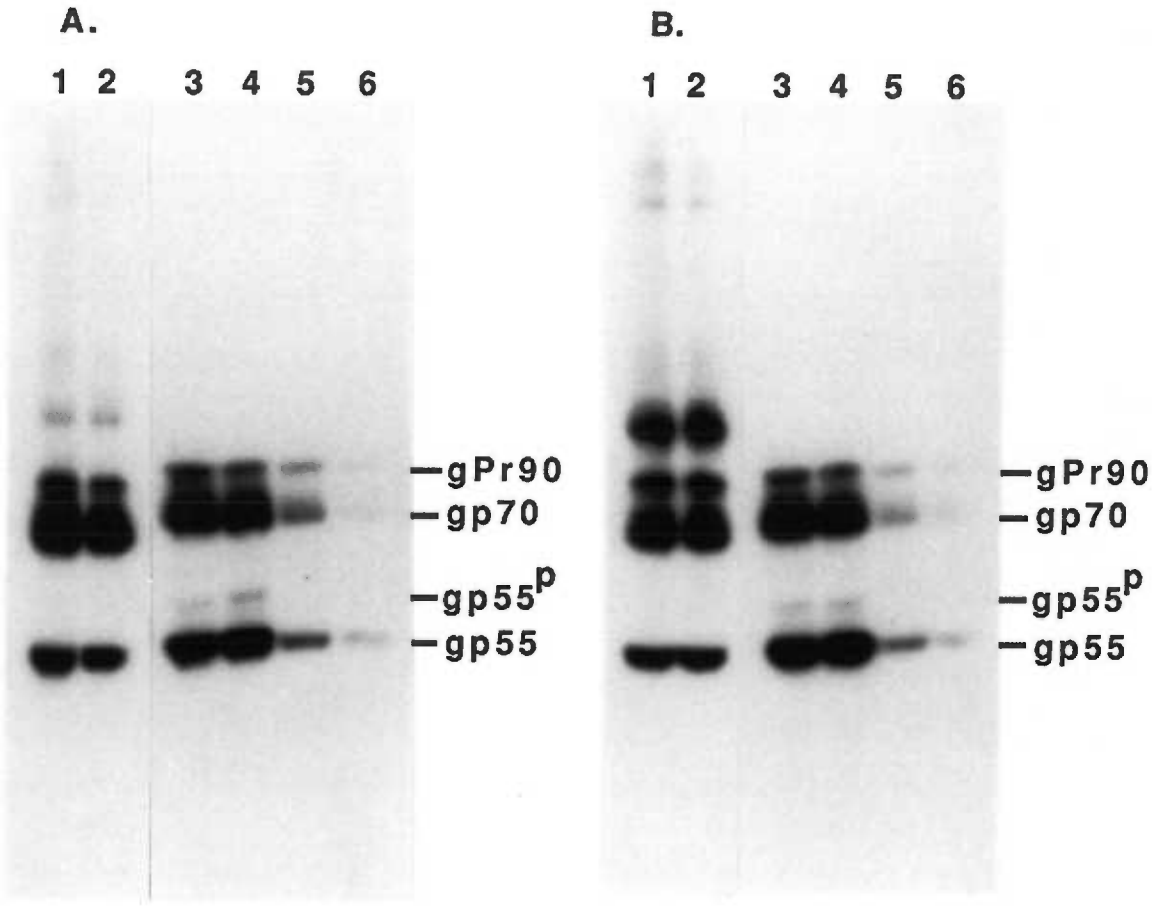
A.
1 2 3 4 5 6
—gPr90
—gp70
—gp55^p
—gp55
B.
1 2 3 4 5 6
—gPr90
—gp70
—gp55^p
—gp55

was prepared without reducing agents and incubated with the resin to remove any components containing free sulfhydryls, the reacted lysate contained the same gp55 glycoproteins as were present in the unreacted control lysate (Fig. 16A, compare lanes 1 and 2). Likewise, analyzing those same lysates by electrophoresis with reduction (lanes 3 and 4) shows they both contain equivalent levels of gp55 and $gp55^{p}$. Only a small percentage of gp55, gp70, and gPr90 were detected following elution of the resin with mercaptoethanol (lanes 5 and 6).

To determine the specificity of this adsorption to the resin, cells were lysed in the presence of the alkylating agent iodoacetamide and then reacted with the organomercurial resin. Iodoacetamide should alkylate any free sulfhydryl groups (113) and block any specific organomercurial binding. A nonreduced control lysate in the presence of 20mM iodoacetamide (Fig. 16B, lane 1) shows a major band appearing above the gPr90 band that was not seen in the control nonreduced lysate without iodoacetamide (Fig. 16A, lane 1) We have identified this component as the disulfide-linked gp70-p15E complex in metabolic labelling experiments (data to be presented). Otherwise, the lysate with iodoacetamide is identical to the lysate without iodoacetamide and no differences in the gp55 components can be observed. Cells lysed in the presence of 20mM iodoacetamide and then reacted with the organomercurial resin (Fig. 16B, lane 2) results in the same pattern as the unreacted control lysate (lane 1). Likewise, the reduced lysates (lanes 3 and 4) and elutants (lanes 5 and 6) show the same patterns as the samples without iodoacetamide (Fig. 16A, lanes 3-6). This suggests that a small amount of viral proteins nonspecifically adheres to the resin and there is no specific binding between the organomerurial reactive group and

gp55 components. Therefore, the results imply that the gp55 components do not have free sulfhydryl groups.

C. Discussion

The results presented in this chapter provide additional information about the structural differences between the various processed forms of the gp55 molecules. In particular, the results suggest that gp55, gp55^{P}, and gp55^{S} have substantial size differences in their carboxyl-terminal regions. The processing of the high-mannose N-linked oligosaccharides of gp55 into the complex sialyated, fucosylated and galactosylated oligosaccharides that occur in gp55^{P} probably contribute slightly to the size increase between gp55 and gp55^{P} (90). However, gp55 only contains 4 Asn-linked oligosaccharides (89) and it is unlikely that the conversion from high mannose N-linked oligosaccharides to complex oligosaccharides would so substantially alter the glycoprotein's size. Moreover, the V-1 domain contains two of these oligosaccharide attachment sites and yet its size is very similar in both the gp55 and gp55^{P} molecules (Fig. 12). Therefore, it is likely that additional post-translational processing modifications must occur in the carboxyl-terminus. These may include the addition of O-linked oligosaccharides in the Golgi apparatus (114) or perhaps the addition of a phospholipid-type membrane anchor structure (115).

The shed gp55 is ~2,500-daltons smaller than the cell surface molecules. This size difference appears to be localized to the carboxy-terminus and may be caused by the removal membrane anchor found within this region to generate a soluble gp55^{S} molecule (Figs. 12 and 13). This hydrolysis may be mediated by a cell associated protease that acts on both dimer subunits coordinately. Both the dimeric and monomeric forms of gp55 can be detected in the medium. However, since gp55^{P} occurs on cell surfaces only as a dimer, the SFFV envelope

glycoprotein must be shed as a dimer and a portion of the molecules must then be reduced.

Analysis of the reduced and nonreduced intracellular gp55 reveals the presence of intrachain disulfide bonds within these molecules (Figs. 14 and 15). Proteolytic analysis of gp55 has confirmed the two domain model of the envelope glycoprotein and supports the presence of intrachain disulfide bonds within each domain, but not between them. The independent folding of these domains is further supported by the fact that the primary V8 protease cleavage site located between these domains remains very accessible even when the protein is nonreduced (Fig. 15).

In addition, the results imply that gp55 may lack free sulfhydryl groups (Fig. 16). If so, then all 12 of its cysteines are involved in disulfide bonding both in the monomeric gp55 and in the disulfide-linked dimers. This implies that the subunits in the gp55 dimers must be linked together by an even number of disulfide bonds. Linkage by only one disulfide bond would necessitate the presence of a free sulfhydryl on each subunit. We do not detect such a free sulfhydryl. This result also implies that dimerization of gp55 could not be achieved by oxidation of prefolded monomeric gp55 molecules because cross-linking would require partial reduction of at least one gp55 monomer followed by a disulfide interchange process. Alternatively, dimerization could occur during the initial oxidation of newly synthesized gp55 molecules. Evidence presented in the next chapter suggests that dimerization can occur only shortly after gp55 biosynthesis. Thus, the fully-folded gp55 monomers apparently are stable and do not undergo partial reduction and disulfide interchange reactions *in vivo.*

V. Characterization of gp55 Biosynthesis, Oligomerization, and Post-translational Processing.

A. Abstract

Dimerization of gp55 is an essential post-translational processing step for cell surface expression of this glycoprotein. Analysis of metabolically labelled gp55 suggests that it is synthesized as precursor molecule that obtains its mature electrophoretic mobility within 1 min after synthesis. No disulfide-bonded intermediates can be detected during this maturation process. Dimerization is an early post-translational modification and apparently can only occur when free sulfhydryls are present on gp55 prior to complete folding and disulfide bond formation. However, not all of the dimers formed within the rough endoplasmic reticulum (RER) are transported to the cell surface. Therefore, we propose that the initial folding and dimerization of nascent gp55 molecules results in a structurally heterogeneous population of dimers formed within the RER. Only those dimers that are "correctly folded" and obtain a unique conformation can escape the RER. This would imply that a stringent structural requirement exists for gp55 transport. There appears to be no equilibrium between the pools of intracellular monomers and dimers to continually generate transport competent molecules. These results imply that the intracellular gp55 components are not being actively isomerized to produce the conformation required for cell surface expression. Therefore, our evidence implies that no interchange enzyme, such as a putative protein disulfide-isomerase, could participate in disulfide bond formation or isomerization of gp55. The nontransported gp55 components are not stably bound by specific RER proteins or form a "precipitant-like" aggregate. Instead, retention in the RER appears to be mediated by a less specific mechanism.

B. General introduction

Proteins destined for the plasma membrane are synthesized in the rough endoplasmic reticulum and transported through the Golgi apparatus. Each step of the processing pathway is characterized by specific post-translational modifications (e.g. glycosylation, proteolysis, etc.). However, not all proteins synthesized in the rough endoplasmic reticulum (RER) are processed to the plasma membranes. Some proteins localize in the RER and Golgi apparatus (e.g. specific glycosidases, etc.) or are sequestered in lysosomes. Others, like gp55, are inefficiently processed to the cell surface.

The rate limiting step in processing proteins to the cell surface is usually the transport from the RER to the Golgi apparatus (116, 117). Different proteins have characteristic rates in reaching the cell surface, but once out of the RER the proteins quickly acquire complex carbohydrates and reach the plasma membrane. Two models have been proposed to explain this variation in transport: 1) newly synthesized proteins are actively retarded in the RER until some maturation process occurs to permit their release, 2) newly synthesized proteins are actively transported out of the RER at different rates by binding to an undefined carrier protein in a rate limiting manner (reviewed 118).

Recent reports have provided experimental evidence for the retardation model. When an acylated tripeptide which contains the consensus sequence for N-linked glycosylation was added to cells, these cells were able to take up this tripeptide and glycosylate it (119). The glycosylation effectively "trapped" the tripeptide within the lumen of the RER. This tripeptide was then secreted from the cell at a faster rate than that measured for any endogenous glycoproteins. Since

this tripeptide is presumably free in the lumen of the RER, the rate of transport out of the RER and through the Golgi apparatus was interpreted to be a measure of bulk liquid flow through these organelles. Therefore, it was concluded that endogenous glycoproteins, which have different slower rates of transport, are specifically retarded in their release from the RER until a specific state of maturation has been achieved.

An RER protein has been described that binds to proteins that are defective in transport to the cell surface. This binding protein is referred to as BiP. BiP was first described in association with heavy chain immunoglobulins in pre-B lymphocytic cell lines that do not synthesize light chain immunoglobulins (120). BiP has been postulated to prevent the heavy chain from exiting the RER until it complexes with the light chain immunoglobulins (121). In normal immunoglobulin secreting cells, BiP is displaced from the heavy chain by light chains post-translationally (121). BiP has also been found associated with proteins in non B-cell lines. Mutant influenza hemagglutinin membrane glycoproteins are also associated with BiP (122). Proteins such as BiP have been referred to as "chaperone" proteins (reviewed 123).

Regardless of which model proves to be correct for the transport of proteins out of the RER, the "correct folding" of a protein seems to be an essential requirement for export of newly synthesized polypeptide. Mutating a membrane protein usually results in the inability of this protein to be transported to the cell surface. For example, site-directed mutagenesis that disrupted the disulfide bond formation in the histocompatibility complex class I antigen resulted in failure in transport to the membrane (124). Likewise, mutations in the structure of the

influenza hemagglutinin glycoprotein that prevented trimer formation resulted in the accumulation of this protein in the RER (122). Disruption of vesicular stomatitis virus G glycoprotein oligomerization prevented its transport to the plasma membrane (125). Similarly, mutations in gp55 prevent its processing to the cell surface (79, 83). These examples help demonstrate that the cell surface transport of a membrane protein has a specific and fairly stringent structural requirement.

A primary factor in determining the overall three-dimensional structure of secreted and membrane proteins is disulfide bonding. Formation of disulfide bonds is an early step in the modification of proteins and begins as the protein is being synthesized (113, 126, 127). Earlier *in vitro* studies suggested that an enzyme protein disulfide-isomerase (PDI) had the ability to catalyse sulfhydryl oxidation and thiol/disulfide interchange, leading to the formation of the set of disulfide bonds representing the most stable state of the protein (reviewed 128, 129). With the subcellular localization of PDI determined to be microsomal membranes, it was proposed that PDI catalysed the formation of disulfide bonds *in vivo*. However, the role of PDI has not been universally accepted because very little convincing *in vivo* evidence has been available to support its activity in protein folding. In addition, its function *in vitro* is usually very slow, in contrast to the rapid folding of proteins that occurs *in vivo*.

In this chapter we have analyzed the biosynthesis, oligomerization, and processing of gp55 to the cell surface. We have paid particular attention to the possible role of mixed disulfide intermediates in gp55 folding, and to the importance of dimerization in cell surface transport, We conclude this chapter with an overall summary of how gp55's structure, biosynthesis, and

oligomerization is related to the inefficient processing of this glycoprotein to cell surfaces.

C. Results

1. Metabolic labelling analysis of gp55 biosynthesis

To study the post-translational processing of the SFFV envelope glycoproteins, erythroleukemia cells were pulsed for 5 min with [^{35}S]-methionine and [^{35}S]-cysteine and then chased for up to 60 min with unlabeled medium. The erythroleukemia suspension cells were removed at various times from the culture and immediately lysed in an equal volume of 2x immunoprecipitation buffer containing 20mM iodoacetamide. The iodoacetamide was included in the lysis buffer to alkylate any free sulfhydryls that may be present on the freshly labeled proteins. In this way, any transient intermediates that contained a free sulfhydryl during biosynthesis or post-translational processing would be "trapped" (113, 130). These intermediates may include various forms of the unfolded glycoproteins disulfide-linked to components that might be important in catalyzing protein oxidation and folding. Molecules postulated to participate in this process include PDI (129), glutathione (131), and cystamine (132).

Immunoprecipitation of the viral proteins and gel electrophoresis under nonreducing conditions should demonstrate the presence of these intermediates. Thus, for example, a mixed disulfide complex between PDI (M_r~70,000) and gp55 would form a relatively large (M_r ~125,000) intermediate. Since these intermediates would be disulfide-bonded, reduction would eliminate this complex and labelled gp55 should be released. Mixed disulfides with smaller molecules such as glutathione would probably also be detectable because they would contain fewer disulfide bonds than mature gp55. This would cause the precursor to have a more open structure and a relatively slow electrophoretic mobility (e.g.,

see Fig. 14, Chap. IV).

The pulse-chase analysis of the Friend virus envelope glycoproteins is shown in Fig. 17. The MuLV gPr90 and SFFV gp55 were the most prominently labeled bands after a 5 min pulse and analysis in nonreducing conditions (Fig 17A, lane 1). The gPr90 appears initially as a very heterogeneous band and does not form a sharp band until ~25 min (lane 6) into the chase period. In contrast, reduction of these samples (Fig. 17B) yields a relatively tight gPr90 band after the initial 5 min pulse (lane 1). This suggests that the heterogenity observed early in the biosynthesis is caused by heterogeneous disulfide bonding and folding of this precursor protein. Within 30 min after synthesis, the glycoprotein has folded into its mature form and obtains a relatively homogeneous electrophoretic mobility.

The gPr90 is processed in the classic precursor-product relationship as previous described (31, 32, 105). Briefly, the gPr90 accumulates in the RER and is slowly released for transport to the cell surface. During transport through the Golgi apparatus or immediately thereafter, the precursor molecule is proteolytically cleaved to its gp70 and p15E components. Our pulse-chase analysis shows that cleavage begins by 30 min (lane 7) after synthesis. Both gp70 and disulfide bonded gp70-p15E can be seen in nonreducing conditions (Figure 20A, lanes 7-9). The identity of the disulfide bonded gp70-p15E complex was initially established by two-dimensional electrophoretic analysis (Fig. 9, Chap. III). The concurrent appearance of this complex with gp70 confirms this identification. Coinciding with the appearance of the processed gp70 is the gradual decrease in labelled gPr90.

In contrast to gPr90, the SFFV gp55 appears as a sharp band after the initial

Figure 17. Pulse-chase analysis of synthesis and processing of viral envelope glycoproteins in erythroleukemia cells. F745 erythroleukemia cells were labelled for 5 min with [^{35}S]-methionine and [^{35}S]-cysteine (50 uCi/ml) at (1x10^{6} cells/ml) in met- and cys-free EMEM. Cells were resuspended in complete medium and chased for a total of 60 min. Aliquots (1 ml) were removed and added directly to 2 x immunoprecipitation buffer plus 20 mM iodoacetamide at 4^{o}C. Lysates were immunoprecipitated with anti-gp70 serum, electrophoresed in 10-20% acrylamide gel containing 0.1% SDS, and then processed for autoradiography. Samples were analyzed without (panel A) and with (panel B) reduction. Samples correspond to 5 min pulse (lane 1); 5 min chase (lane 2); 10 min chase (lane 3);15 min chase (lane 4); 20 min chase (lane 5); 25 min chase (lane 6); 30 min chase (lane 7); 45 min chase (lane 8); 60 min chase (lane 9).

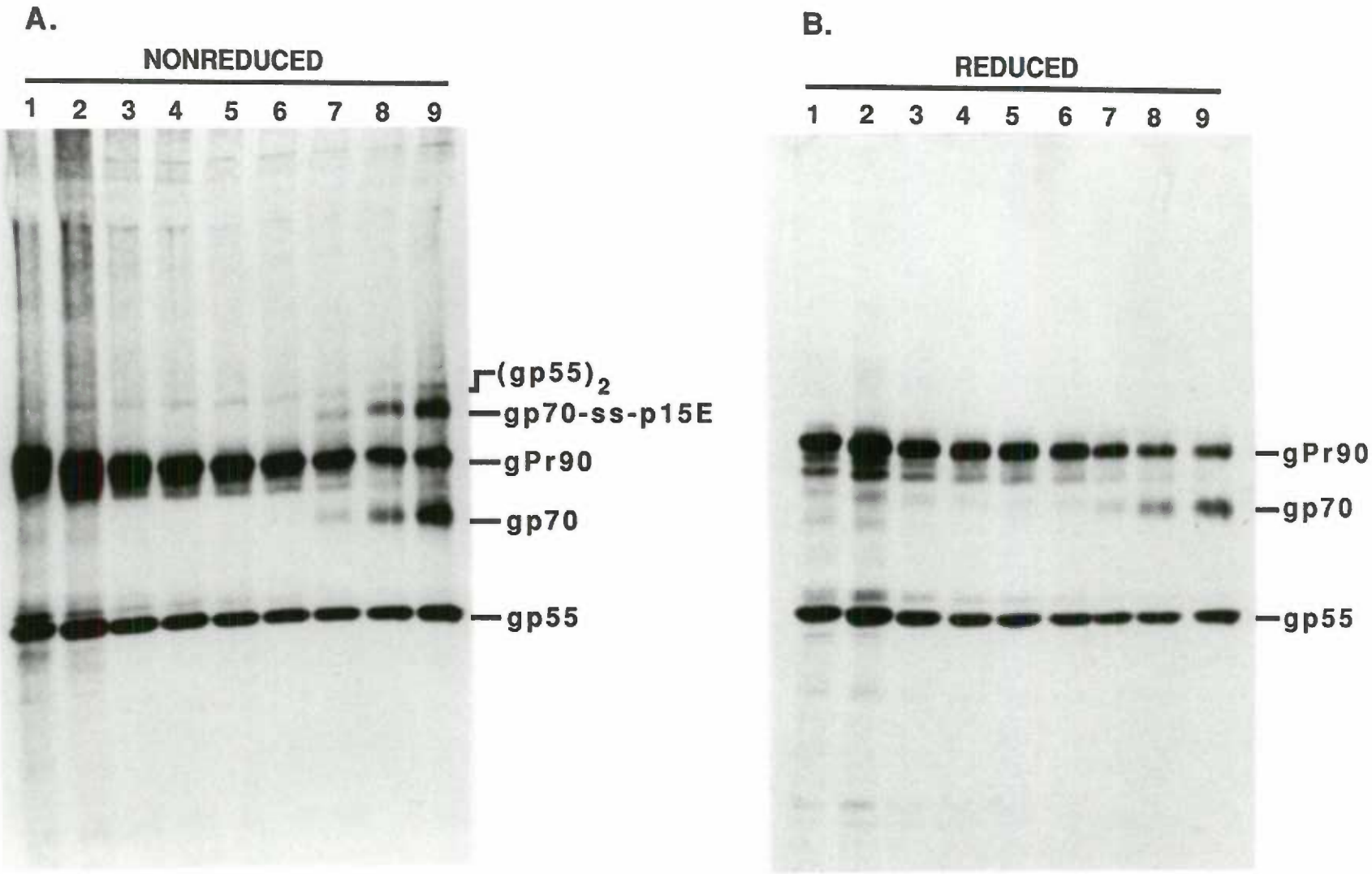
A.
NONREDUCED
1 2 3 4 5 6 7 8 9
(gp55)2
gp70-ss-p15E
gPr90
gp70
gp55
B.
REDUCED
1 2 3 4 5 6 7 8 9
gPr90
gp70
gp55

5 min pulse-labelling (lane 1) and undergoes no significant change in mobility or loss of signal intensity during the chase period (lanes 2-9). This suggests that the majority of gp55 is present in its mature form soon after synthesis and is not rapidly processed to other gp55 forms. A faint gp55 dimer band is detected after the pulse period (lane 1) in the absence of a reducing agent and remains with relatively the same intensity through the chase (lanes 2-9). As expected, with reduction (Fig. 17B) the dimer is no longer detectable. The lack of change in the dimer band intensity during the chase is consistent with the previous observation that the gp55 monomer is not continually being dimerized. In addition, the presence of gp55 dimer 60 min into the chase (Fig. 17A, lane 9) suggests that this component is not being efficiently processed to the cell surfaces. A distinct cell surface form of $gp55^{p}$ was not detected in this 5 min labelling experiment. This is expected because the minor $gp55^{p}$ form is very difficult to label and its visualization requires a longer pulse period.

No major precursor components are seen in the absence of reducing agents that are eliminated by reduction. A minor band with a slightly slower mobility than gp55 is metabolically labelled and disappears within 20 min of the chase (Fig. 17A, lanes 1-5). These pulse-chase kinetics suggest that this component may be a precursor to the main gp55 band. With reduction this band still remains and it is not resolved into the main gp55 band (Fig. 17B). This demonstrates that the slower electrophoretic mobility of this component is not mediated by disulfide bonding differences or disulfide-linkage to some other factor. Rather, this minor band probably has some covalent difference from mature gp55. Therefore, we conclude that gp55 does not form any mixed disulfide precursors that are

detectable by this method. Attempts by others to detect mixed disulfide complexes of newly made proteins to glutathione or to cystamine by direct chemical studies have also given only negative results (113, 127).

The previous pulse-chase analysis demonstrated that the majority of gp55 was in its mature conformation after a 5 min pulse labelling. To determine when the first mature gp55 molecule was detectable, we pulsed erythroleukemia cells with [^{35}S]-methionine and [^{35}S]-cysteine and rapidily removed aliquots for analysis. Once again, cell lysis was performed in the presence of iodoacetamide to stabilize any potential transient intermediates. Pulsed erythroleukemia cells were sampled every 15 sec for the first minute, and then every minute through a total of 3 min. Analysis of pulse labelled cells under nonreducing conditions is shown in Fig. 18. Because the cells are in the continuous presence of [^{35}S]-methionine and [^{35}S]-cysteine, the intensities of the viral bands increases with time.

The first detectable band with an electrophoretic mobility of mature gp55 can be seen at 0.75 min (Fig. 18). Normal goat serum control precipitations contain no radioacivity to confirm the specificity of the labelled bands seen in this analysis (data not shown). Prior to the appearance of mature gp55, possible precursor bands with electrophoretic microheterogenity are detected in the gp55 region of the gel. Consistent with Fig. 17, reduction of these samples did not reveal the presence of any disulfide-bonded intermediates (data not shown). These results, and those presented in the pulse-chase analysis (Fig. 17), suggest that gp55 folds into its mature disulfide-bonded configuration within approximately 0.75-1 min after its release from ribosomes. More precise delineation of the folding

Figure 18. [^{35}S]-Pulse analysis of Friend viral envelope glycoprotein synthesis. F745 erythroleukemia cells at 1x10^{6} cells/ml were pulsed with [^{35}S]-methionine and [^{35}S]-cysteine in met- and cys-free EMEM. Aliquotes (1 ml) were removed at the indicated times and added directly to an equal volume of 2 x immunoprecipitation buffer plus 20 mM iodoacetamide at 4^{o}C. Samples were immunoprecipitated with anti-gp70, electrophoresed in a 10-20% acrylamide gel containing 0.1% SDS in the absence of reducing agent, and processed for autoradiography.

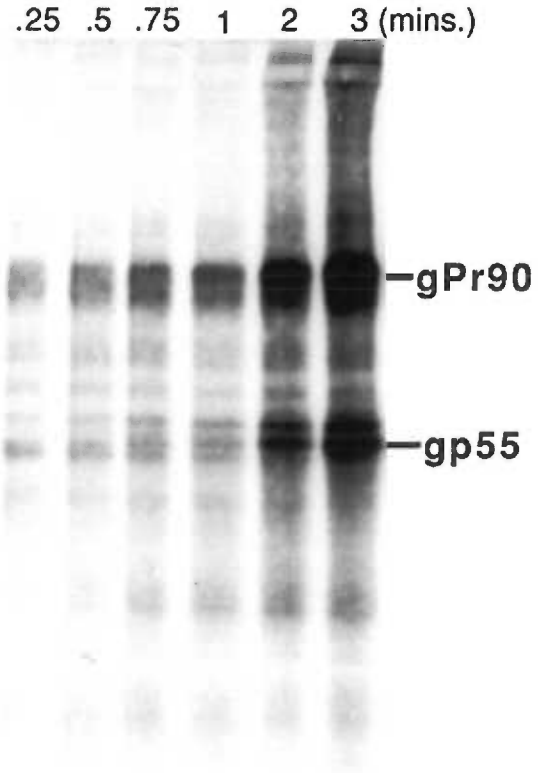
.25 .5 .75 1 2 3 (mins.)
gPr90
gp55

pathway or of its kinetics have not been possible for this or other proteins *in vivo* because of the small quantities of precursors and their short lifespans.

2. Envelope glycoprotein processing and turnover

The precursor-product relationships of the gp55 components were analyzed using a longer period of metabolic labelling. Erythroleukemia cells were labelled for up to 90 min and nonreduced aliquots were analyzed throughout this time (Fig. 19). The major gp55 band is detectable at 5 min and continues to accumulate throughout the 90 min pulse. In agreement with Fig.17, the $(gp55)_2$ component also forms rapidily and gradually becomes more intense between 45 and 90 min. The cell surface $(gp55^p)_2$ begins to appear only after 45 min and becomes slightly more intense by 90 min. At no time could any monomeric $gp55^p$ components be detected in the cells. This suggests that the cell surface dimers are probably derived from the intracellular dimers and not from the dimerization of monomers at the plasma membrane.

Cells were pulsed labelled for two hours and then both the cells and medium were analyzed at various times through a 24 h chase period to follow the processing and turnover of the viral glycoproteins (Fig. 20). Labelling erythroleukemia cells allowed us to follow the processing of both MuLV and SFFV envelope glycoproteins. The MuLV gPr90 is completely converted to the processed gp70 form within 6 h after labelling (Fig. 20, left panel). A disulfide-linked gp70-p15E band is not seen during the processing of gPr90 because this particular analysis was not performed in the presence of iodoacetamide. We have found that alkylation is required to maintain the disulfide-bonded gp70-p15E complex during cell lysis. In contrast, alkylation has no apparent effect on gp55 components (Figs. 16 and 17, experiments not shown).

Figure 19. [^{35}S]-Pulse analysis of Friend viral envelope synthesis and processing in erythroleukemia cells. F745 erythroleukemia cells at 1x10^{6} cells/ml were pulsed with [^{35}S]-methionine and [^{35}S]-cysteine in met- and cys-free EMEM. Aliquotes (1 ml) were removed at the indicated times and added directly to an equal volume of 2 x immunoprecipitation buffer at 4^{o}C. Samples were immunoprecipitated with anti-gp70, electrophoresed in a 10-20% acrylamide gel containing 0.1% SDS in the absence of reducing agent, and processed for autoradiography.

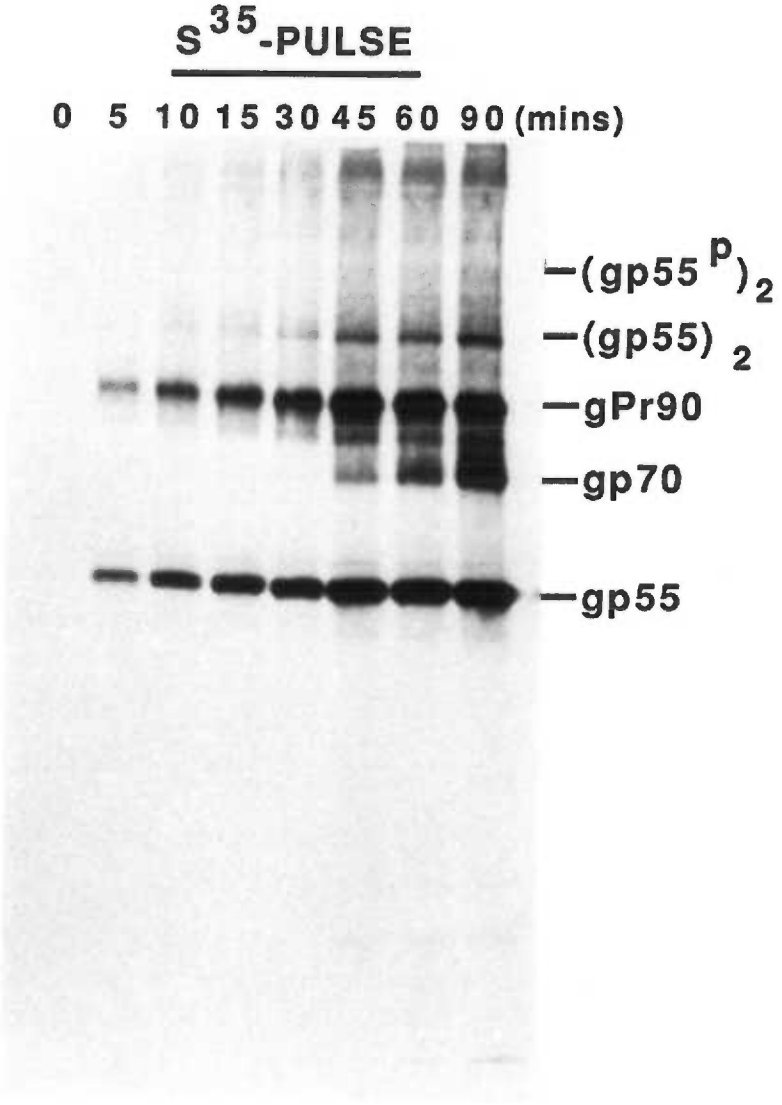
S 35 -PULSE
0 5 10 15 30 45 60 90 (mins)
—(gp55 P)2
—(gp55) 2
—gPr90
—gp70
—gp55

Figure 20. Pulse-chase analysis of post-translational processing and shedding of viral envelope glycoproteins. F745 erythroleukemia cells ($1x10^6$ cells/ml) were pulsed labelled with [^{35}S]-methionine and [^{35}S]-cysteine for 2 h in met- and cys-free EMEM. Cells were resuspended in complete medium and chased for the indicated time. Aliquots (1 ml) were removed and cells were separated from the medium by centrifugation and lysed in 1 ml immunoprecipitation buffer. Both the cell lysate and medium samples were immunoprecipitated with anti-gp70, electrophoresed in a 10-20% acrylamide gel containing 0.1% SDS, and processed for autoradiography. Both the cell immunoprecipitants (left panel) and medium immunoprecipitants (right panel) were analyzed without reduction. These cells were not lysed in the presence of alkylating agent and the level of disulfide-bonded gp70-p15E was low (see text). In this figure, the cell associated autoradiograph represents a 24 hour exposure and the medium autoradiograph a 96 hour exposure.

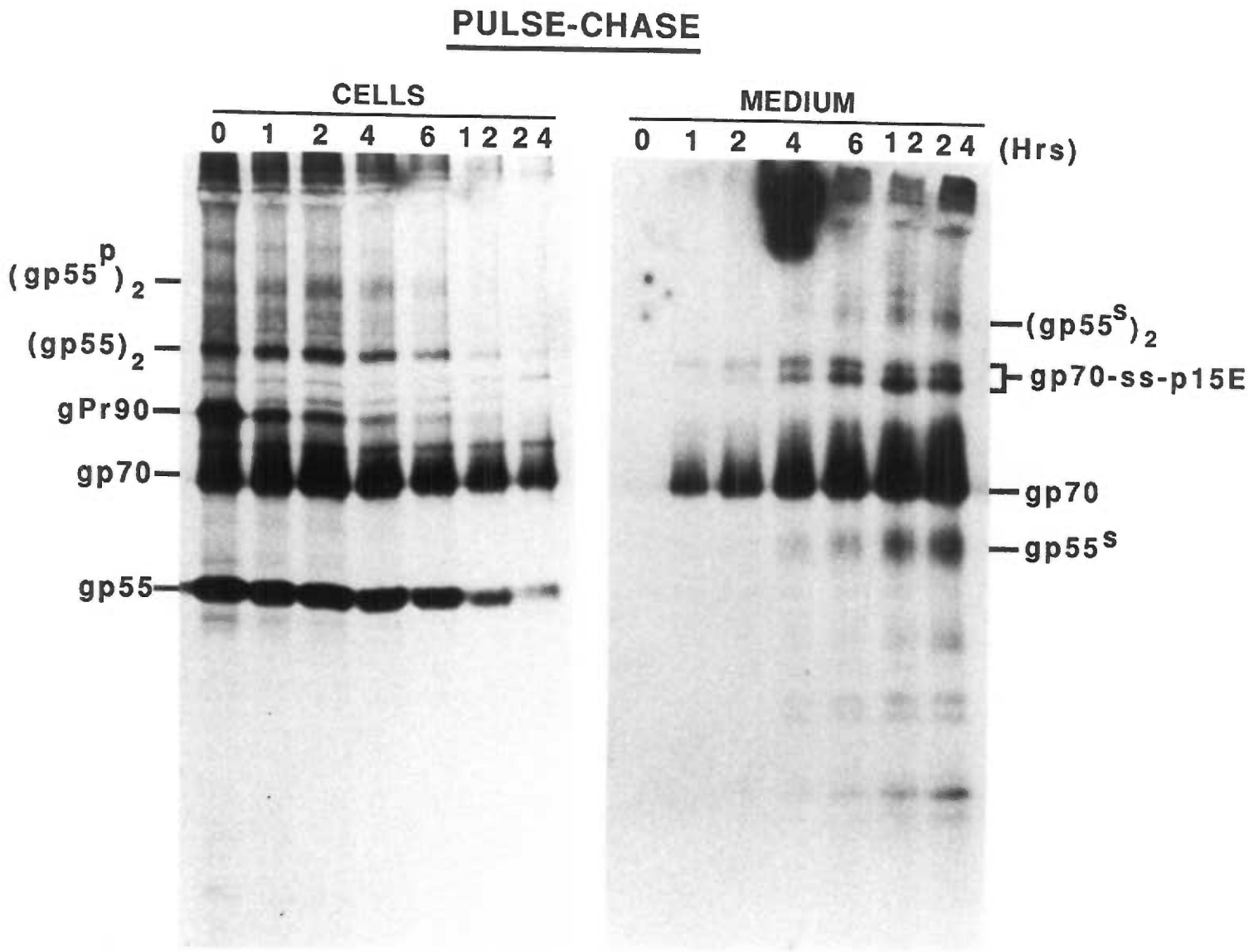
PULSE-CHASE
CELLS
MEDIUM
0 1 2 4 6 12 24
0 1 2 4 6 12 24 (Hrs)
(gp55p)2
(gp55)2
gPr90
gp70
gp55
(gp55s)2
gp70-ss-p15E
gp70
gp55s

Although some gp70 remains associated with the cell 24 h after labelling, the majority has been shed into the medium and incorporated into virions (right panel). Here it is found both as soluble gp70 and as disulfide-bonded gp70-p15E. In this experiment, a gp70-p15E doublet is seen in the medium which probably represents both gp70-p15E and gp70-p12E. The p12E is a proteolytic clipped form of the p15E forms after virion budding (32, 106).

Both the gp55 monomer and $(gp55)_2$ components decline in relative intensity during the chase period, however both intracellular forms can still be detected in association with the cells 24 h after labelling. In contrast, $(gp55^P)_2$ accumulates at the cell surface to its greatest extent within 2 h and then is slowly shed into the medium. Between 6 and 12 h $(gp55^P)_2$ is completely lost from the cells. Concurrently, gp55 can be detected in the medium 4 h into the chase and becomes more prominent as $gp55^P$ is lost from the cell surfaces. Both $(gp55^S)_2$ and $gp55^S$ can be detected simultaneously in the medium. Since the cells lack monomeric $gp55^P$, we infer that the monomeric $gp55^S$ must form from $(gp55^S)_2$ shortly after shedding. These results suggest that both the gp55 monomer and intracellular dimer are not efficiently processed to the cell surface and shed into the medium. Instead, both appear to remain intracellular and are eventually degraded. This implies that the intracellular $(gp55)_2$ dimers do not all serve as an efficient pool of precursors for the formation of $(gp55^P)_2$. In Fig. 20, the cell associated autoradiograph represents a 24 hour exposure while the medium autoradiograph represents a 96 hour exposure to help visualize the $gp55^S$ components which are very faint after a 24 h exposure.

To further analyze these precursor-product relationships, we repeated the

Figure 21. Quantitation of gp55 post-translational processing and shedding. F745 erythroleukemia cells were pulsed and chased up to 48 h exactly as described in Fig. 20. Immunoprecipitates were reduced, separated in a 10-20% acrylamide gel containing 0.1% SDS, and processed for autoradiography. Relative intensities were determined by quantitative densitometric scanning of autoradiographs using various exposures. The intensities of gp55, $gp55^{P}$, and $gp55^{S}$, were plotted in comparison to the relative intensity of gp55 at time 0 h which was set to equal 100.

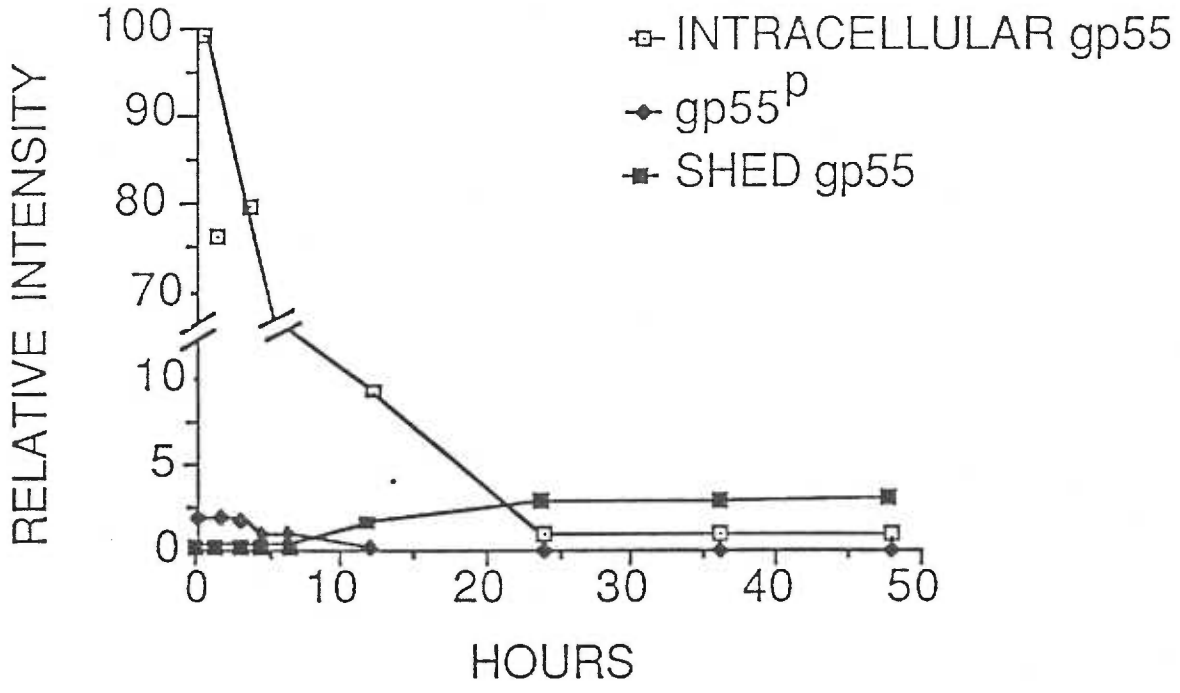
INTRACELLULAR gp55
gp55^{p}
SHED gp55
RELATIVE INTENSITY
100
90
80
70
10
5
0
0
10
20
30
40
50
HOURS

pulse-chase analysis and quantitated by densometric scanning the amount of gp55 that remained intracellular, the amount that was processed to $gp55^{p}$, and the amount that was shed into the medium (Fig. 21). The results clearly show that the quantity of $gp55^{s}$ that was eventually shed into the culture medium was very similar to the quantity of $gp55^{p}$ that was initially at the cell surface after the 2 h pulse-labelling period and never exceeded 4% of the total gp55 labelled. The $gp55^{p}$ remained associated with the cells for up to 4 h before it was shed. Although $(gp55)_2$ dimers were not analyzed in this study, they constituted approximately 10% of the total labelled gp55 components (see Fig. 20) and they seemed to be degraded within the cells with the same kinetics as the gp55 monomers. We conclude from this analysis that $gp55^{p}$ is the precursor to $gp55^{s}$ and that continual processing of intracellular gp55 does not occur. In addition, the results suggest that the $(gp55^{p})_2$ molecules form within 1-2 h from their precursors and that the unprocessed gp55 monomers and dimers that remain after this time are not capable of being processed to the cell surfaces. These molecules are eventually degraded within the cell.

3. Sucrose Velocity Centrifugation

Previous reports have indicated that cellular proteins can noncovalently bind to proteins to retain them in the ER (120, 121). To explore the possibility of noncovalent associations between gp55 and any other proteins, erythroleukemia cells were lysed in conditions to maintain noncovalent bonds. The cell lysate was then fractionated by rate zonal centrifugation in a sucrose density gradient. The gradient was fractionated, immunoprecipitated, and analyzed by immunoblotting under nonreducing (Fig. 22, top) and reducing conditions (Fig. 22, bottom). Viral

proteins forming a noncovalent complex would have a greater sedimentation coefficient, in comparison to the unassociated protein, and would migrate into the denser portion of the gradient. However, as seen in Fig. 22, the viral envelope glycoproteins are localized only in the lower density portion of the gradient and show no indication of abnormal sedimentation. The $gp55^{p}$ component could be visualized with a longer exposure of the autoradiographs (data not shown). Consistent with the other viral glycoproteins, $gp55^{p}$ was localized exclusively in the lower density portion of the gradient. We conclude from this analysis that the Friend virus glycoproteins do not form noncovalently associated complexes that are stable in the conditions used for this analysis.

Figure 22. Sucrose gradient analysis of viral glycoproteins. Approximately $2.5x10^6$ F745 cells were lysed in 500 ul 50 mM Tris-HCl, pH 7.5, 150 mM NaCl, and 1% Triton X-100. The lysate was layered onto a 5-30% continuous sucrose gradient that overlaid a 0.5 ml 60% sucrose cushion. Centrifugation was carried out at 45,000 rpm in a SW55Ti rotor for 15 hrs at 4^oC. Fractions were collected, diluted with an equal volume of 2x immunoprecipitation buffer, and immunoprecipitated with anti-gp70 serum. Immunoprecipitates were electrophoresed without (Top) and with (Bottom) reduction. Viral glycoproteins were detected by immunoblotting using anti-gp70 serum.

NONREDUCED

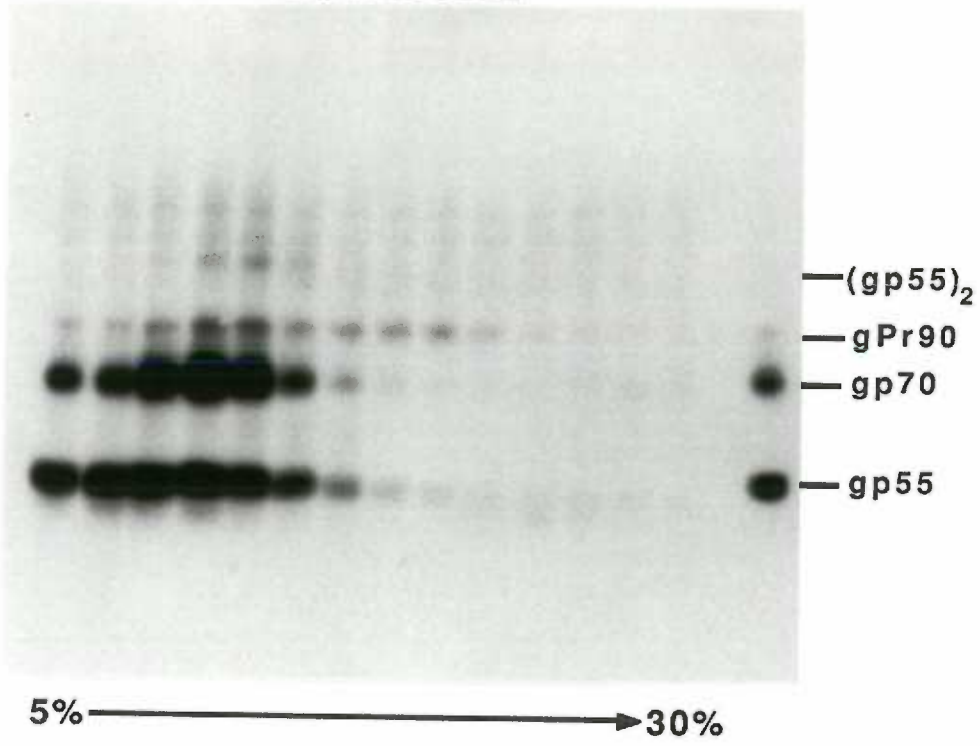

REDUCED

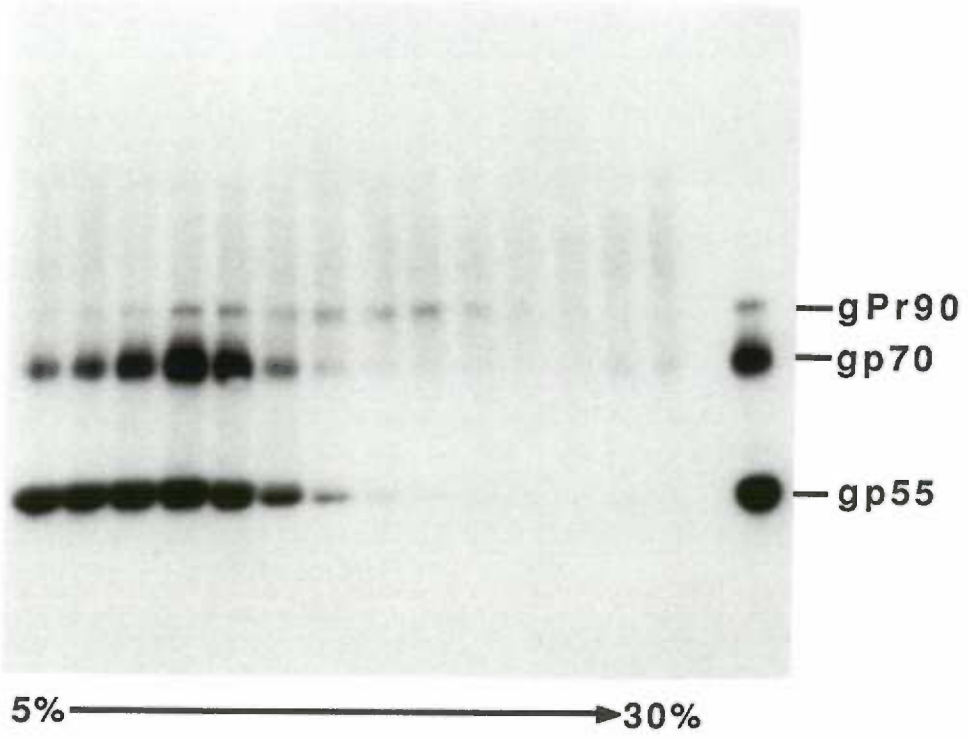

D. Discussion

1. Summary of Friend envelope glycoprotein processing

The post-translational processing of the MuLV envelope glycoproteins described in this chapter is in good agreement with previous studies (31, 32, 105). The gPr90 is synthesized in the RER and is slowly transported to the cell surface (summarized, Fig. 23). Within 12 h after metabolic labelling (Fig. 20), all of the gPr90 precursor polyprotein has been processed. The first proteolytic processing to the gp70 and disulfide-linked gp70/p15E components can be observed approximately 30 min after synthesis (Fig. 17). As with other proteins (133), this proteolysis step presumably occurs within the Golgi apparatus or shortly thereafter. Localization at the cell surface occurs within 5-10 min after this cleavage (116). A portion of the cell surface gp70 remains associated with the cell surface up to 24 h after labelling (Fig. 20). However, the majority of gp70 is found in the medium both as a soluble molecule and incorporated into virions.

We have clearly demonstrated that additional post-translational processing is necessary for the intracellular transport of the SFFV envelope glycoprotein (summarized, Fig. 23). The vast majority of gp55 is found as a monomer in the RER, but a portion of the intracellular gp55 molecules are dimerized. Moreover, all of the cell surface gp55 molecules are dimerized (Figs. 19 and 20). The $gp55^{p}$ remains stably associated with the plasma membrane for up to 4 h (Figs. 20 and 21), but is eventually shed into the medium presumably after cleavage of its carboxy-terminus membrane anchor. In the medium gp55 can be found both as a dimer and monomer (Fig. 20).

2. gp55 Biosynthesis

Figure 23. Overall summary of Friend viral envelope processing in erythroleukemia cells. See text for complete explanation.

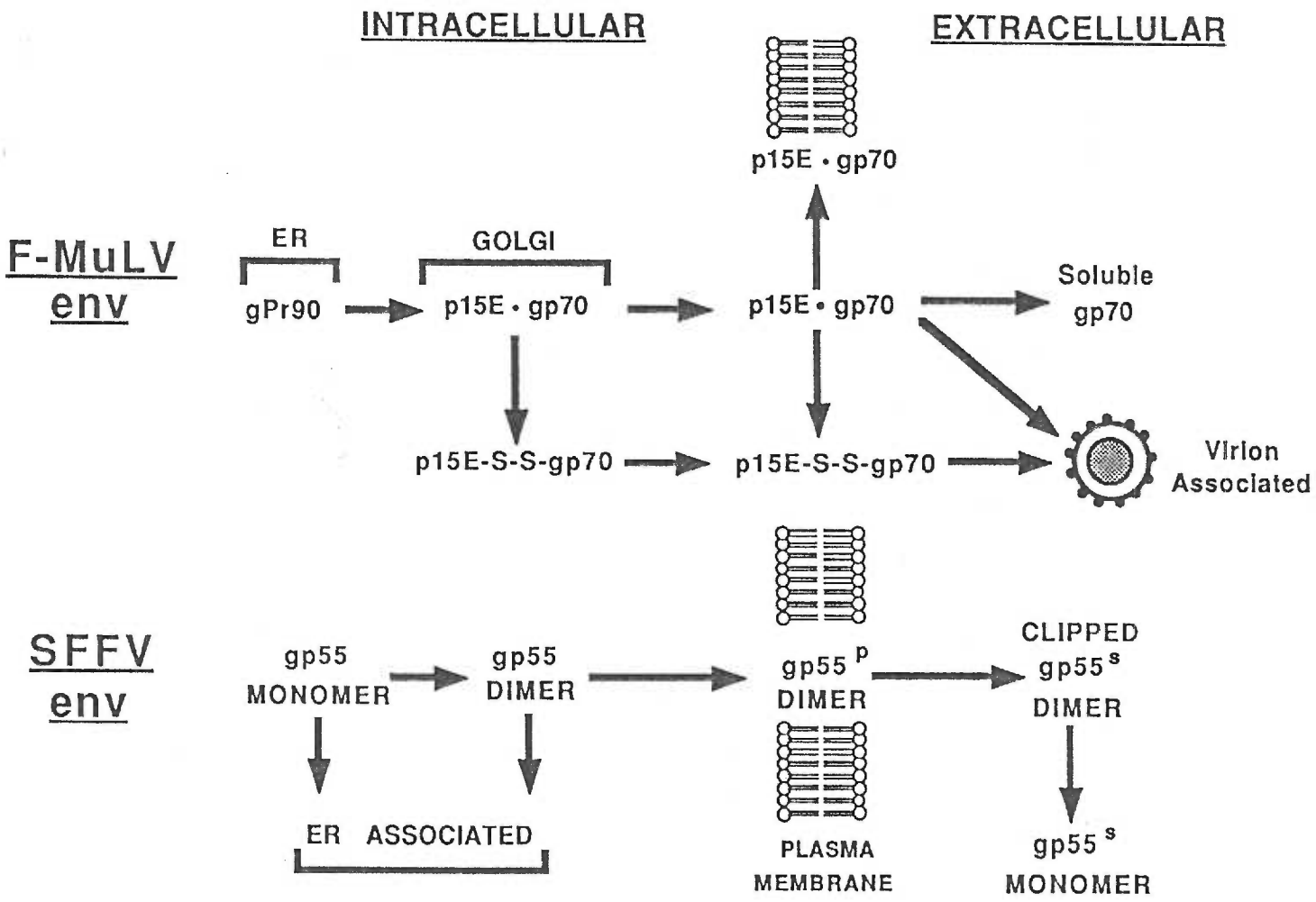
INTRACELLULAR
EXTRACELLULAR
F-MuLV env
ER
GOLGI
gPr90
p15E • gp70
p15E • gp70
p15E • gp70
Soluble gp70
p15E-S-S-gp70
p15E-S-S-gp70
Virion Associated
SFFV env
gp55 MONOMER
gp55 DIMER
gp55 p DIMER
CLIPPED gp55 s DIMER
ER ASSOCIATED
PLASMA MEMBRANE
gp55 s MONOMER

The importance of cell surface expression of gp55 in the development of erythroleukemia has been well documented (79, 81, 83). Therefore, we have thoroughly characterized the biosynthesis, assembly, and post-translational processing of the newly discovered cell surface dimer. These results have provided us with a working model for the inefficient intracellular transport of gp55 (summarized, Fig. 24). Details of this model are presented below.

The SFFV envelope glycoprotein is synthesized on endoplasmic reticulum bound ribosomes. The first biosynthetically labelled gp55 molecules with the electrophoretic mobility of the mature glycoprotein can be seen within 1 min after labelling (Fig. 18). Prior to the appearance of this component, bands can be seen with both slower and faster electrophoretic mobilities. These may represent gp55 precursor molecules that are quickly converted to the mature gp55 form. Possible post-translational modifications to the nascent gp55 polypeptide may include leader sequence removal (134), carbohydrate trimming (135), and complete disulfide bond formation and protein folding (113, 126, 127).

The folding of newly synthesized proteins requires the oxidation of sulfhydryl groups to form disulfide bonds. Classic experiments by Anfinsen (reviewed 136) demonstrated that an unfolded ribonuclease could be converted to a homogeneous end product by the slow removal of denaturant and the addition of an oxidizing agent. This folding process was driven entirely by the free energy of conformation that was gained in going to the thermodynamically stable, native structure. However, the kinetics of this process was very slow and the existence of a disulfide interchange enzyme was proposed to catalyze the oxidation and folding *in vivo*. The enzyme that has been termed protein disulfide-isomerase

Figure 24. Proposed model for gp55 biosynthesis, oligomerization, and cell surface transport. See text for complete explanation.

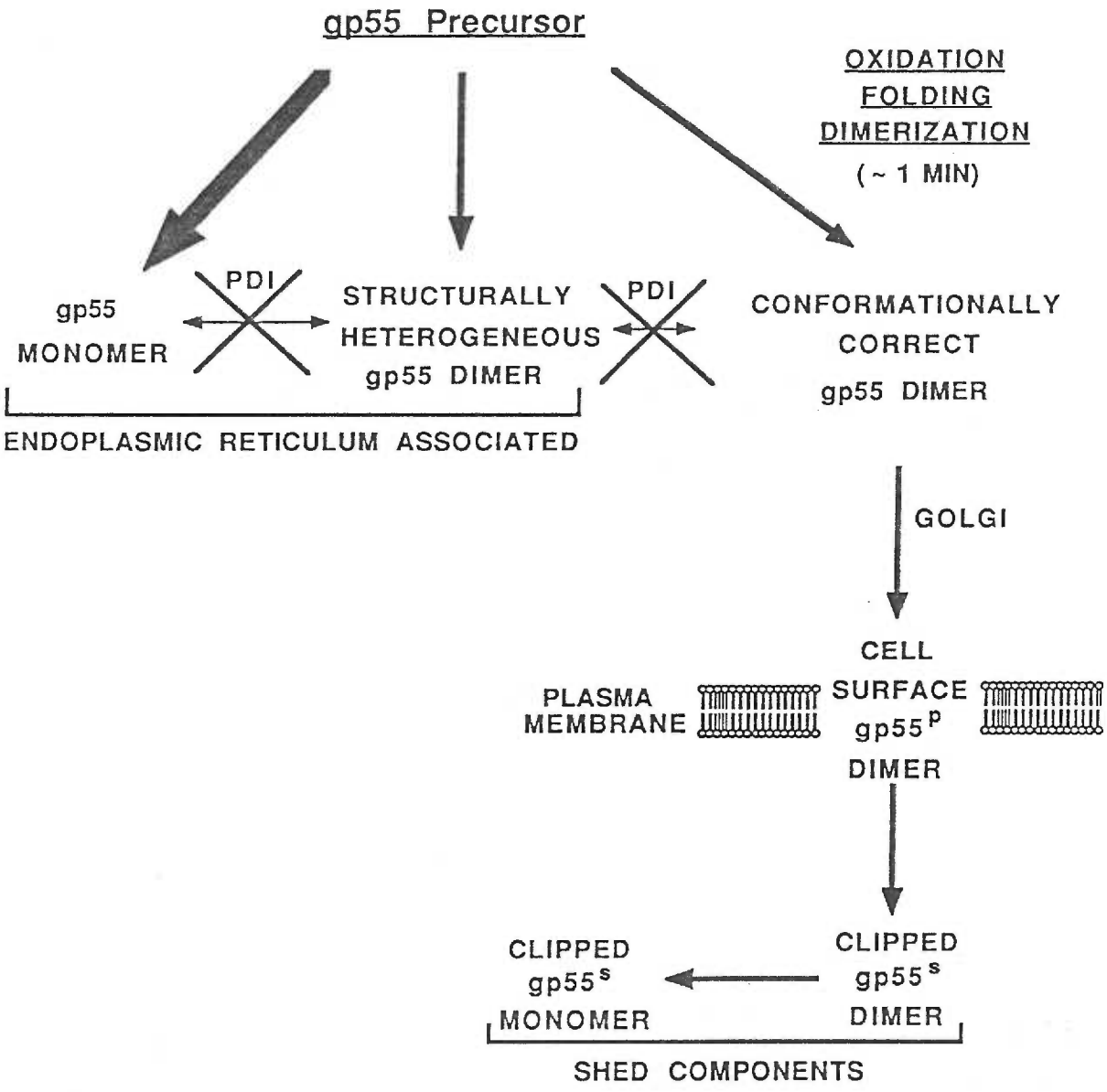
gp55 Precursor
OXIDATION
FOLDING
DIMERIZATION
(~ 1 MIN)
PDI
gp55
MONOMER
STRUCTURALLY
HETEROGENEOUS
gp55 DIMER
PDI
CONFORMATIONALLY
CORRECT
gp55 DIMER
ENDOPLASMIC RETICULUM ASSOCIATED
GOLGI
CELL
SURFACE
gp55 P
DIMER
PLASMA
MEMBRANE
CLIPPED
gp55 S
MONOMER
CLIPPED
gp55 S
DIMER
SHED COMPONENTS

(PDI) has been proposed to be this interchange enzyme (reviewed 128, 129). Although PDI can catalyze refolding *in vitro*, the *in vitro* rate is dramatically slower than the folding rate *in vivo* (113, 126, 127, 139). However, recent cloning analysis suggests that putative PDI may be the beta-subunit of the enzyme prolyl 4-hydroxylase (138, 139). Recent work on some proteins has suggested that glutathione (131) or cystamine (132) may also form mixed disulfide intermediates to catalyze oxidation and isomerization of protein disulfide bonds.

We find no evidence for a disulfide-bonded PDI-gp55 intermediate complex. Such a complex would be expected to have an apparent M_r ~125,000 when analyzed without reduction. This transient intermediate would be expected to disappear gradually during the pulse-chase analysis (Fig. 17) and to form rapidily in the pulse analysis (Fig. 18). We detect no such intermediate in these labelling experiments. Therefore, we have no *in vivo* evidence for the participation of PDI in gp55 oxidation and folding. In addition, the minor bands detected with slower electrophoretic mobilities than that of gp55 (Figs. 17A and 18) do not resolve into the mature gp55 band with reduction (Fig. 17B, data not shown). This suggests that these bands do not represent unfolded precursors of gp55 that contain mixed disulfides with smaller molecules such as glutathione or cystamine. Thus, our results suggest that disulfide-bonded intermediates may not be formed to catalyze free sulfhydryl oxidation and folding of gp55.

3. gp55 Dimerization

The gp55 dimers represent only a small percentage of the total gp55 synthesized. The majority remains as an intracellular monomer within the RER. Therefore, detection of dimer formation during biosynthetic labelling has proven

very difficult. Usually labelling for 5 min or more is required to unambiguously visualize the dimer (e.g., Figs. 17 and 19). However, results presented in Chap. IV suggested that the mature gp55 has no free sulfhydryls. This means that dimerization must take place only within the first minute after synthesis when free sulfhydyrls must exist prior to complete folding. Consistent with this assumption is the pulse-chase analysis in Fig. 17. The dimer level present after a 5 min pulse is equivalent to the dimer level after a 60 min chase period. This demonstrates that the metabolically labelled gp55 monomer is not being continually dimerized after its synthesis. Therefore, we conclude that gp55 dimerization is a very early post-translational modification and can only occur during a short time span (~1 min) after gp55 synthesis.

Previous work on the oligomerization of IgG immunoglobulins is consistent with the dimerization kinetics of gp55. Bergman and Kuehl showed that the initial step in the covalent assembly of immunoglobulins was the disulfide bond formation between a nascent heavy chain and a completed heavy or light chain depending on the cell type (140). Moreover, pulse-chase analysis demonstrated that only freshly made light chains (within ~2 min) could be covalently assembled. These results demonstrate that disulfide bonded oligomerization is often an early post-translational modification.

Our analysis of the post-translational processing of gp55 clearly demonstrates that the glycoprotein must be dimerized to reach the cell surface. However, not all dimerized gp55 molecules escape the RER (Fig. 24). Dimerization in concert with some other factor must be needed to generate a transport competent gp55 molecule. Two-dimensional electrophoresis of the gp55 components (Figs. 7, 8, and 9, Chap III) has suggested that the intracellular

dimers can be separated into a cluster of distinct components while only a single dimer can be found at the cell surface. This would suggests that only a unique homodimer is competent for cell surface expression. In addition, intrachain disulfide bond heterogenity was implied by two-dimensional seperation of gp55 (Figs. 7 and 8, Chap. III). Therefore, we propose that the intracellular gp55 molecules represent a structurally heterogeneous population of molecules. These structural differences would be generated by heterogenity in both intrachain and interchain disulfide bonding and perhaps additionally by simple folding variations. Only the formation of dimers that obtain a unique conformational structure will be able to escape the RER and to be transported to the cell surfaces. The monomers that do not oligomerize and the dimers that fail to obtain this conformation remain trapped within the RER.

4. Oligomerization and intracellular transport

The importance of protein oligomerization for transport to the cell surface has been well studied. Both the vesicular stomatitis virus G protein and the influenza hemagglutinin glycoproteins must form noncovalent associated trimers in order to reach the cell surface (95, 122, 125). Mutations that disrupt this trimer formation result in a blockage of transport and glycoprotein subunits that accumulate in the RER (95, 122, 125). More significantly, a small percentage (~10%) of the hemagglutinin normally does not reach the cell surface and accumulates as a trimer in the RER. Thorough biochemical and biophysical studies on these glycoproteins suggest that the cell surface trimers are folded differently than the nontransported trimers. This has led to the proposal that a "correct" tertiary and quanternary structure may be a general requirement for

transport of transmembrane proteins from their site of synthesis in the RER (95, 122). The processing of the SFFV envelope glycoprotein to the cell surface strongly supports this hypothesis.

Additional evidence supporting the significance of protein folding in oligomerization and cell surface transport was presented for two cellular proteins. The nicotinic acetylcholine receptor was shown to pass through at least two distinct intracellular conformations en route to the plasma membrane (141). During intracellular processing, the alpha-subunit gained the ability to bind to the ligand bungarotoxin and became stably associated with the beta-subunit prior to cell surface detection (142). Likewise, the beta-subunit of human chorionic gonadotropin progressed through various conformations during its post-translational processing (143). The earliest form of beta-subunit detected was incompletely folded and did not oligomerize with the alpha-subunit. Within 4 minutes after synthesis, the beta-subunit was fully folded, dimerized with the alpha-subunit, and was efficiently secreted from the cell. Interestingly, a small portion of the beta-subunits folded differently and formed an unassociated intracellular pool. These results provide strong evidence that a protein's overall conformation can be a critical factor in determining the eventual processing fate of the molecule.

5. No evidence for isomerization

Obtaining the correct overall three dimensional structure appears to be critical for transport to the cell surface. A major factor in determining protein structure is the formation of disulfide bonds. The mechanism of disulfide bonding in proteins *in vivo* is still very poorly understood. *In vitro* studies have indicated

that protein folding is a two-step process. First, randomly cross-linked disulfide bonds are formed. Second, these non-native disulfides are isomerized to native ones through a series of thiol-disulfide interchange reactions (reviewed 128, 129). Previous work with the ribonuclease A and trypsin inhibitor molecules suggested that the final product represented both the biologically active and thermodynamically most stable form of the protein (137). This interchange reaction is believed to be the rate-limiting step in the folding pathway. As previously described, the enzyme protein disulfide-isomerase (PDI) has been shown to have the ability to catalyze the formation of both intrachain (137) and interchain (144) disulfide bonds *in vitro.* Furthermore, PDI can isomerize certain proteins *in vitro* to form the "correct" pattern of disulfide bonds needed for the protein to be biologically active (137, 145, reviewed 128).

The mechanism of disulfide-interchange *in vitro* has been shown to require the formation of disulfide-linked intermediates between the enzyme and substrate (137). As previously discussed, our data indicates that no disulfide bonded larger intermediates are formed during gp55 biosynthesis. Although the PDI-protein substrate complex *in vivo* may be unstable, it should have been stabilized by the lysis in the presence of a sulfhydryl alkylating agent. A second, indirect method of analyzing potential PDI enzymatic activity would be to determine if the newly synthesized gp55 intermediates are isomerized. Previous *in vitro* evidence demonstrated that PDI can isomerize a protein to its biologically active and thermodynamically most stable form (137, 145). The biologically active form of gp55 is the structurally unique dimer that is transported to the cell surface. We have clearly shown that post-translational processing of the large intracellular pool of gp55 does not occur to continually generate the cell surface molecules

(figs. 20 and 21). This indicates that the nontransported gp55 molecules are stable after their formation and that no equilibrium exists between the pools of intermediates. This argues against the structural isomerization of intracellular molecules to form the biological active form of gp55. Therefore, we have no *in vivo* evidence to support the action of PDI, or any other molecule, in the catalysis of oxidation, folding, or isomerization of newly synthesized proteins. Rather, our results suggest that substantial isomerization probably doesn't occur intracellularly. In addition, recent cloning analysis suggests that putative PDI may be the beta-subunit of the enzyme prolyl 4-hydroxylase (138, 139).

6. Endoplasmic reticulum retention

Different membrane proteins exit the RER at characteristic rates (116, 117). Whether this is because a specific interaction with a transport receptor is required or because proteins are retained in the RER until they can enter the bulk flow transport has not been unambiguously established. Regardless of which model proves to be correct, both require the retention of proteins in the RER until they are properly folded to either bind to a receptor or move with the bulk flow. It has been proposed that a family of proteins termed "molecular chaperones" reside in the RER to aid in the correct folding of proteins and to noncovalently retain improperly folded proteins (reviewed 123). This family includes a diverse set of proteins, including heat shock proteins, BiP, PDI, and a binding protein for the large subunit of ribulose biphosphate carboxlyase-oxygenase (Rubisco).

We have no evidence for cellular proteins binding to the gp55 monomer or dimer that remains in the RER. Sucrose velocity gradient analysis (Fig. 22) suggests that the gp55 intermediates do not form stable noncovalent complexes.

This would also mean that gp55 is not aggregating to form a "precipitant-like" complex in the RER. This type of aggregation was recently observed for a mutant VSV G protein defective in cell surface transport (146). The VSV G protein aggregate was easily detectable upon sucrose gradient analysis. Therefore, retention of gp55 in the RER may not be mediated by stable protein binding or aggregation. Instead, as suggested by Pfeffer and Rothman (118), retention in the RER may be less specific and similar to adsorption chromatography. The RER membrane proteins may retain nontransported molecules by nonspecific electrostatic and/or hydrophobic interactions. Only proteins that are folded and/or oligomerized in such a way to minimize these interactions may be able to escape the RER.

7. Signal patch theory for intracellular transport

For a protein to escape the RER it must contain some type of signal or structure that makes it different from the nontransported molecules. As mentioned above, such signals may include charge and hydrophobicity differences. Experimental evidence from a variety of sources suggest that these signals are likely to be composed of regions on the surface of the protein that are directly related to the overall three dimensional structure. These have been referred to as signal patches (reviewed 118). Unlike specific covalent modifications thought to target proteins (i.e. leader sequences), signal patches would be formed from noncontiguous regions of the polypeptide chain and only brought together during protein folding and/or oligomerization. Accordingly, signal patches are conformation-dependent and a wide range of structural mutations can disrupt them and, consequently, cell surface transport.

Our analysis on the processing of gp55 to the cell surface indicates that a strict structural requirement exists for transport out of the RER. Both the proper folding and dimerization are essential. Experimentally, both of these steps occur very early in the biosynthesis of gp55 and may be inextricably associated. The intracellular transport of gp55 does not appear to be controlled by an enzyme-mediated rate-limiting step. Instead, post-translational processing quickly generates gp55 molecules that are either competent or incompetent for transport. No detectable isomerization occurs between these intermediates to continually generate cell surface molecules. Therefore, the inefficient processing of gp55 appears to be intrinsic to the molecule because of the glycoprotein's structure and ultimate folding pattern. Only the "correctly folded" dimers that obtain the necessary signal patches to escape the RER will be transported to the cell surfaces.

VI. Expression of Cellular Oncogenes and SFFV *env* during Friend Erythroleukemia and Differentiation.

A. Abstract

The Friend virus complex causes a progressive murine erythroleukemia. The disease culminates after 4-8 weeks in the formation of leukemia cells that can be cultured indefinitely and that can be induced to differentiate only by treatment with dimethyl sulfoxide (DMSO) or other chemical inducers. We measured the expression of the Friend spleen focus-forming virus (SFFV) *env* glycoprotein (gp55) and of thirteen cellular oncogenes throughout leukemic progression and during DMSO-induced differentiation. The transcripts of SFFV *env*, c-*myc*, c-*myb*, p53, and c-Ha-*ras* increased substantially in the final stage of leukemic progression, in parallel with a reduction in spontaneous erythropoiesis. Genomic blot analyses of three independently formed advanced leukemias revealed that the c-*myc* oncogene was variably amplified in its copy number (0-20 fold), and that the p53 gene was rearranged in one cell line. DMSO-induced differentiation rapidly reduced transcript levels for all four of these cellular oncogenes. Moreover, a rapid transient reduction in the quantity of gp55 on the plasma membranes occurred very early in the differentiation process and was caused by enhanced shedding into the culture medium. We propose that increases in expression of SFFV *env* and of cellular oncogenes may contribute to leukemic progression by interfering with erythropoiesis.

B. General introduction

Friend virus causes a progressive erythroleukemia in susceptible mice (reviewed 2, 3). The early phase of the disease is characterized by extensive erythroid hyperplasia, development of macroscopic spleen foci, splenomegaly, and polycythemia or anemia depending on the strain of virus. However, the infected erythroid cells from this stage appear to be premalignant as judged by their limited proliferative capacity and inability to cause tumors. The infected erythroblasts spontaneously embark on the erythropoietic pathway *in vivo* and in cell culture, although the process is abnormal and is substantially ineffective (54-57). In contrast, approximately 3-8 weeks post-infection malignant Friend cells begin to form. These cells can be maintained in long term culture, are capable of producing tumors in syngeneic mice, and can be induced to differentiate only if they are treated with dimethylsulfoxide (DMSO) or certain other compounds (64-66). Therefore, the Friend system provides an excellent model for studying leukemic progression and erythroid differentiation.

An understanding of the relevance of Friend cell differentiation to normal differentiation requires information about the pathologic effects of the virus and about changes that occur during leukemic progression and establishment of the cell lines in culture. Such an integrated understanding has been lacking and is especially important because leukemic progression may involve changes that reduce the ability of the neoplastic cells to differentiate (15, 16). Presumably, induction of differentiation *in vitro* must include abrogation of these leukemic abnormalities.

It is currently believed that the aberrant expression of cellular oncogenes can play an important role in the initiation, maintenance, and progression of cellular malignancies (147, 148). Experimental evidence suggesting a critical role

for cellular oncogenes in neoplastic growth comes from several sources (reviewed 147-149). They include: 1) sequence homology between cellular oncogenes and known transforming viral oncogenes; 2) transfection studies showing the transforming potential of cellular oncogenes in NIH 3T3 cells and primary embryo fibroblasts; 3) the localization of cellular oncogenes at or near the site of specific, tumor-associated chromosomal translocations; and 4) amplification of cellular oncogenes in some human tumors. In addition, cell growth after mitogenic stimulation increases cellular oncogene expression, while terminal differentiation decreases expression. In this study we present a comprehensive analysis of cellular oncogene and SFFV *env* expression throughout progression and differentiation of Friend erythroleukemia.

C. Results

1. Stages of erythroleukemic progression

The principal targets for the Friend virus complex are immature erythroblasts classified as burst-forming units erythroid (58). When infected with SFFV, these cells proliferate and migrate to the spleen (54). By 14 days, the spleen is enlarged 15-20 fold due to proliferating erythroblasts and their differentiating hemoglobin-containing derivatives in the red pulp. However, these cells are premalignant as judged by their limited self-renewal capacity and by their ability to differentiate (54-57). We used normal spleens and spleens from mice with phenylhydrazine-induced hemolytic anemia (72, 150) as controls. Anemia causes murine spleens to become a major site for erythropoiesis (72, 150) and to increase severalfold in size. Comparisons also included spleens from mice 14 days after intravenous injection with a polycythemic strain of Friend virus (91) and several independently isolated erythroleukemia cell lines.

The relative quantities of actin and ß-globin transcripts were analyzed in the poly (A)+ RNAs by the Northern blot method. As seen in Fig. 25A (right panel), the relative proportion of ß-globin mRNA was increased about 5-fold in anemic spleens (lane 2) and about 10-fold in 14 day post-infected spleens (lane 3) compared with normal spleens (lane 1). In contrast, the advanced leukemias are blocked in the proerythroblast stage of differentiation (151) and their relative quantities of ß-globin mRNA are correspondingly very low (lanes 4 and 5). These results are consistent with histological results and with other evidence (151) that progression of erythroleukemia is associated with a reduced tendency of the neoplastic cells to differentiate. The polycythemia strain of SFFV used for these studies causes an initial polycythemia. However, transplantation of resulting

Figure 25. Gene expression during erythroleukemic progression. (A) Expression of actin, pAC269 (152) and ß-globin, *Hind* III probe B (153). (B) Expression of cellular oncogenes Ha-*ras* , HB-11 (154); N-*ras*, pAt8.8 (155); *myc* , pM104 BH (156); *myb* , pVM2 (157); and p53, pp53-208 (158) through progression. RNA was isolated from uninfected spleens (Lane 1), anemic spleens (Lane 2), 2 week post-infected spleens (Lane 3), and independently isolated erythroleukemia cell lines F745 (Lane 4) and F4.6 (Lane 5). Size markers are in kilobases.

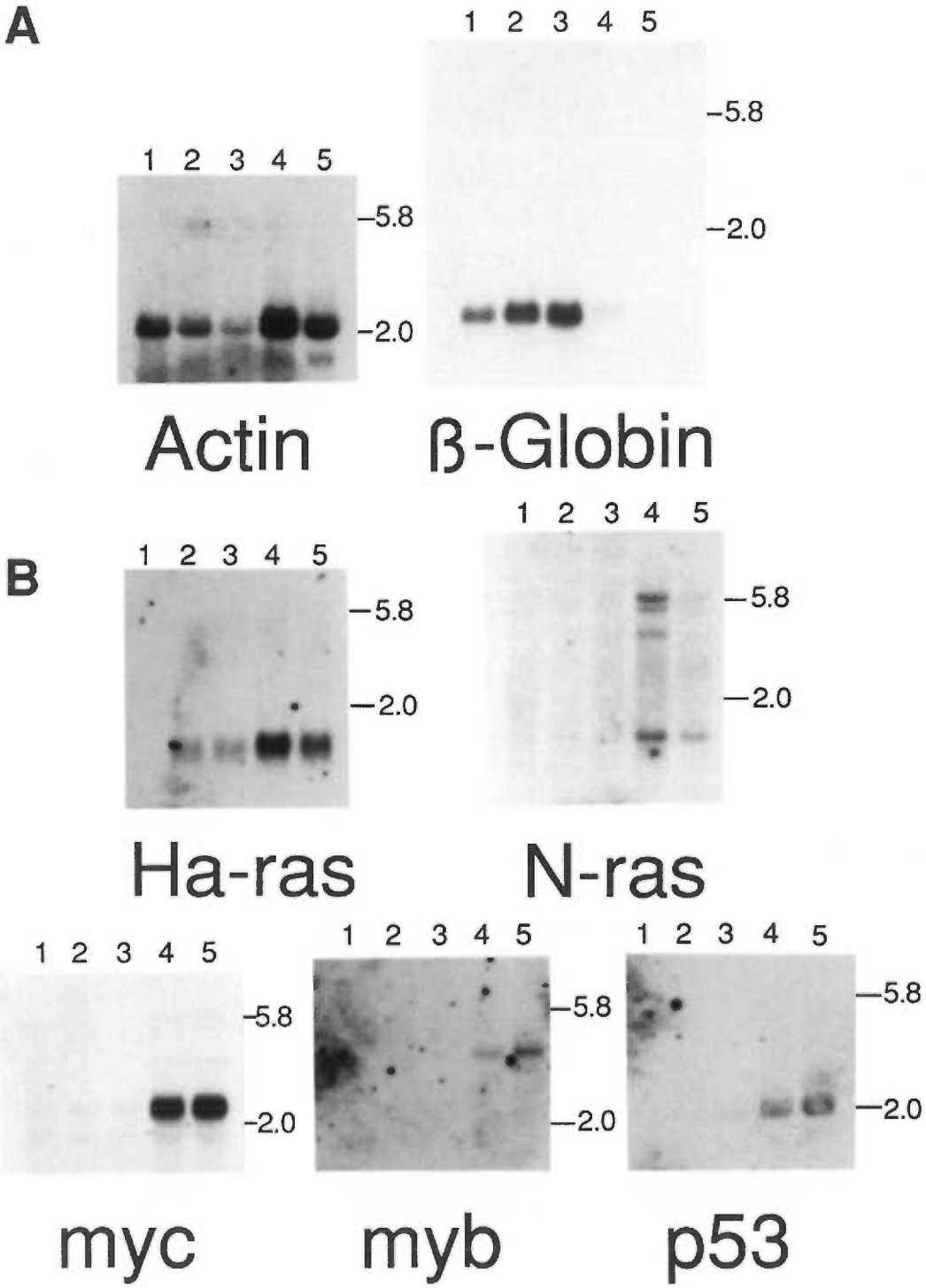
A
1 2 3 4 5
-5.8
-2.0
Actin
1 2 3 4 5
-5.8
-2.0
β-Globin
B
1 2 3 4 5
-5.8
-2.0
Ha-ras
1 2 3 4 5
-5.8
-2.0
N-ras
1 2 3 4 5
-5.8
-2.0
myc
1 2 3 4 5
-5.8
-2.0
myb
1 2 3 4 5
-5.8
-2.0
p53

advanced leukemias into secondary recipients causes a severe anemia. Thus, progression is associated with a reduction *in vivo* in erythropoiesis (C. Spiro, unpublished results).

2. Expression of cellular oncogenes and SFFV env during erythroleukemic progression

We screened for expression of thirteen oncogenes during erythroleukemic progression. These included *erb* A, *erb* B, *fes, fms, fos, fps, mos, myb, myc*, Ha-*ras*, N-*ras*, p53 and *src*. Fig. 25B shows the oncogenes for which transcripts were detected by Northern blot analysis. The c-Ha-*ras* transcript had the expected 1.2 kb size and was seen both in the anemic and infected erythroid cells. The expression of c-Ha-*ras* in the anemic spleen (lane 2), but not in the normal spleen (lane1), suggests that the transcript occurs in immature erythroid cells. In contrast, N-*ras* is expressed primarily in the F745 cell line (lane 4) and gives a range of transcript sizes. In addition to the 5.8 kb band which may be the primary N-*ras* transcript (155) , there are several smaller RNAs of unknown origin. The oncogenes c-*myc*, c-*myb*, and p53 are expressed primarily in the erythroleukemia cell lines. These three oncogenes formed transcripts with the expected sizes of 2.3 kb, 3.8 kb, and 2.0 kb, respectively. In contrast to an earlier report (159), we do not detect an appreciable quantity of c-*myc* transcript in the 2 week post-infected spleens.

Analysis of the SFFV *env* transcripts and protein levels during erythroleukemic progression is shown in Fig. 26. The 5.8 kb RNA is the full length SFFV genome and the 2.1 kb transcript is the processed *env* message (Fig. 26A). In addition, several minor RNAs are also detected and probably represent additional processing events. As can be seen, the SFFV *env* transcripts are greatly increased (c.a., 50-fold) in advanced leukemias (lanes 4 and 5)

Figure 26. Expression of SFFV *env* gene and gp55 glycoprotein through progression. (A) Northern blot analysis of SFFV transcripts using the SFFV BE probe (82). Lanes 1-5 contain 5.0ug of poly A+ RNA isolated from uninfected spleens (Lane 1), anemic spleens (Lane 2), 2 week post-infected spleens (Lane 3), and erythroleukemia cell lines F745 (Lane 4) and F4.6 (Lane 5). (B) Detection by Western blotting of the SFFV *env* glycoproteins using the F-MuLV gp70 antibody. Equivalent amounts of protein (150ug) were analyzed from normal spleen (Lane 1), 2 week post-infected spleens (Lane 2), and cell lines F745 (Lane 3) and F4.6 (Lane 4).

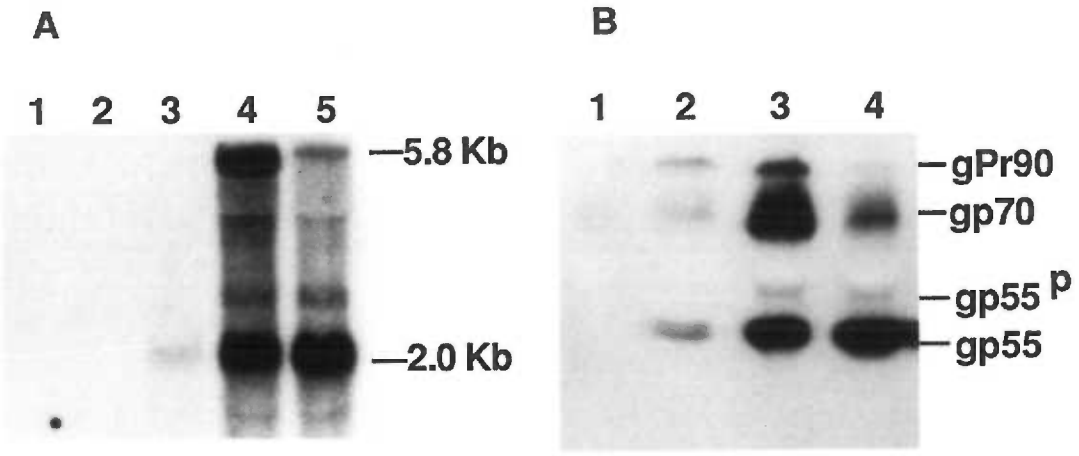
A
1 2 3 4 5
—5.8 Kb
—2.0 Kb
B
1 2 3 4
—gPr90
—gp70
—gp55 p
—gp55

compared with 14 day post-infected spleens (lane 3). The SFFV *env* glycoprotein quantities were analyzed by Western immunoblotting as shown in Fig. 26B. The SFFV-encoded *env* glycoprotein occurs as two components (reviewed 2). The majority has an apparent M_r 55,000 and occurs in the rough endoplasmic reticulum. A second component (designated $gp55^p$), constituting only 2-5% of the total, occurs on cell surfaces . The $gp55^p$ form has a larger apparent M_r (65,000) that is partly caused by processing of its asparagine-linked oligosaccharides in the Golgi apparatus (2, 90). The gp70 and gPr90 components are the MuLV *env* glycoprotein and precursor, respectively. In agreement with the transcriptional analysis, dramatic increases in the gp55 components accompany leukemic progression.

3. Genomic analyses

The DNA from different stages of erythroleukemic progression were analyzed for possible structural alterations in the c-*myc*, c-*myb*, and p53 genes. The FVT/A erythroleukemia cell line (91) was also included in this analysis. Hybridization with a c-*myc* specific probe (Fig. 27A) detected the expected 21 kb *Eco* RI fragment (160) and showed variable amplification in the three erythroleukemia cell lines analyzed (lanes 5,6,7). As an internal control for the amount of DNA transferred to the filters and to estimate the copy number of the c-*myc* gene, we hybridized the blot using both c-*myc* and ß-globin specific probes (Fig. 27B). In addition to the 21 kb fragment detected by the *myc* probe, 18 kb and 6.3 kb fragments were detected with the ß-globin probe (Fig. 27B). The relative c-*myc* intensities were determined by quantitative densitometric scanning of autoradiograms using the ß-globin 6.3 kb signal as the denominator to normalize for experimental variation in quantity of DNA. This analysis indicated a 3- to 5-fold c-*myc* gene copy number amplification in the F4.6 line (lane 6) and

Figure 27. Genomic analysis of c-*myc*, p53, and ß-globin. Blots were probed with ^{32}P-labled *myc,* (panel A); *myc* and ß-globin, (panel B); and p53, (panel C). High molecular weight DNA was isolated from normal livers (Lane1), normal spleens (Lane 2), anemic spleens (Lane 3), 2 week post-infected spleens (Lane 4), and cell lines F745 (Lane 5), F4.6 (Lane 6), and FVT/A (Lane 7). Size markers are in kilobases.

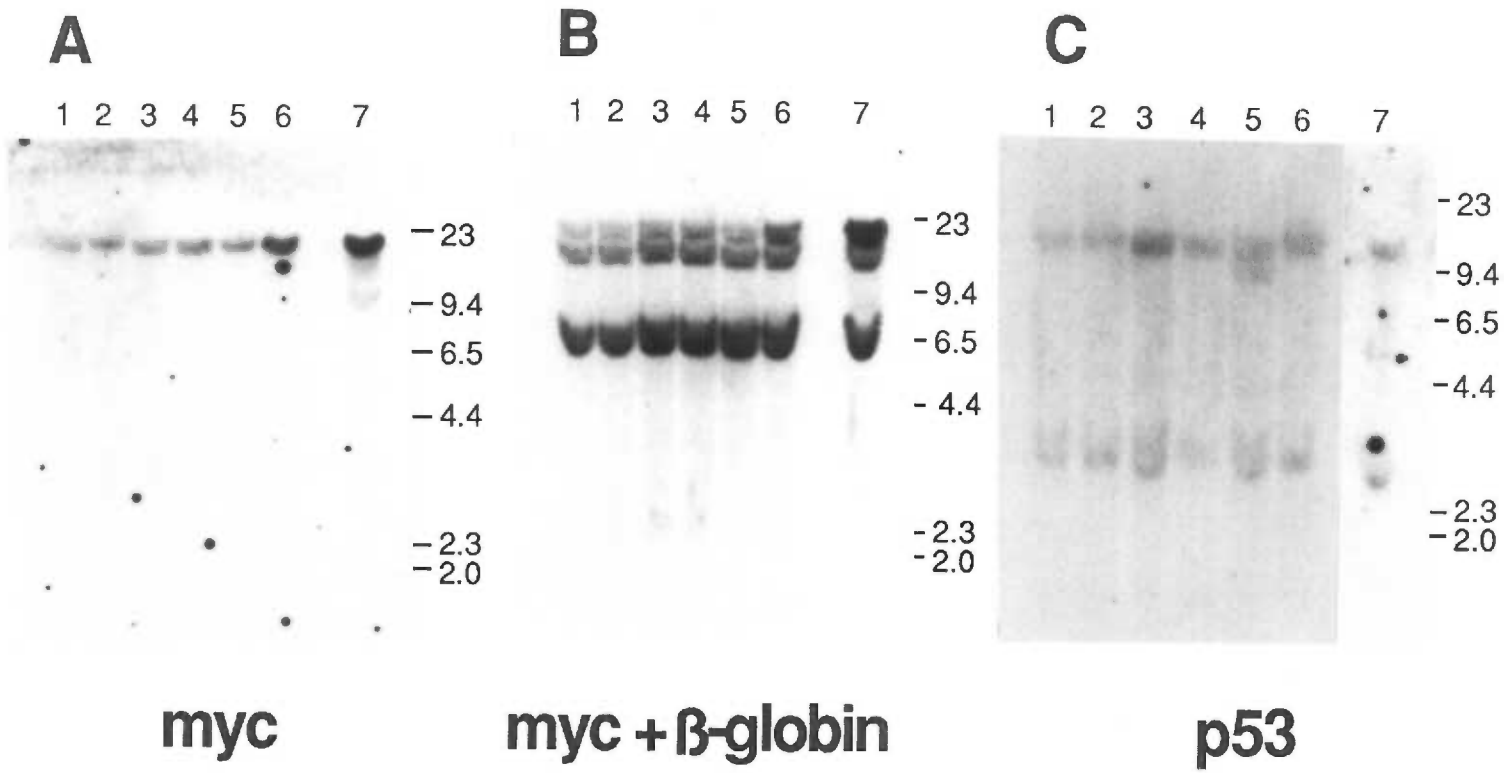
A
1 2 3 4 5 6 7
23
9.4
6.5
4.4
2.3
2.0
myc
B
1 2 3 4 5 6 7
23
9.4
6.5
4.4
2.3
2.0
myc + β-globin
C
1 2 3 4 5 6 7
23
9.4
6.5
4.4
2.3
2.0
p53

a 15- to 20-fold amplification in the FVT/A line (lane 7). In contrast, c-*myc* was not amplified in line F745 (lane 5).

Analysis of *Eco* RI digested DNA samples with a p53 specific probe detected two fragments at 12 kb and 2.8 kb (Fig. 27C). In addition, the F745 line contained a unique fragment at 9.5 kb. Variable rearrangement of the p53 gene was previously reported (161, 162). Hybridization with a c-*myb* specific probe revealed no structural alterations (data not shown).

4. Effect of DMSO-induced differentiation on expression of oncogenes and of SFFV gp55^{p}

Addition of 1.8% DMSO to murine erythroleukemia cell lines induces them to differentiate (66, reviewed 163), but has only a slight effect on cell proliferation within the first 48 h (100). Between 48 and 72 h the cells cease mitosis, and they begin to die after about 100 h (100). Expression levels of actin and ß-globin during terminal differentiation are shown in Fig. 28A. The transcript levels for actin were constant. As expected (66,163), the ß-globin transcript appeared at 48 h and became abundant by 72 h.

Cellular oncogene expression throughout differentiation is shown in Fig. 28B. Expression of c-Ha-*ras* dropped to background levels by 48 h and reproducibly reappeared at a relatively low level during the later stages differentiation. In comparison with the data in Fig. 25B, these results suggest that c-Ha-*ras* transcripts occur predominantly in the erythroblasts of both uninfected and infected mice. In contrast, N-*ras* expression remained constant. In agreement with several earlier studies (164-168), the expression of c-*myc*, c-*myb*, and p53 declined rapidly during DMSO induced differentiation (Fig. 28B). Expression of these oncogenes declines within 3-12 h, although the c-*myc* transcript transiently reforms at 18 h (164-166, results not shown). The transcript

Figure 28. Gene expression during DMSO-induced differentiation. F745 PC4 D2 cells were cultured with 1.8% DMSO and RNA was isolated at 24 h intervals through 96 h. Northern blot analysis was performed with radiolabeled probes described in Fig. 25. (A) Expression of actin and ß-globin. (B) Oncogene expression through differentiation. Size markers are in kilobases.

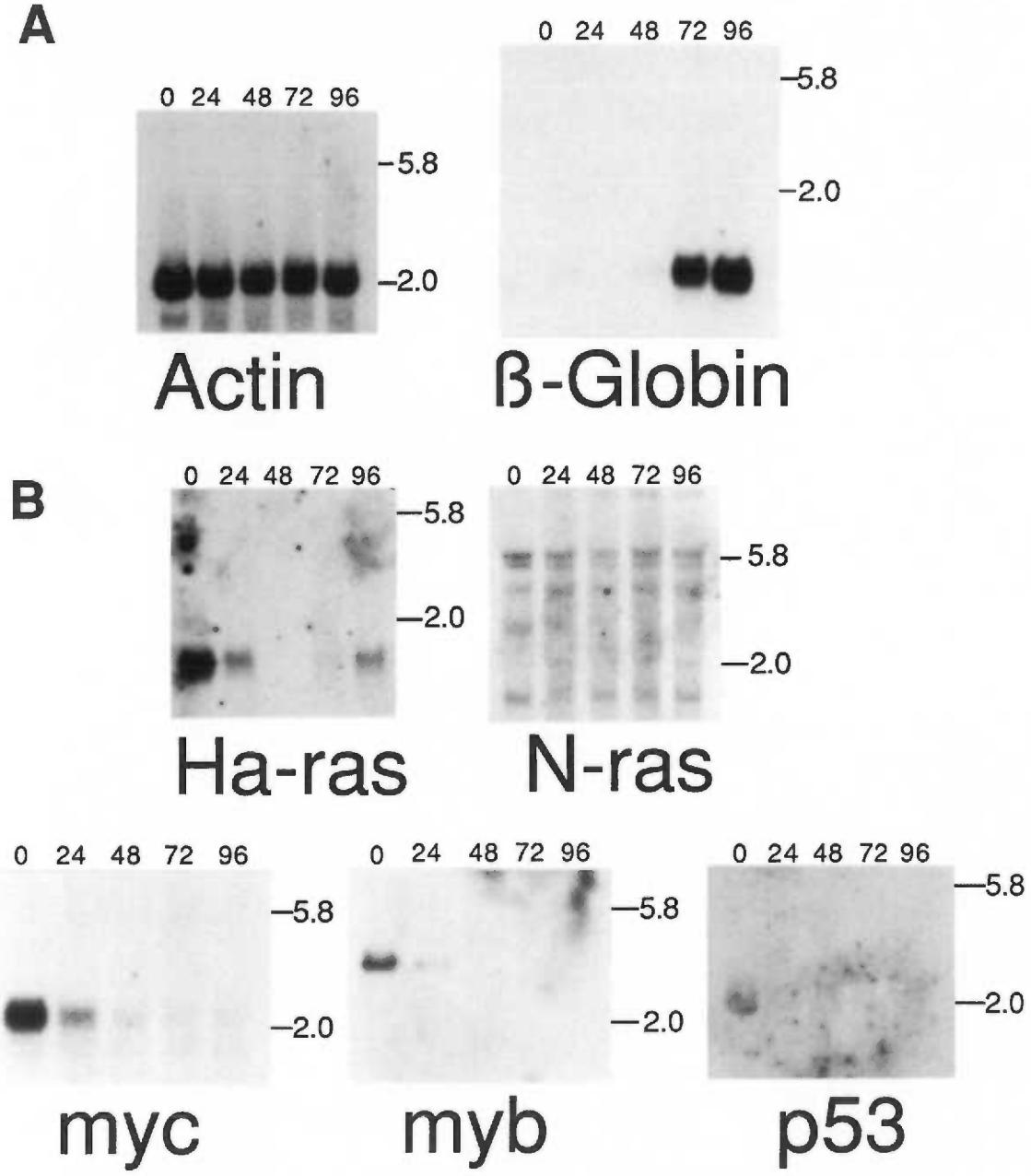
A
0 24 48 72 96
5.8
2.0
Actin
0 24 48 72 96
5.8
2.0
ß-Globin
B
0 24 48 72 96
5.8
2.0
Ha-ras
0 24 48 72 96
5.8
2.0
N-ras
0 24 48 72 96
5.8
2.0
myc
0 24 48 72 96
5.8
2.0
myb
0 24 48 72 96
5.8
2.0
p53

Figure 29. Detection of gp55 glycoprotein and SFFV transcripts during DMSO-induced differentiation. (A) Western blot detection of the gp55 glycoprotein using the 7C-10 monoclonal antibody. (B) Northern blot analysis of SFFV transcripts. RNA was analyzed as described in Fig. 26A.

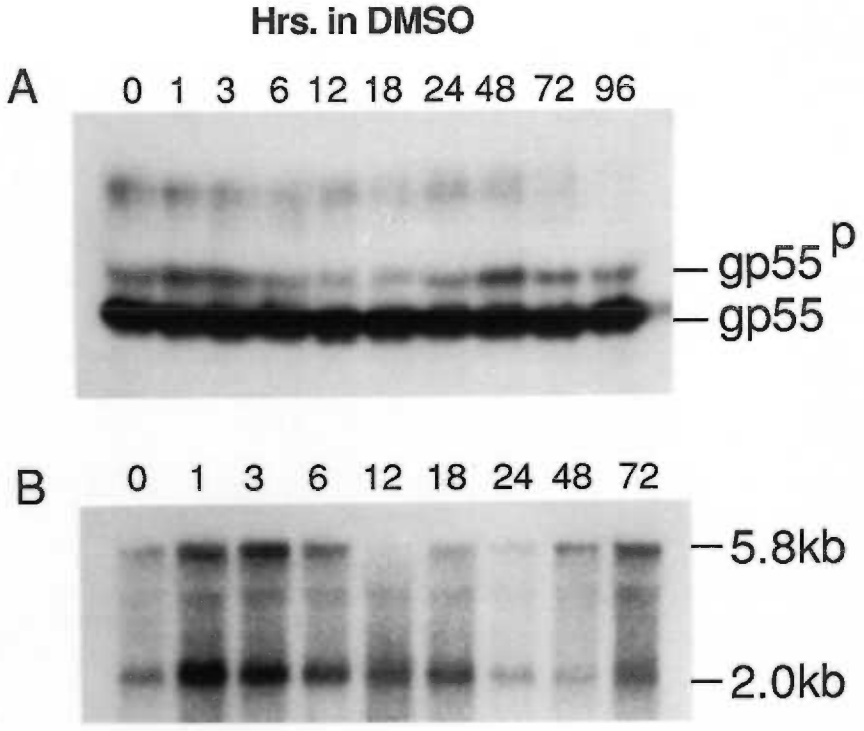
Hrs. in DMSO
A
0 1 3 6 12 18 24 48 72 96
gp55 p
gp55
B
0 1 3 6 12 18 24 48 72
5.8kb
2.0kb

levels for these three oncogenes were near background in our studies by 24 h. Analysis of the gp55 components during DMSO induced differentiation is shown in Fig. 29A. We have reproducibly observed a specific transient decline in the quantity of $gp55^{p}$ during the early phase of DMSO-induced differentiation. The quantity of $gp55^{p}$ began to decline at approximately 3-6 h; it reached a minimum by 12 h; and it increased again between 18-48 h. Densitometry indicated that $gp55^{p}$ was reduced to approximately 20% of the uninduced amount by 12 h. Densitometry of weakly exposed autoradiograms indicated no change in content of the major gp55 component. A similar transient reduction was observed between 12 and 24 h when hypoxanthine was used to induce differentiation (data not shown).

Analysis of the SFFV transcripts is shown in Fig. 29B. The quantities of SFFV RNAs increased sharply within 1 h after DMSO induction. This was followed by a rapid decline in the 5.8 kb RNA and by a slower decline in the 2.1 kb *env* mRNA between 3 and 24 h. Between 24 and 72 h, the quantities of the SFFV RNAs increased. Morphological and biochemical studies have shown that erythroleukemia cell lines efficiently release virions during the early stages of differentiation (91,169). However, as the cells stop proliferating, virion release ceases and virions accumulate within intracellular vacuoles (91,169). This presumably contributes to the increase in viral 5.8 kb RNA after 48 h.

Recent work has shown that $gp55^{p}$ is shed into the medium (52). The effect of DMSO-induced differentiation on $gp55^{p}$ shedding is shown in Fig. 30. The addition of DMSO causes an increase in $gp55^{p}$ shedding during the first 6 h after treatment. However, the quantity of shed gp55 is lower than the untreated control by 12 h and becomes dramatically lower after 18 h. Shedding of gp55 continues through 72 h of DMSO exposure, but at a rate approximately 20% that of the

Figure 30. Analysis of DMSO-induced shedding of the gp55 glycoprotein. Cells were induced to differentiate and the medium was analyzed at the indicated times as described in the Materials and Methods. Relative intensities were determined by quantitative densitometric scanning of autoradiograms using various exposures. The intensity of the 18 h sample without DMSO was set at 1.0 and all other sample values are plotted in comparison to this level.

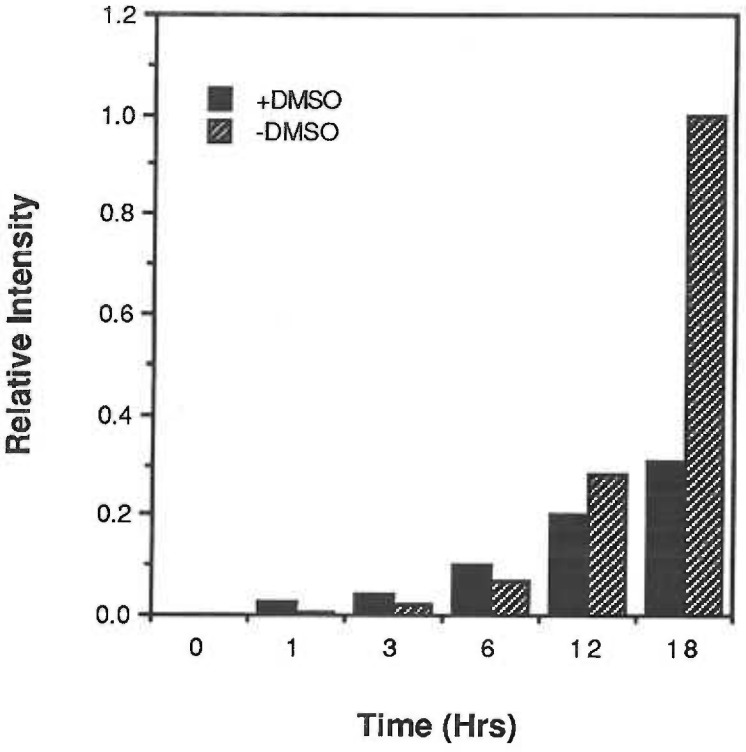
1.2
1.0
0.8
0.6
0.4
0.2
0.0
+DMSO
-DMSO
Relative Intensity
0
1
3
6
12
18
Time (Hrs)

untreated cells (data not shown).

D. Discussion

1. Changes in cellular oncogene expression during leukemogenic progression and differentiation

Expression of c-*myc*, c-*myb*, p53, and c-Ha-*ras* were higher in erythroleukemia cell lines than in uninfected spleens or 2 week post-infected spleens (Fig. 25B). In addition, the quantities of these transcripts declined during DMSO induced differentiation (Fig. 28B). It is unclear from this evidence whether the apparent increased expression of these oncogenes in the late stages of leukemic progression occurred because of a decline in the proportion of terminally differentiating cells or because of an augmentation in expression of these genes within the infected BFU-E. Distinguishing between these possibilities would require analyses of oncogene expression in unavailable pure populations of normal proliferating BFU-E. Despite this uncertainty, our genomic structural studies demonstrated amplifications of c-*myc* gene copy numbers and p53 gene rearrangements in Friend erythroleukemias (Fig. 27). p53 gene rearrangements were previously described in Friend cells (161, 162). As recently reviewed (148), such results imply that changes in expression of these genes were selected during erythroleukemic progression. Therefore, we infer that abnormal expression of c-*myc* and p53 contributes to progression

Chemically-induced differentiation of Friend cells results in a rapid reduction of c-*myc*, c-*myb*, p53, and c-Ha-*ras* transcripts (Fig. 28B). It is unclear from this evidence whether the reduced expression of these genes may cause, or be a consequence of, the differentiation process. However, it was recently shown that constitutive expression of c-*myc* can block Friend cell differentiation (170, 171). This result supports the idea that enhanced expression of c-*myc* could contribute to leukemic progression by interfering with

differentiation.

2. Changes in expression of SFFV env and of gp55 quantities during progression and differentiation

We have observed a substantial increase in SFFV transcripts and gp55 quantities within the erythroleukemia cell lines compared with the infected erythroid cells present in the 2 week post-infected spleens (Fig. 26). This was unexpected because of an earlier report (167) and because the 14 day infected spleens are greatly enlarged (15-20X) and they consist of a 90-95% pure population of erythroid cells that are proliferating under the influence of the SFFV *env* gene (71-73). As with other retroviruses, independently integrated SFFV proviruses are transcribed to widely differing extents depending presumably on their sites of integration in the host chromosomes (49). Therefore, the initially formed neoplasm must contain cells with differing quantities of SFFV gene expression. Presumably, proviral integrations continue to occur during the course of the disease and we propose that progression preferentially selects high-expresser clones.

DMSO-induced differentiation of Friend cells causes a rapid and complex set of changes to the SFFV *env* components (Figs. 29 and 30). Rapid increases in SFFV transcripts and in shedding of $gp55^{p}$ into the culture medium are associated with a transient decrease in the quantity of $gp55^{p}$ that is attached to the cells (Fig.29A). Subsequently, the SFFV transcript quantities decrease (Fig. 29B). Although differentiation does not result in a permanent loss of any of these components, $gp55^{p}$ shedding into the culture medium becomes severely reduced after approximately 10-12 h (Fig. 30). Clearly, substantial changes in SFFV *env* expression occur within the first few hours of DMSO induction. These changes include increased $gp55^{p}$ shedding and changes in gp55 synthesis. This

time period is known to be critical for the commitment of Friend cells to the differentiation pathway (100, 163).

The Friend 745 (164, 172) and F4.6 (91) erythroleukemia cell lines contain anemia and polycythemia strains of SFFV, respectively. Earlier reports suggested that gp55 produced by anemia strains of SFFV were not processed to form $gp55^p$ cell surface components (2, 104). Our Western blot studies establish that both of these cell lines contain similar quantities of $gp55^p$ (Fig. 26B). Cell surface iodination studies confirmed that these $gp55^p$ components were on plasma membranes (data not shown).

3. A possible role for $gp55^p$ in leukemogenic progression and Friend cell differentiation

Faletto et al. (173) recently reported that an early decrease in phosphotidylinositol turnover occurred upon the induction of Friend cell differentiation and that this preceded the decrease in c-*myc* expression. These results suggested that secondary messengers generated at the plasma membrane can stimulate oncogene expression in Friend cells and that this pathway is inhibited during chemical-induced differentiation. Other evidence also suggests that c-*myc* expression can be induced by growth factor binding to membrane receptors (174, 175).

We have previously shown that the SFFV *env* gene is essential for initiating the erythroblastosis that occurs after infection of mice with the Friend virus (79, 80, 83). More recently, using site-directed *env* mutants and spontaneous pathogenic revertants that have second-site (suppressor type) mutations in their *env* genes (82), we have obtained evidence that the pathogenic SFFVs all encode *env* glycoproteins that are expressed on cell surfaces, whereas the nonpathogenic mutant glycoproteins are exclusively

intracellular. The pathogenic *env* glycoproteins also specifically interact with the cell surface receptors for dual tropic MuLVs (83). Consequently, we have proposed that $gp55^{p}$ causes erythroblastosis by binding to a plasma membrane receptor. This interaction presumably generates a constitutive transmembrane signal that stimulates proliferation of infected erythroblasts. We propose that the DMSO-induced loss of $gp55^{p}$ would reduce this receptor-mediated signalling and that this might initiate changes in expression of cellular oncogenes and thereby lead to erythropoiesis.

VII. Identification of SFFV Integration Sites with a "Tagged" Helper-free Virus.

A. Abstract

A colinear molecular clone of the Lilly-Steeves polycythemia strain of Friend spleen focus-forming virus (SFFV) was modified by inserting a 215 base pair "tag" of SV40 DNA into its nonfunctional *pol* gene region. The DNA was then transfected into Psi-2 packaging cells and helper-free tagged SFFV was recovered in the culture medium. Injection of this helper-free virus into NIH/Swiss mice caused transient mild splenomegaly and formation of spleen foci at 9-10 days. Although the vast majority of infected erythroblast clones then differentiated and died out, rare cells that were present in only 20-30% of the mice grew extensively by 26-33 days to form transplantable leukemias. Clonality of these leukemias was established by a Southern blot analysis of their DNAs, using several restriction endonucleases and the SV40 tag as a hybridization probe. All transplantable leukemias lacked helper virus contamination and contained a single tagged SFFV provirus that actively expressed the mitogenic *env* gene product gp55. The SFFV proviruses in these leukemias also appeared to be integrated into a few tightly clustered sites in the cellular genome. Although the tagged SFFV caused polycythemia during the polyclonal early stage of erythroblastosis, growth of the helper-free clonal erythrleukemia caused severe anemia. These results suggest that a single SFFV can cause mitosis of erythroblasts, and that cell immortalization also occurs if the provirus integrates into a critical site of the host genome. Because the immortalizing integrations also interfere with erythriod differentiation, mice with clonal stage leukemia become anemic. This system provides a relatively direct and background-free approach for identifying and studying genomic integration sites that contribute specifically to erythroblast immortality.

B. General Introduction

To analyze both the clonal aspects of progression and which cellular genes may contribute to the pathogenesis of Friend erythroleukemia, it would be very useful to have methods for identifying SFFV integration sites in the host cell genome. This has been a major problem because SFFV lacks a classical oncogene and contains only MuLV-related nucleic acid sequences that occur in large numbers in the normal mouse genome (40, 86, 176-178). Moreover, SFFV pathogenesis is restricted to mice (68, 69) and a species with a heterologous DNA background can not be used. Despite these difficulties, previous studies have suggested that the progression of Friend erythroleukemia involves selective outgrowth of cell clones that have a proliferative advantage (162, 176, 177). Moreau-Gachelin and co-workers have analyzed the DNA from Friend leukemia cells using a small SFFV-derived hybridization probe that reacts in stringent conditions with only a few endogenous sequences of the murine genome (177). Their identification of only a few "extra" SFFV proviral bands in Southern blots of leukemia cell DNAs suggested that the tumors arose from one or a few cells (177). Recently, they examined an erythroleukemia that contained helper MuLV and five SFFV proviruses (178). Using a genomic library, they cloned SFFV-host junction fragment DNAs from four of these integrations and screened each of these against other independently isolated erythroleukemias. By this screening process, they identified a locus (Spi-1) that was rearranged in 95 % of the highly progressed Friend erythroleukemias that were examined. The roles of Spi-1 proviral integration and of other SFFV and MuLV integrations that had occurred in these advanced leukemia cells remain unknown.

We have independently developed a different method to address this problem. Specifically, we have modified a colinear molecular clone of

polycythemia strain of SFFV by inserting a 215 base pair "tag" of SV40 DNA into its nonfunctional pol gene region. This tagged virus is pathogenic and in the absence of helper virus it causes at a low frequency transplantable Friend erythroleukemias. Moreover, single provirus integration sites can be detected in the infected host's genome using the SV40 fragment as a hybridization probe. The system described here provides a relatively defined and efficient background-free method for identifying and analyzing genes that can contribute specifically to erythroblast immortality.

Activation of cellular genes by proviral integration has been termed insertional mutagenesis. Evidence for the importance of cellular gene activation in the development of retroviral-induced tumors has been provided by studies on the mouse mammary tumor virus (MMTV), Mo-MuLV, and avian leukosis virus (ALV). MMTV has been shown to preferentially integrate within two areas of the mouse genome termed int-1 and int-2 (179-181). In the Mo-MuLV induced lymphomas, proviruses have been shown to be integrated in at least five independent cellular DNA domains, with one site being the c-*myc* region (182-184). The ALV provirus can increase the expression of c-*myc* in pre-B cells to induce a lymphoid leukosis (185) or activate the c-*erb B* gene during the development of erythroleukemia (186). These studies have provided direct evidence that proviral integrations can increase cellular gene activity as well as influence the type of tumor development.

The work described in this chapter was performed in collaboration with Dr. Craig Spiro who is a post-doctoral fellow Dr. David Kabat's laboratory. Dr. Spiro initiated this project by constructing the "tagged" SFFV described in Fig. 31 and by demonstrating the pathogenicity of this modified virus. At this point, we collaborated equally in the animal studies summarized in Table 1. The Western

and Southern blots presented in this chapter (Figs. 32, 33, and 34) were performed by myself.

C. Results

1. Tagged SFFV causes Friend erythroleukemia.

To identify Friend SFFV integrations in the mouse genome, we modified a polycythemic molecular clone of SFFV by inserting a 215 base pair fragment of SV40 DNA into its nonfunctional *pol* gene region (see Fig. 31). This plasmid, pSVSF, was transfected into psi-2 packaging cells (102) and a clone (psi-2/SVSF 4-4) was selected to stably express the gp55 glycoprotein that is encoded by SFFV. Virus harvested from the culture medium of psi-2/SVSF 4-4 cells caused NIH/3T3 fibroblasts to synthesize gp55, but helper virus glycoproteins were absent even after several weeks of culturing (results not shown).

As a first test to analyze pathogenicity of this tagged virus, we injected female NIH/Swiss mice intravenously with SVSF to which MuLV helper was added. As shown in Table 1, these mice developed an enduring splenomegaly and became polycythemic as indicated by their hematocrits. This result was expected because the molecularly cloned Lilly-Steeves SFFV causes a variable degree of polycythemia when coinjected with helper MuLV (77, 83, 187). As described below, it is relevant that the disease induced in these conditions also remains predominantly polyclonal at the cellular level (see below).

The SVSF virions released from psi-2/SVSF 4-4 cells were then analyzed for their pathogenicity in the absence of added helper MuLV. As shown in Table 1, the mice that were analyzed between 8-12 days after infection contained slightly enlarged spleens with numerous foci that became visible after placement in Bouin's fixative. The hematocrits were also slightly increased compared with the controls. Although most of the animals subsequently recovered, approximately 20-30% of the mice in four different experiments developed a large splenomegaly by 26-33 days. These results agree with previous evidence that

Figure 31. Structures of the retroviral clones used in this study. (A) The plasmid pL2-6K is a full length colinear Friend SFFV molecular clone that was derived from the Lilly-Steeves polycythemic strain of SFFV (77). The SFFV env sequences are located entirely 3' to the Bam HI site and designated by the hatched box. The LTRs are represented by solid boxes and the vector sequences by dashed lines. (B) The plasmid pSVSF was constructed by inserting the 215-base pair Hind III fragment of SV40 DNA into the unique Hind III site of the colinear SFFV pL2-6K. This insertion did not disrupt the splice acceptor site for the *env* gene which is located 3' to the Hind III site. In addition to the restriction sites shown in pL2-6K, pSVSF contains the additional sites shown. These sites were utilized in the localization of the integrated tagged provirus (see text).

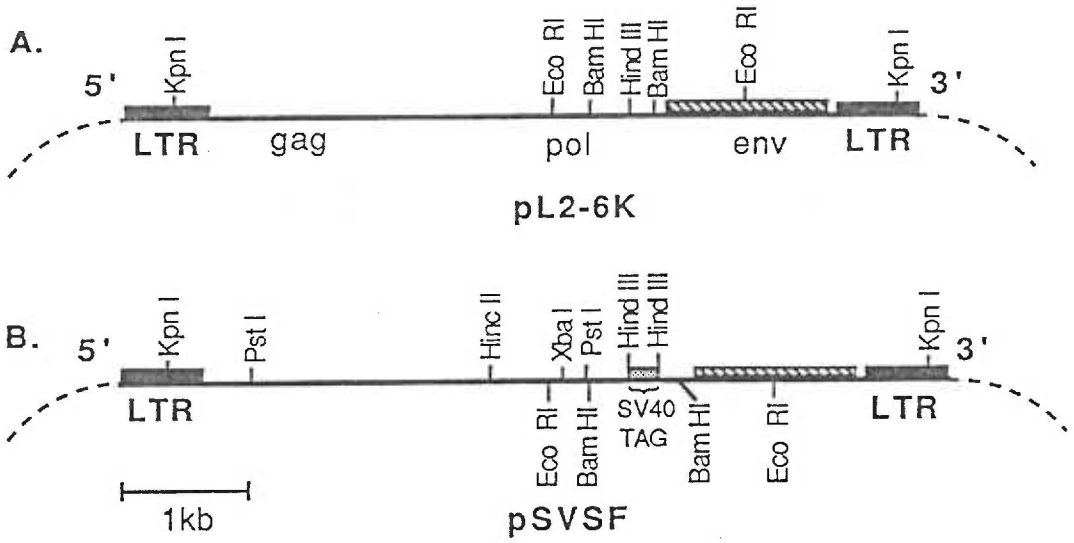
A.
5'
Kpn I
Eco RI
Bam HI
Hind III
Bam HI
Eco RI
Kpn I
3'
LTR
gag
pol
env
LTR
pL2-6K
B.
5'
Kpn I
Pst I
Hinc II
Xba I
Pst I
Hind III
Hind III
Kpn I
3'
LTR
Eco RI
Bam HI
SV40
TAG
Bam HI
Eco RI
LTR
1kb
pSVSF

Table I. Summary of mouse injections with the SVSF tagged virus.

Abbreviations used:

N.D. Not determined

a Spleen weight in grams (hematocrit is % of red blood cells).

b Deceased mouse. Hematocrit not determined.

c Spleens from these mice were used for studies described below and are designated by letters A-J in order of their appearance in the table. Thus, A is 35 day spleen of 1.68 g with hematocrit of 68%; B, 35 day, 2.60 g, 80%; C, 26 day, 1.33 g, 31%; D, 26 day, 1.35 g, 39%; E, 26 day, 1.18 g; F, 26 day, 1.35 g; G, 29 day, 1.60 g, 33%; H, 29 day, 2.27 g, 26 %; I, 29 day, 1.11 g, 42%; J, 33 day, 1.16 g.

TABLE I

Virus Injected.	Days After Infection.	Spleen Foci.	Spleen Weights (Hematocrit)*
None	12	None	0.09-0.13 (42-45)
SVSF + MuLV	35	N.D.	0.78 (73), 0.80 (46), 1.68 (68)c, 2.60 (80)c
SVSF	8	+	0.14 (53)
	11	+	0.10 (50)
	12	+,+, N.D.	0.18 (N.D.), 0.21 (N.D.), 0.13 (N.D.)
	14	-	0.11 (47)
	26	N.D.	0.11 (47), 0.21 (47), 0.11 (45), 0.09 (47), 0.09 (42), 0.14 (45), 1.33 (31)c, 1.35 (39)c, 1.18 (b)c, 1.35 (b)c
	27	N.D.	12 mice 0.09-0.14 (43-47) 2.31 (b), 1.86 (b), 1.48 (42), 0.86 (44), 2.19 (N.D.)
	29	N.D.	0.09 (47), 0.16 (46), 0.09 (45), 0.11 (47), 0.13 (48) 1.60 (33)c, 2.27 (26)c, 1.11 (42)c
	31-33	N.D.	12 Mice 0.11-0.14 (37-45) 0.98 (b), 1.01 (b), 1.16 (b)c

nearly all erythroblasts infected with helper-free SFFV have a limited self-renewal capability (71, 72), and with the results of Wolff and co-workers (73, 74), that a proportion of mice infected with the Lilly-Steeves polycythemia SFFV develop persistent erythroleukemia. However, we unexpectedly observed that the mice with persistent disease also became anemic (Table 1).

The persistent erythroleukemias recovered from mice 26-33 days after injection of SVSF in the absence of helper MuLV were readily transplantable into secondary recipients. By 14 days after intravenous injection of 5 x 10^5 spleen cells, the spleens of the secondary recipients were enlarged (1-2 g) and the hematocrits became reduced to 30-40%. Moreover, when these erythroleukemia cells were injected intraperitoneally, they all formed tumors on the omenta of the secondary recipients, and the omenta became enlarged from approximately 10 mg to at least 100 mg. The latter mice also all developed splenomegaly and anemia. Therefore, all of the persistent neoplasms formed by SVSF injections (Table 1) were readily transplantable. However, consistent with an earlier study, (26), these transplantable leukemia cells are not routinely culturable. At this time, only one of the leukemias recovered from secondary recipient mice has become adapted to permanent growth in culture.

2. Analysis of these spleens for synthesis of the SFFV *env* glycoprotein gp55 and for the MuLV *env* glycoprotein gPr90 and gp70.

Previous studies of SFFV packaged on psi-2 cells have shown that replication-competent MuLV can occur in some preparations in low amounts (71, 72). Theoretically, such MuLV could account for the persistent splenomegaly that occurred in a proportion of the mice infected with SVSF virus, although the associated anemia would be anomalous. To address this issue, the proteins from enlarged spleens were analyzed by polyacrylamide gel electrophoresis, followed

by Western blot analysis using an antiserum that reacts with both the SFFV glycoprotein gp55 and the MuLV *env* glycoproteins gPr90 and its processed product gp70. As shown in Fig. 32A, the enlarged spleens from mice that had been injected with SVSF and MuLV contained both gp55 and gPr90/gp70. In contrast, as illustrated in Fig. 32A, all the enlarged spleens taken from mice 26-33 days after injection with only SVSF contained gp55 but not gPr90/gp70 (e.g. lanes 1-6).

3. Southern blot analyses of genomic DNA from the spleens of mice that had been injected with SVSF virus in the presence or absence of helper MuLV.

To determine whether the enlarged spleens described above contained polyclonal or monoclonal neoplasms, the spleen DNAs were analyzed by the Southern blot method using restriction enzymes that can cut only one side of the tag site in SVSF and using SV40 tag DNA as the hybridization probe. The resulting cleavages should produce tagged SVSF-host DNA junction fragments that are unique for each SVSF proviral integration site. As shown in Fig. 33, the enlarged spleens from mice that have been infected with SVSF plus helper MuLV (lanes 2 and 3) contained a heterogeneous array of tagged junction sites, suggesting that these neoplasms were at least predominantly polyclonal. This was expected because the efficient disease persistence that occurs only in the mice that received helper MuLV (see Table 1) implies that this persistence involves virus replication and continuous infection of new erythroblast target cells. Although there was relatively little tagged virus in the small spleens of mice that had been injected 12 days earlier with SVSF, this early phase of helper-free erythrobalsts was also polyclonal as indicated by the heterogeneity of the junction fragment DNAs (e.g., Fig. 33, lane 4).

On the contrary, the DNAs isolated from the enlarged spleens of mice 26-33

Figure 32. Immunoblotting of viral envelope glycoproteins synthesized in infected spleens. The immunoblot was reacted with F-MuLV anti-gp70 serum as previously described (83). Equivalent amounts of lysate derived from $5x10^5$ cells were analyzed in each lane. The F745 erythroleukemia cell lysate was included as a positive control for both MuLV (gPr90/gp70) and SFFV (gp55/$gp55^P$) envelope glycoprotein synthesis. For identification of specific spleens, see Table I, footnote c. (A) Spleen lysates from infection with SVSF plus MuLV helper. Lane 1, spleen A; lane 2, spleen B; and lane 3, Friend 745 cell line. (B) Spleen lysates from infection with helper-free SVSF . Lane 1, spleen F; lane 2, spleen C; lane 3, spleen D; lane 4, spleen G; lane 5, spleen H; lane 6, spleen I; and lane 7, Friend 745 cell line. The $gp55^P$ band is the cell surface form of gp55 and could be visualized in the spleen lysates with a longer exposure.

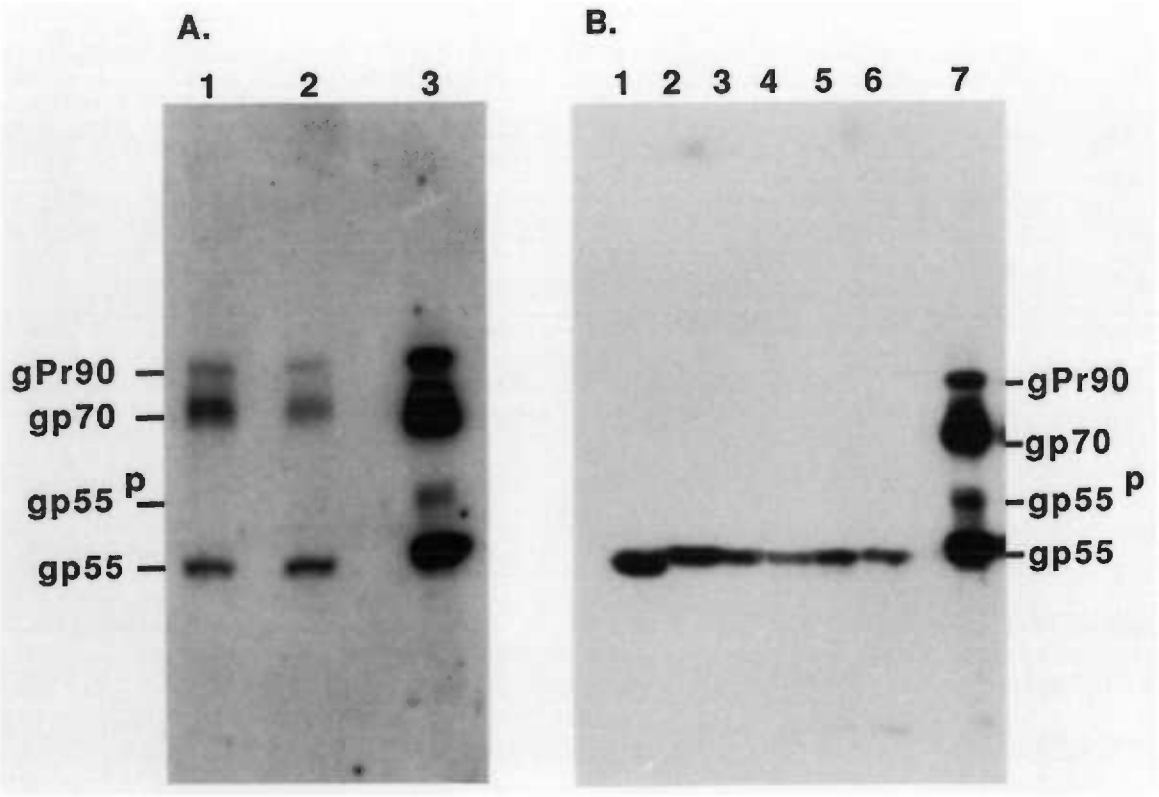
A.
1
2
3
gPr90
gp70
gp55 p
gp55
B.
1
2
3
4
5
6
7
gPr90
gp70
gp55 p
gp55

Figure 33. Southern blot analysis of the tagged provirus from mice that had been infected either in the presence and absence of MuLV helper virus. High molecular weight DNA was digested with Pst I and probed with the 215 bp SV40 DNA fragment. For identification of specific spleens, see Table I, footnote c.Lane 1, uninfected spleen DNA; lane 2, SVSF plus MuLV (spleen A); lane 3, SVSF plus MuLV (spleen B); lane 4, SVSF helper-free 12 day post-infection; lane 5, SVSF helper-free (spleen E); and lane 6, SVSF helper-free (spleen J).

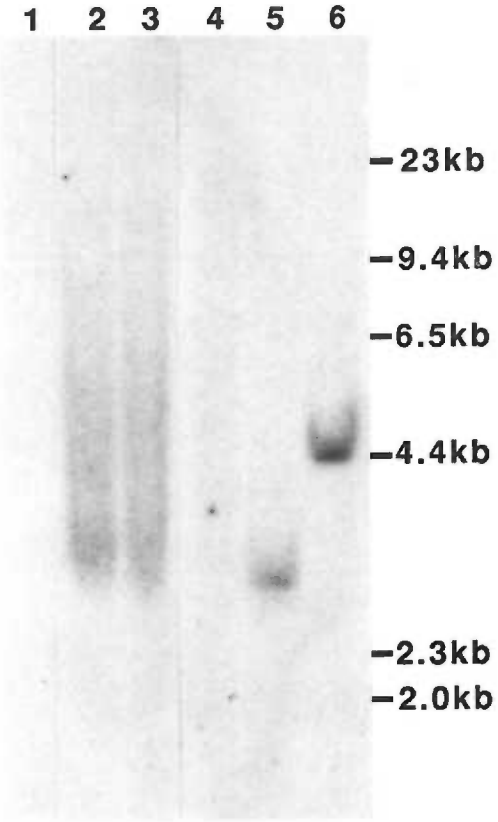
1
2
3
4
5
6
23kb
9.4kb
6.5kb
4.4kb
2.3kb
2.0kb

days after injection of helper-free SVSF clearly contained only single tagged SVSF-host DNA junction fragments (Fig. 33, lanes 5 and 6). These results indicated that these persistent leukemias are clonal neoplasms that contain single SVSF proviruses. Therefore, progressive and persistent Friend erythroleukemia can be induced in the absence of MuLV by a single SVSF virion. The restriction enzyme Kpn I cleaves within each of the SVSF LTRs and therefore should release a tagged DNA fragment of 5.8 kb, regardless of the genomic site of SVSF proviral integration. Studies of different DNAs using KpnI digestions revealed this expected 5.8 kb fragment, suggesting that the SVSF proviruses in the clonal erythroleukemias did not contain detectable deletions or rearrangements (results not shown).

4. Evidence for common integration sites in SVSF-induced clonal erythroleukemias.

As described above, all of the transplantable leukemias that were recovered from the spleens of mice 26-33 days after infection with SVSF contained single SVSF-host DNA junctions fragments, as indicated by Southern blot analysis of their DNAs. Surprisingly, however, as indicated in Fig. 34A, the tagged junction fragments in Hinc II digests of 8 different tumor DNAs seemed to cluster predominantly into two size groups, Within each group, the junction fragments had sizes that were tightly clustered within approximately ± 0.3 kilobases. One clustered group included three DNAs designated spleen E, spleen C, and spleen G (lanes 2,5, and 7) and the other group included three DNAs designated spleen J, spleen F, and spleen D (lanes 3, 4, and 6). For identification of specific spleens, see Table I, footnote c. These results raised the possibility that the SVSF integrations in these transplantable leukemias might occur with common proviral orientations at a few tightly clustered sites in the host DNA. To further test this

Figure 34. Southern blot analysis of helper-free tagged proviral integration sites. High molecular weight genomic DNAs were digested with Hinc II (panel A), Pst I (panel B), or Xba I (panel C). All blots were probed with the 215 bp SV40 DNA. For identification of specific spleens, see Table I, footnote c. The DNAs used were as follows: Lane 1, uninfected spleens; lane 2, SVSF helper-free spleen E; lane 3, SVSF helper-free spleen J; lane 4, SVSF helper-free spleen F; lane 5, SVSF helper-free spleen C; lane 6, SVSF helper-free spleen D, lane 7, SVSF helper-free spleen G; lane 8, SVSF helper-free spleen H; lane 9, SVSF helper-free spleen I.To ensure identification of faint bands that were clearly seen on the original autoradiographs, black dots were placed to the right of each band in the leukemic DNA samples.

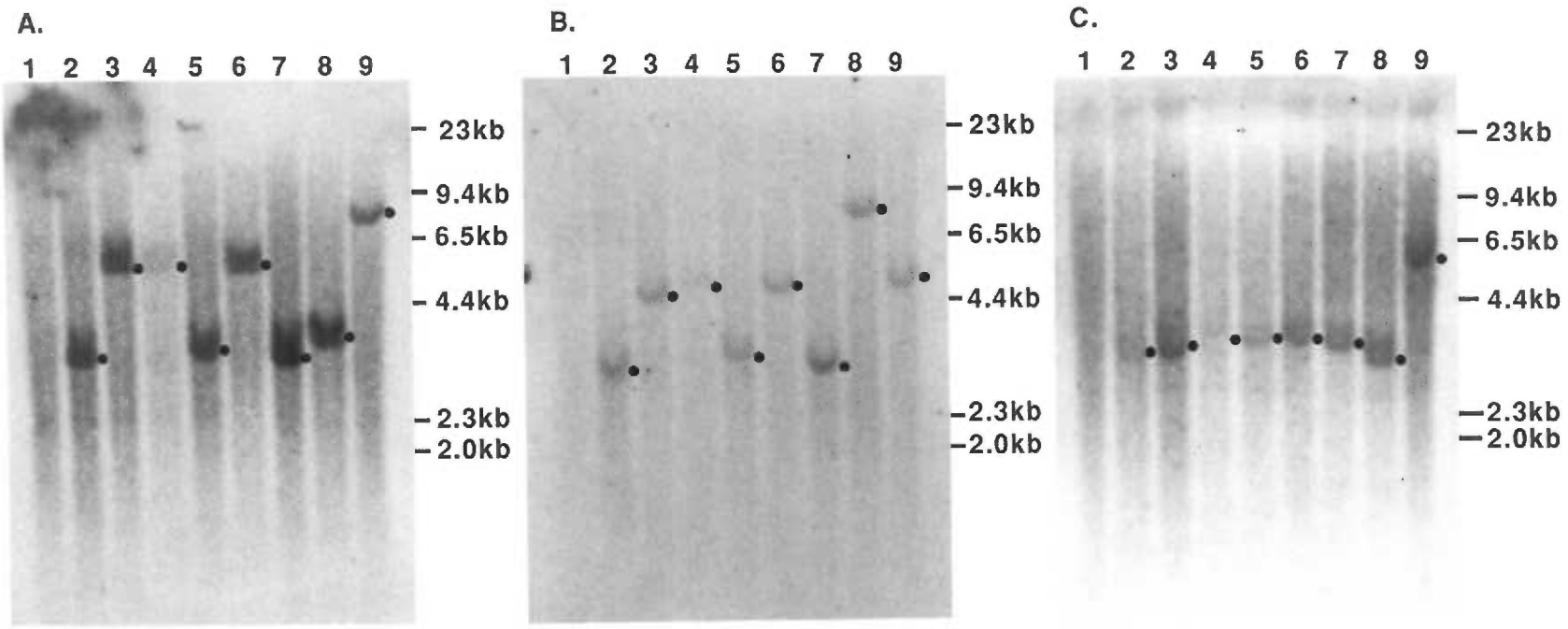
A.
1 2 3 4 5 6 7 8 9
23kb
9.4kb
6.5kb
4.4kb
2.3kb
2.0kb
B.
1 2 3 4 5 6 7 8 9
23kb
9.4kb
6.5kb
4.4kb
2.3kb
2.0kb
C.
1 2 3 4 5 6 7 8 9
23kb
9.4kb
6.5kb
4.4kb
2.3kb
2.0kb

hypothesis, we digested these same splenic DNA preparations with the restriction enzymes Pst I and Xba I. These enzymes, like Hinc II, also cleaves SVSF only on the 5' side of the SV40 tag. As shown in Fig. 34B and 34C, each group of three DNAs (i.e., lanes 2, 5, 7 and lanes 3, 4, and 6) maintained the tight association with one another that was originally suggested by the Hinc II digest. These results demonstrated that the DNAs from spleen E, spleen C, and spleen G all contain SVSF proviruses in the same orientation with the 3' LTR approximately 0.2 kb upstream of a Hinc II site, 0.1 kb upstream of a Pst I site, and 0.2 kb upstream of a Xba I site. Similarly, DNAs from spleen J, spleen F, and spleen D contain SVSF proviruses in a common orientation with their 3' LTRs integrated 2.2 kb upstream of a Hinc II site, 1.7 kb upstream of a Pst I site, and 0,2 kb upstream of a Xba I site. Moreover, the small differences in the placement of SVSF proviruses within each putative group were maintained in the analyses using different restriction enzymes. DNAs from spleen H and spleen I did not occur within either of these putative groups. After this work was completed, Moreau-Gachelin et al. (178) identified an SFFV proviral integration site (Spi-1) that was occupied in nearly all Friend virus-induced leukemias they examined. The integrations within Spi-1 also occurred in several tightly clustered groupings (see Discussion).

D. Discussion

1. Clonal analysis of Friend erythroleukemia.

A major problem in analyzing the clonal progression and pathogenesis of Friend erythroleukemia has derived from the difficulty of unambiguously identifying SFFV proviral integration sites in the host genome (39, 40, 86, 176-178). This inherent difficulty has been exacerbated because SFFV has been almost exclusively analyzed in the presence of helper MuLV which creates opportunities for multiple infections of tumor cells (176-178) and for continual infection of previously uninfected erythroblasts *in vivo*. Despite these difficulties, evidence has accumulated that Friend disease can be separated into an initial polyclonal erythroblastosis in which the proliferating cells have limited lifespans and continue to differentiate, and a later stage that may be clonal, in which the cells have a greater self-renewal capability (5, 176, 177). The numbers of steps involved in this progression and their temporal relationships have not been previously known. Recent studies by Wolff and co-workers have suggested that progressive Friend erythroleukemia can be initiated in certain circumstances by helper-free SFFV (73, 74).

The tagged virus SVSF provides an advantageous background-free model for analyzing the growth of cell clones during the development of Friend erythroleukemia, and for identifying critical proviral integration sites in the host genome. Thus, we believe our studies of SVSF in the presence and absence of helper MuLV provide relatively clear and unambiguous evidence that the disease progresses from a phase in which numerous clones of infected cells proliferate and then die out within 8-12 days to a clonal leukemia in which the cells have an indefinite self-renewal capability as indicated by their persistent growth *in vivo* (Table 1), and by their transplantability. The disease persists efficiently in the

presence of helper MuLV because erythroblasts continuously become newly - infected, whereas in the absence of helper, the polyclonal phase of disease disappears by approximately 12 days and most mice then rapidly recover. As described below, our results also suggest that the transplantable leukemias caused by SVSF contain single functional SVSF proviruses and that the acquisition of the immortality in these rare cell clones may be caused by SVSF integration into a specific site in the host genome. Thus, our results suggest that the "stages" of Friend disease may actually be caused by a rare one-hit process, the integration of a single functional SFFV provirus into a critical site in the host genome.

Our results support earlier evidence that helper-free SFFV efficiently stimulates polyclonal proliferation and differentiation of infected BFU-E erythroblasts (71-74). This mitogenic stimulation of BFU-E apparently requires expression of the SFFV *env* gene product gp55 on the surfaces of infected cells (83). All of the transplantable leukemias that we have obtained following their helper-free SVSF injections have continued to express gp55 (e.g., Fig 32), suggesting that the proviruses remain functionally active. Moreover, Southern blot analyses using Kpn I digestions also have implied the the SVSF proviruses appear to be structurally intact. These results are in contrast with studies of avian leukosis virus-induced bursal lymphomas in which continued viral gene expression is not required and in which proviruses are often structurally rearranged (185, 188).

2. Evidence for common sites of proviral integration in immortalized Friend erythroleukemia cells.

The clonal leukemias that we have isolated from NIH/Swiss mice 26-33 days after injections of helper-free SVSF can be considered "immortal" based on the

functional criterion that they can be transplanted indefinitely in secondary recipients. Clearly, this is a striking difference between these clones and other clones of infected erythroblasts that proliferate briefly and then die out 8-12 days after SVSF injections (Table 1) and the BFU-E clones that grow briefly for approximately 5-8 days before terminally differentiating in bone marrow cultures (57). In addition, our results suggest that these clonal leukemias contain single SVSF proviruses that may occur in only a few tightly clustered integration sites in the cellular genome. This evidence is based on Southern blot analyses of eight different randomly selected transplantable leukemias using three different restriction endnucleases (Hinc II, Pst1 and Xba I) that cut SVSF only on the 5' side of the SV40 tag (see Figs. 31, 33 and 34) to generate tagged viral-host junction fragment DNAs that are characteristic of the proviral integration sites. Two putative groups of common integrations were observed, each of which contained three members. Within each putative group, the junction fragments generated by a given restriction enzyme differed in size by only approximately ± 0.3 kb (see Fig. 34), suggesting that the polarity of the proviruses and the specific distances between the junction fragment restriction sites were common within each group. Within each group, the small differences in placement of the apparent integrations were also maintained within experimental error in the results observed with the different restriction enzymes. We believe these results support the hypothesis that SVSF proviruses are integrated in a few tightly clustered common sites in the genomic DNAs of the transplantable leukemias. These different clustered proviral groups could occur at different genes or with different orientations and/or placements around a single gene. Currently we are cloning these integration sites in order to definitively test these interpretations.

Recently in an independent study, Moreau-Gachelin, et al. (178) described a common SFFV integration site in Friend virus-induced leukemias. Using a

hybridization probe that reacts with only a few endogenous sequences in the mouse genome (176-178), and by screening at least five different SFFV integrations that occurred in an advanced leukemia, they obtained evidence that one of these integration sites, Spi-1, was altered in approximately 95% of the independently derived erythroleukemias that they analyzed. These alterations of Spi-1 were caused by tightly clustered SFFV integrations in a common orientation, and they activated expression of an adjacent cellular gene (178). Because the advanced leukemia that they examined contained other potentially functional SFFV integrations and an unknown number of MuLV integrations, the functional role of Spi-1 integrations could not be unambiguously inferred.

The leukemias that we have examined were derived from NIH/Swiss mice, whereas the leukemias studied by Moreau-Gachelin et al. were derived from ICFW, CBA or DBA/2 mice (178). By analogy with the int-1 and int-2 loci in mouse mammary tumor viruse-induced disease, different loci might be involved in Friend disease in genetically different mice (179-181). Cloning and further examination of the integration sites in our SVSF-derived leukemias should clarify their relationship to Spi-1.

3. Acquisition of immortality by Friend leukemias appears to be associated with inhibition of differentiation.

During the polyclonal initial phase of Friend disease that is induced by polycythemic strains of SFFV, the infected and proliferating BFU-E erythroblasts continue to differentiate from erythrocytes. This differentiation, which occurs in the apparent absence of erythropoietin, is believed to be responsible for the polycythemia that occurs *in vivo* (3, 57, 187). Although the SVSF derivative virus also caused polycythemia in the presence and absence of helper MuLV whenever the disease was at a polyclonal stage, we were surprised to observe

that the clonal phase of erythroleukemia was associated with anemia (e.g., Table 1 and Fig. 33). Moreover, secondary recipients that received these transplantable leukemias all became severely anemic. This striking difference between the polyclonal and clonal stages of leukemogenesis would be difficult to observe in leukemias that contain MuLV because the transplant would induce a polyclonal disease in the recipient mice. Based on these results, we propose that the SVSF proviral integrations that cause immortalization of erythroblasts concomitantly interfere with cellular differentiation *in vivo*. According to this interpretation of our results, the polyclonal phase of the disease would result in polycythemia, whereas clonal helper-free leukemia cells would crowd out the uninfected erythroblasts *in vivo* and cause anemia. Presumably, therefore, identification and analysis of the SVSF integration sites in transplantable leukemias could provide information not only about genes that contribute to "immortality", but also about the genetic controls that establish a commitment to differentiate.

VIII. Summary

The Friend virus complex causes a progressive murine erythroleukemia. The early phase of the disease is considered premalignant because the infected erythroblasts have a limited proliferative capacity and continue to differentiate. In contrast, 3-8 weeks post-infection malignant Friend cells emerge that can be maintained in culture, are transplantable, and appear to be blocked at the proerythroblast stage of differentiation. Thus, the Friend cells have escaped the commitment to differentiate and now have the capacity for unlimited self-renewal and are considered immortal.

Expression of gp55 at the cell's surface provides the mitogenic signal for the initial erythroblastosis. Previous work had demonstrated that the SFFV gp55 was inefficiently processed to the surface and the majority remained within the rough endoplasmic reticulum. We have shown that the majority of gp55 is still present as an intracellular monomer, but a portion of the intracellular molecules are dimerized by disulfide bonds and all of the cell surface molecules are dimerized. We have demonstrated that the intracellular dimers are the precursors to the cell surface dimers, however not all of the dimers formed reach the cell surface. Instead, it appears that several different forms of the dimer can be detected intracellularly, while only one dimer form is found at the cell surface.

We have proposed that the initial folding and dimerization of gp55 generates a structurally heterogeneous population of molecules. Only those dimers that are "correctly folded" can escape the rough endoplasmic reticulum. This would imply that the transported molecules would be conformationally unique from the intracellular dimers. We find no evidence that the intracellular gp55 components are being continually processed to generate the cell surface dimer. Instead, gp55 folds and dimerizes very quickly after synthesis and this generates transport

competent or incompetent molecules. Those molecules that are incompetent for transport remain in the RER. This would imply that isomerization is not being catalyzed *in vivo* by a disulfide interchange enzyme such as protein disulfide-isomerase. Thus, only the conformationally correct dimers that are formed shortly after gp55 synthesis are transported to the surface and generate a mitogenic signal.

The initial viral infection is characterized by massive proliferation of erythroblasts that have a limited self-renewal capability and continue to differentiate. The disease culminates after 4-8 weeks post-infection in the formation of tumorigenic leukemia cells that can be cultured indefinitely. We have shown that the erythroleukemic progression is associated with an increase in the relative expression levels of the cellular oncogenes c-*myc*, c-*myb*, and p53 in the erythroleukemia cell lines. In addition, our genomic structural studies demonstrated amplifications of c-*myc* copy numbers and p53 rearrangements. Such results imply that changes in expression of these cellular oncogenes were selected during progression and may contribute to the proliferation and tumorigenicity of these cells. Progression is associated with a decreased tendency in cellular differentiation and an increased capacity for self-renewal. This has led to the hypothesis that leukemias represent a block in differentiation. Friend cells can still be induced to differentiate with compounds such as DMSO. This induction results in a rapid decrease in c-*myc*, c-*myb*, and p53 transcript levels. These results are consistent with the belief that increased expression of cellular oncogenes may contribute to leukemic progression by interfering with erythropoiesis.

The importance of cell surface expression of gp55 in the development of erythroleukemia has been well documented. Nonpathogenic *env* mutants, both spontaneous and site-directed, lack the expression of this envelope glycoprotein

at the cell surface. From this and other evidence, our laboratory has proposed a model of gp55 action in which the cell surface form binds to a specific receptor to stimulate erythroblast mitosis. Results presented in this thesis have suggested that the continued expression of gp55 may also be important in both the progression and maintenance of the erythroleukemia. The Friend erythroleukemia cell lines express gp55 at a much higher level than the premalignant cells and all SVSF helper-free leukemias continue to express the SFFV gp55. This is consistent with the previous observation that while some erythroleukemia cell lines derived from mice infected with SFFV fail to express SFFV *gag* proteins, they all continue to express SFFV envelope glycoprotein. This suggests that the continued expression of the SFFV *env* glycoprotein may play an important role in maintaining a constitutive mitogenic stimulus necessary for the high self-renewal capacity of transformed cells. Conceivably, this mitogenic stimulus may activate the cellular oncogenes found to be expressed in the erythroleukemia cell lines.

Whereas gp55 expression will stimulate erythroblastosis, the expression of gp55 alone is not sufficient to generate immortal leukemia cells. Clearly, the vast majority of the infected cells proliferate for a limited period, differentiate, and then die out. Our proviral integration studies demonstrate that a single clonal population eventually emerges to form the advanced leukemia. Moreover, common integration sites are suggested by the clustering of the proviruses in only a few areas of the genome. This implies that the "stages" of erythroleukemia may only involve a single critical proviral integration event. The continued expression of gp55 may contribute to the progression by providing a constitutive mitogenic stimulus, whereas the proviral integration may allow the erythroblasts to escape from its commitment to erythroid differentiation and become immortalized. Thus,

the SFFV proviral integration may represent a primary genetic alteration to the infected erythroblast that eventually culminates in a transformed cell. Cloning and characterizing these proviral integration sites should provide a significant new insight into Friend erythroleukemia.

IX. References

1. Friend, C. (1957) Cell-free transmission in adult Swiss mice of of a disease having the character of a leukemia. J Exp. Med., 105:307-318.

2. Ruscetti, S., and L. Wolff. (1984) Spleen focus-forming virus: relationship of an altered envelop gene to the development of a rapid erythroleukemia. Curr. Topics in Micro. and Immuno. 112:21-44.

3. Teich, N., J. Wyke, T. Mak, A. Bernstein, and W. Hardy. (1982) Pathogenesis of retrovirus-induced disease. p. 785-999. In Weiss, R., N. Teich, H. Varmus, and J. Coffin. (eds.). RNA Tumor Viruses. Cold Spring Harbor Laboratory, Cold Spring Harbor, New York.

4. Mirand, E.A., T.C. Prentice, J. Hoffman, and J. Grace, Jr. (1961) Effect of Friend virus in Swiss and DBA/1 mice on Fe^{59} uptake. Proc. Soc. Exp. Biol. Med., 106:423-426.

5. Sassa, S., F. Takaku, and K. Nakao. (1968) Regulation of erythropoiesis in the Friend leukemia mouse. Blood, 31:758-765.

6. Mirand, E.A., R. Steeves, R. Lange, and J. Grace. Jr. (1968) Virus-induced polycythemia in mice: erythropoiesis without erythropoietin. Proc. Soc. Exp. Biol. Med., 128:844-849.

7. Rauscher, F.J. (1962) A virus-induced disease of mice characterized by erythrocytopoiesis and lymphoid leukemia. J. Natl. Cancer Inst., 29:515-543.

8. Bestwick, R., B. Boswell, and D. Kabat. (1984) Molecular cloning of biologically active Rauscher spleen focus-forming virus and the sequence of its *env* gene and long terminal repeat. J. Virol., 51:695-705.

9. Vogt, M., C. Haggblom, S. Swift, and M. Hass. (1985) Envelope gene and long terminal repeat determine the different biological properties of Rauscher, Friend, and Moloney mink cell focus-inducing viruses. J. Virol., 55:184-192.

10. Metcalf, D., J. Furth, R. Buffett. (1959) Pathogenesis of mouse leukemia caused

by Friend virus. Cancer Res., 19:52-60.

11. Tambourin, P., and F. Wendling. (1971) Malignant transformation and erythroid differentiation by polycythemia-inducing Friend virus. Nature, 234:230-233.

12. Axelrad, A., and R. Steeves, (1964) Assay for Friend leukemia virus: Rapid quantitative method based on enumeration of macroscopic spleen foci in mice. Virology, 24:513-518.

13. MacDonald, M., F.H. Reynolds, W. Van de Ven , J. Stephenson, T. Mak, and A. Bernstein. (1980) Anemia- and polycythemia-inducing isolates of Friend spleen focus-forming virus. Biological and molecular evidence for two distinct viral genomes. J. Exp. Med., 151:1477-1492.

14. Clark, S.C., and R. Kamen. (1987) The human hematopoietic Coloney-stimulating factors. Science, 236:1229-1237.

15. McCulloch, E. A. (1983) Stem cells in normal and leukemic hemopoiesis. Blood 62:1-13.

16. Clarkson, B., P. A. Marks, and J. E. Till (eds.). (1978) Differentiation of normal and neoplastic hematopoietic cells, Cold Spring Harbor conferences on cell proliferation. Vol. 5. New York, Cold Spring Harbor Symposium.

17. Weiss, R. Host susceptibility and resistance. In: Weiss, R., N. Teich, H. Varmus, and J. Coffin. (Eds.) (1984) pp. 226-235.

18. Varmus, H., and R. Swanstrom. Replication of retroviruses. In: Weiss, R., N. Teich, H. Varmus, and J. Coffin. (Eds.) (1984) pp. 369-512.

19. Dickson, C., R. Eisenman, H. Fan, E. Hunter, and N. Teich. Protein biosynthesis and assembly. In: Weiss, R., N. Teich, H. Varmus, and J. Coffin. (Eds.) (1984) pp. 513-648.

20. Pluznik, D., and L. Sachs. Quantitation of a murine leukemia virus with a spleen colony assay. J. Natl. Cancer Inst., (1964) 33:535-546.

21. Steeves, R.A. (1975) Spleen focus-forming virus in Friend and Rauscher leukemia virus preparations. J. Natl. Cancer Inst,. 54:289-297.

22. Maisel, J., V. Klement, M. Lai, W. Ostertag, and P. Duesberg. (1973) ribonucleic acid components of murine sarcoma and leukemia viruses. Proc. Natl. Acad. Sci. USA, 70:3536-3540.

23. Dube, S., H.-J. Kung, W. Bender, N. Davidson, and W. Ostertag. (1976) J. Virol., 20:264-272.

24. Evans, L., M. Nunn, P. Duesberg, D. Troxler, and E. Scolnick. (1980) RNAs of defective and nondefective components of Friend anemic and polycythemic virus strains identified and compared. Cold Spring Harbor Symp. Quant. Biol., 44:823-835.

25. Coffin, J. Structure of the retroviral genome. In: Weiss, R., N. Teich, H. Varmus, and J. Coffin. (Eds.) (1984) pp. 226-235.

26. Yoshinaka, Y., I. Katoch, T. Copeland, and S. Oroszlan. (1985) Murine leukemia virus protease is encoded by the *gag-pol* gene and is synthesized through suppression of an amber termination codon. Proc. Natl. Acad. Sci. USA, 85:234-237.

27. Luftig, R., and Y. Yoshinaka. (1978) Rauscher leukemia virus populations enriching for immature virions contain increased amounts of gp70, the *gag* gene product. J. Virol., 25:416-421.

28. Edwards, S.A., and H. Fan. (1979) gag-related proteins of Moloney murine leukemia virus: evidence for independent synthesis of glycosylated and unglycosylated forms. J. Virol., 30:551-563.

29. Witte, O.N., and D. Baltimore. (1978) Relationship of retrovirus polyprotein cleavages to virion maturation studied with temperature-sensitive murine leukemia virus mutants. J. Virol., 26:750-761.

30. Van Zaane, D., A. Gielkins, W. Hasselink, and H. Blomers. (1977) Identification of Rauscher murine leukemia virus-specific mRNAs for the synthesis of *gag* and *env* gene products. Proc. Natl. Acad. Sci. USA, 74:1855-1859.

31. Famulari, N.G., D.L. Buchhagen, H.D. Klenk, and E. Fleissner. (1976) Presence of murine leukemia virus envelope proteins gp70 and p15E in a common polyprotein of infected cells. J. Virol. 20:501-508.

32. Naso, R.B., L.J. Arcement, W.L. Karshin, G.A. Jamjoom, and R.B. Arlinghaus. (1976) A fucose-deficient glycoprotein precursor to Rausher leukemia virus gp69/71. Proc. Natl. Acad. Sci. USA, 73:2326-2330.

33. Leamnson, R.N., M.H. Shander, and M.S. Halpern. (1977) A structural protein complex in Moloney leukemia virus. Virology 76:437-439.

34. Pinter, A, E Fleissner. (1977) The presence of disulfide-linked gp70-p15E complexes in AKR murine leukemia virus. Virology, 83:417-422.

35. Pinter, A., J. Lieman-Hurwitz, and E. Fleissner. (1978)The nature of the association between the murine leukemia virus envelope proteins. Virology, 91:345-351.

36. Bolognesi, D.P., A.J. Langlois, and W. Schafer. (1975) Polypeptides of mammalian oncornaviruses IV. Structural components of murine leukemia virus released as soluble antigens in cell culture. Virology, 68:550-555.

37. Troxler, D.H., W.P. Parks, W.C. Vass, E.M. Scolnick. (1977) Isolation of a fibroblast nonproducer cell line containing the Friend strain of spleen focus-forming virus Virology, 76:602-615.

38. Bernstein, A., T.W. Mak, and J.R. Stephenson. (1977) The Friend virus genome: evidence for the stable association of MuLV sequences and sequences involved in erythroleukemic transformation. Cell, 12:287-294.

39. Troxler, D.H., J.K. Boyars, W.P. Parks, and E.M. Scolnick. (1977) Friend strain of spleen focus forming virus: a recombinant between mouse type C ecotropic viral sequences and sequences related to xenotropic virus. J. Virol., 22:361-372

40. Troxler, D.H., D. Lowy, R. Howk, H. Young, and E.M. Scolnick. (1977) Friend strain of spleen focus-forming virus is a recombinant ecotropic murine type C virus and the *env* gene region of xenotropic type C virus. Proc. Natl Acad. Sci USA, 74:461-4675.

41. Famulari, N. (1983) Murine leukemia viruses with recombinant *env* genes: a discussion of their role in leukemogenesis. Curr. Top. Microbiol. Immunol., 103:76-108.

42. Ruscetti, S.K., L. Davis, J. Field, and A. Oliff. (1981) Friend murine leukemia virus-induced leukemia is associate with the formation of mink cell focus-inducing viruses and is blocked in mice expressing endogenous mink cell focus-inducing xenotropic viral envelope-related glycoproteins. J. Exp. Med. 154:907-920.

43. Barbacid, M., D.H. Troxler, E.M. Scolnick, and S.A. Aaronson. (1978) Analysis of translational products of Friend strain of spleen focus-forming virus. J. Virol., 27:826-830.

44. Evans, L.H., P.H. Duesberg, D.H. Troxler, and E.M. Scolnick. (1979) Spleen focus-forming Friend virus: identification of genomic RNA and its relationship to helper virus RNA. J. Virol., 31:133-146.

45. Ruscetti, S., D.H. Troxler, D. Linemeyer, and E.M. Scolnick. (1980) Three laboratory strains of spleen focus-forming virus: comparison of their genomes and translational products. J. Virol., 33:140-151.

46. Bilello, J.A., G. Colleta, G. Koch, D. Frisby, I.B. Pragnell, and W. Ostertag. (1980) Analysis of the expression of spleen focus-forming virus (SFFV)-related RNA and gp55, a Friend and Rauscher virus specific protein. Virology, 107:331-334.

47. Yoshida, M., and H. Yoshikura. (1980) Analysis of spleen focus-forming virus-specific RNA sequences coding for spleen focus-forming virus-specific glycoprotein with a molecular weight of 55,000 (gp55). J. Virol., 33:587-596.

48. Ruscetti, S., D. Linemeyer, J. Feild, D. Troxler, and E.M. Scolnick. (1979) Characterization of a protein found in cells infected with the spleen focus-forming virus that shares immunological cross-reactivity with the gp70 found in mink cell focus-inducing virus particles. J. Virol., 30:787-798.

49. Dresler, S., M. Ruta, M. J. Murray, and D. Kabat. (1979) Glycoprotein encoded by the Friend spleen focus-forming virus. J. Virol. 30:564-575.

50. Ruta, M., and D. Kabat. (1980) Plasma membrane glycoproteins encoded by cloned Rauscher and Friend spleen focus-forming virus. J. Virol, 35:844-853.

51. Ruscetti, S., D. Linemeyer, J. Feild, D. Troxler, and E. Scolnick. (1978) Type-

specific radioimmunoassays for the gp70s of mink cell focus-inducing leukemia viruses: expression of a cross-reacting antigen in cells infected with Friend strain of the spleen focus-forming virus. J. Exp. Med., 148:654-663.

52. Pinter, A., and W. J. Honnen. (1985) The mature form of the Friend spleen focus-forming virus envelope protein, gp65, is efficiently secreted from cells. Virology 143:646-650.

53. Troxler, D.H., S.K. Ruscetti, D.L. Linemeyer, and E.M. Scolnick. (1980) Helper-independent and replication-defective erythroblastosis-inducing viruses contained within anemia-inducing Friend virus complex (FV-A). Virology, 102:28-45.

54. Wendling, F., P. Tambourin, O. Gallien-Lartigue, and M. Charon. (1974) Comparative differentiation and numeration of CFUs from mice infected either by the anemia- or polycythemia-inducing strains of Friend viruses. Int. J. Cancer 13:454-462.

55. Horoszewicz, J. S., S. S. Leong, and W. A. Carter. (1975) Friend leukemia: rapid development of erythropoietin-independent hematopoietic precursors. J. Natl. Cancer Inst. 54:265-268.

56. Liao, S-K., and A. A. Axelrad. (1975) Erythropoietin-independent erythroid colony formation *in vitro* by hemopoietic cells of mice infected with Friend virus. Int. J. Cancer 15:467-482.

57. Hankins, W. D., and D. Troxler. (1980) Polycythemia- and anemia-inducing erythroleukemia viruses exhibit differential erythroid transforming effects *in vitro*. Cell 22:693-699.

58. Kost, T. A., M. J. Koury, W. D. Hankins, and S. B. Krantz. (1979) Target cells for Friend virus-induced erythroid bursts *in vitro*. Cell 18:145-152.

59. Kost, T.A., M.J. Koury, and S.B. Krantz. (1981) Mature erythroid burst forming units are target cells for Friend virus-induced erythroid bursts. Virology, 108:309-317.

60. Hankins, W.D., T.A. Kost, M.J. Khoury, and S.B. Krantz. (1978) Erythroid bursts produced by Friend leukemia virus *in vitro*. Nature, 276:506-508.

61. Steinheider, G., H.J. Seidel, and L. Kreja. (1979) Comparison of the biological effects of anemia inducing and polycythemia inducing Friend virus complex. Experientia, 35:1173-1175.

62. Koury, M.J., M.C. Bondurant, D.T. Duncan, S.B. Krantz, and W.D. Hankins. (1982) Specific differentiation events induced by erythropoietin in cells infected *in vitro* with the anemia strain of Friend virus. Proc. Natl. Acad. Sci. USA, 79:635-639.

63. Friend, C., and J.R. Haddad. (1960) Tumor formation with transplants of spleen or liver from mice with virus-induced leukemia. J. Natl. Cancer Inst. 25:1279-1289.

64. Wendling, F., F. Moreau-Gachelin, and P. Tambourin. (1981) Emergence of tumorigenic cells during the course of Friend virus leukemias. Proc. Natl. Acad. Sci. USA, 78:3614-3618.

65. Mager, D. L. , T. W. Mak, and A. Bernstein. (1981) Quantitative colony method for tumorigenic cells transformed by two distinct strains of Friend leukemia virus. Proc. Natl. Acad. Sci. USA 78:1703-1707

66. Friend, C., W. Scher, J. G. Holland, and T. Sato. (1971) Hemoglobin synthesis in Murine virus-induced leukemic cells *in vitro* : stimulation of erythroid differentiation by dimethyl sulfoxide. Proc. Natl. Acad. Sci. USA 68:378-382.

67. Mager, D., T.W. Mak, and A. Bernstein. (1981) Friend leukemia virus transformed cells, unlike normal stem cells, form spleen colonies in Sl/Sld mice. Nature, 288:592-594.

68. Dawson, P.J., W.M. Rose, and A.H. Fieldsteel. (1966) Lymphatic leukemia in rats and mice inoculated with Friend virus. Br. J. Cancer, 20:114-121.

69. Steeves, R.A., R.J. Eckner, M. Bennett, E.A. Mirand, and P.J. Trudel. (1971) Isolation and characterization of a lymphatic leukemia in the Friend virus complex. J Natl. Cancer Inst., 46:1209-1217.

70. Dawson, P.J., W.M. Rose, and A.H. Fieldsteel. (1966) Lymphatic leukemia in rats and mice induced by Friend lymphatic leukemia virus in T-cell-depleted

mice. Cancer Res. 39:1611-1615.

71. Berger, S. A., N. Sanderson, A. Bernstein, and W. D. Hankins. (1985) Induction of the early stages of Friend erythroleukemia with helper-free Friend spleen focus-forming virus. Proc. Natl. Acad. Sci. USA, 82:6913-6917.

72. Bestwick, R. K., W. D. Hankins, and D. Kabat. (1985) Roles of helper and defective retroviral genomes in murine erythroleukemia: studies of spleen focus-forming virus in the absence of helper. J. Virol., 56:660-664.

73. Wolff, L., and S. Ruscetti. (1985) Malignant transformation of erythroid cells *in vivo* by introduction of a nonreplicating retrovirus vector. Science, 228:1549-1552.

74. Wolff, L., P. Tambourin, and S. Ruscetti (1986) Induction of the autonomous stage of transformation in erythroid cells infected with spleen focus-forming virus; helper virus is not required. Virology, 152:272-276.

75. Anand, R., F. Lilly, and S. Ruscetti. (1981) Viral protein expression in producer and nonproducer clones of Friend erythroleukemia cell lines. J. Virol., 37:654-660.

76. Amanuma, H., K. Akiko, M. Obata, N. Sagata, and Y. Ikawa. (1983) Complete nucleotide sequence of the gene for the specific glycoprotein (gp55) of Friend spleen focus-forming virus. Proc. Natl. Acad. Sci. USA, 80:3913-3917.

77. Linemyer, D.L., S.K. Ruscett, J.G. Menke, and E.M. Scolnick. (1980) Recovery of biologically active spleen focus-forming virus from molecularly cloned spleen focus-forming virus-pBR322 circular DNA by cotransfection with infectious Type C retroviral DNA. J. Virol., 35:710-721.

78. Linemeyer, D.L., S.K. Ruscetti, E.M. Scolnick, L.H. Evans, and P.H. Duesberg. (1981) Biological activity of the spleen focus-forming virus DNA. Proc. Natl. Acad. Sci. USA, 78:1410-1405.

79. Ruta, M., R. K. Bestwick, C. Machida, and D. Kabat. (1983) Loss of leukemogenicity caused by mutations in the membrane glycoprotein structural gene of Friend spleen focus-forming virus. Proc. Natl. Acad. Sci. USA, 80: 4704-4708.

80. Machida, C.A., R.K. Bestwick, and D. Kabat. (1984) Reduced leukemogenicity caused by mutations in the membrane glycoprotein gene of Rauscher spleen focus-forming virus. J. Virol., 49:394-402.

81. Machida, C., R. K. Bestwick, B. A. Boswell, and D. Kabat. (1985) Role of a membrane glycoprotein in Friend virus induced erythroleukemia: studies of mutant and revertant viruses. Virology, 144:158-172.

82. Li, J-P., R. K. Bestwick, C. Machida, and D. Kabat. (1986) Role of a membrane glycoprotein in Friend virus erythroleukemia: nucleotide sequences of nonleukemogenic mutant and spontaneous revertant viruses. J. Virol., 57:534-538.

83. Li, J-P., R. K. Bestwick, C. Spiro, and D. Kabat. (1987) The membrane glycoprotein of Friend spleen focus-forming virus: evidence that the cell surface component is required for pathogenesis and that it binds to a receptor. J. Virol., 61:2782-2792.

84. Clark, S.P., and T.W. Mak. (1983) Complete nucleotide sequences of an infectious clone of Friend spleen focus-forming provirus: gp55 is an envelope fusion glycoprotein. Proc. Natl. Acad. Sci. USA, 80:5037-5041.

85. Wolff, L., E. Scolnick, and S. Ruscetti. (1983) Envelope gene of the Friend spleen focus-forming virus: deletion and insertion in 3' gp70/p15E-encoding region have resulted in unique features in the primary structure of its protein product. Proc. Natl. Acad. Sci. USA, 80:4718-4722.

86. Chattopadhyay, S.K., M.W. Cloyd, D.L. Linemeyer, M.R. Lander, E. Rands, and D.R. Lowy. (1982) Cellular origin and role mink cell focus-forming virus in murine thymic lymphomas. Nature, 295:25-31.

87. Rein, A. (1982) Interference grouping of murine leukemia viruses: a distinct receptor for the MCF-recombinant viruses on mouse cells. Virology, 120:251-257.

88. Srinvas, R.V. and R.W. Compans. (1983) Membrane association and defective transport of spleen focus-forming virus glycoproteins. J. Biol. Chem., 258:14718-14724.

89. Polonoff, E., C.A. Machida, and D. Kabat. (1982) Glycosylation and intracellular transport of membrane glycoproteins encoded by murine leukemia viruses. J. Biol. Chem., 257:14023-14028.

90. Ruta, M., S. Clarke, B. Boswell, and D. Kabat. (1982) Heterogeneous metabolism and subcellular localization of a potentially leukemogenic membrane glycoprotein encoded by Friend erythroleukemia virus. J. Biol. Chem., 257:126-134.

91. Sherton, C. C., L. H. Evans, E. Polonoff, and D. Kabat. (1976) Relationship of Friend murine leukemia virus production to growth and hemoglobin synthesis in cultured erythroleukemia cells. J. Virol., 19:118-125.

92. Laemmli, U.K. (1970) Cleavage of structural proteins during the assembly of the head of bacteriophage T4. Nature, 227:680-685.

93. Wolff, L., R. Koller, and S. Ruscetti. (1982) Monoclonal antibody to spleen focus-forming virus-encoded gp52 provides a probe for the amino-terminal region of retroviral envelope proteins that confers dual tropism and xenotropism. J. Virol., 43:472-481.

94. Brenner, M.B., I.S. Trowbridge, and J.L. Strominger. (1985) Cross-linking of human T cell receptor proteins: Association between the T cell idiotype beta-subunit and the T3 glycoprotein heavy subunit. Cell, 40:183-190.

95. Copeland, C.S., R.W. Doms, E.M. Bolzau, R.G. Webster, and A. Heleinius. (1986) Assembly of influenza hemagglutinin trimers and its role in intracellular transport. J. Cell Biol.,103:1179-1191.

96. Chirgwin, J. M., A. E. Przybyla, R. J. MacDonald, and W. J. Rutter. (1982) Isolation of biologically active ribonucleic acid from sources enriched in ribonuclease. Biochem., 18:5294-5299.

97. Maniatis, T., E. F. Fritsch, and J. Sambrook. (1982) Molecular cloning: a laboratory manual. Cold Spring Harbor Laboratory, Cold Spring Harbor, N.Y.

98. Thomas, P. S. (1983) Hybridization of denatured RNA transferred or dotted to nitrocellulose paper. Methods in Enzymology, 100:255-266.

99. Southern, E. M. (1975) Detection of specific sequences among DNA fragments

separated by gel electrophoresis. J. Mol. Biol., 98:503-517.

100. Gusella, J., R. Geller, B. Clarke, V. Weeks, and D. Housman. (1976) Commitment to erythroid differentiation by Friend erythroleukemia cells: a stochastic analysis. Cell, 9:221-229.

101. Fiers, W., R. Contreras, G. Haegeman, R. Rogiers, A. Van de Voorde, H. Van Heuverswyn, J. Van Herreweghe, G. Volckaert, and M. Ysebaert. (1978) Complete nucleotide sequence of SV40 DNA. Nature, 273:113-120.

102. Mann, R., R.C. Mulligan, and D. Baltimore. (1983) Construction of a retrovirus packaging mutant and its use to produce helper-free defective retrovirus. Cell, 33:153-159.

103. Southern, P.J., and P. Berg. (1982) Transformation of mammalian cells to antibiotic resistance with a bacterial gene under the control of the SV40 early region promoter. J. Mole. Appl. Genet., 1:327-341.

104. Ruscetti, S. K., J. A. Field, and E. M. Scolnick. (1981) Polycythemia- and anemia-inducing strains of spleen focus-forming virus differ in post-translational processing of envelope-related glycoproteins. Nature. 294:663-665.

105. Karshin, W.L., L.J. Arcement, R.B. Naso, and R.B. Arlinghaus. (1977) Common precursor for Rauscher leukemia virus gp69/71, p15E, and p12E. J. Virol. 23:787-798.

106. Montelaro, R.C, S.J. Sullivan, and D.P. Bolognesi. (1978) An analysis of type-C retrovirus polypeptides and their associations in the virion. Virology, 84:19-31.

107. Troxler, D.H., and E.M. Scolnick. (1978) Rapid leukemia induced by cloned Friend strain of replicating murine type-C virus. Virology, 85:17-27.

108. Bosselman, R.A., F. van Straaten, C. Van Beveren, I.M. Verma, and M. Vogt. (1982) Analysis of the *env* gene of a molecularly cloned and biologically active Moloney mink cell focus-forming proviral DNA. J. Virol. 44:1931.

109. Holland, C.A., J. Wozney, and N. Hopkins. (1983) Nucleotide sequence of the gp70 gene of murine retrovirus MCF 247. J. Virol., 47:413-420.

110. Koch, W., W. Zimmermann, A. Oliff, and R. Friedrich. (1984) Molecular analysis of the envelope gene and long terminal repeat of Friend mink cell focus-inducing virus: implications for the functions of these sequences. J. Virol. 49:828-840.

111. Sun, I., E.M. Johnson, and V.G. Allfrey. (1980) Affinity purification of newly phosphorylated protein molecules. J. Biol. Chem. 255:742-747.

112. Shami, Y., S. Ship, and A. Rothstein. (1977) Rapid quantitative separation of the major glycoproteins (PAS 1, 2, and 3) from other human red cell membrane proteins in a nondenaturing medium by affinity chromatography. Anal. Biochem., 80:438-445.

113. Peters, T., and L.K. Davidson. (1982) The biosynthesis of rat serum albumin. J. Biol. Chem., 257:8847-8853.

114. Schacter, H., and S. Roseman. (1980) Mammalian glycosyltransferases: their role in the synthesis and function of complex carbohydrates and glycolipids. In W. Lennarz (Ed.) The biochemistry of glycoproteins and proteoglycans. pp 85-160. Plenum Press. New York.

115. Sefton, B.M., and J.E. Buss. (1987) The covalent modification of eukaryotic proteins with lipid. J. Cell Biol. 104:1449-1453.

116. Fitting, T., and D. Kabat. (1982) Evidence for a glycoprotein "signal" involved in transport between subcellular organelles. J. Biol. Chem., 257:14011-14017.

117. Lodish, H.F., N. Kong,M. Snider, and G.J. Strous. (1983) Hepatoma secretory proteins migrate from rough endoplasmic reticulum to Golgi with characteristic rates. Nature, 304:80-83.

118. Pfeffer, S.R., and J.E. Rothman. (1987) Biosynthetic protein transport and sorting by the endoplasmic reticulum and Golgi. Ann. Rev. Biochem., 56:829-852.

119. Wieland, F.T., M.L. Gleason, T.A. Serefini, and J.E. Rothman. (1987) The rate of bulk flow from the endoplasmic reticulum to the cell surface. Cell, 50:289-300.

120. Haas, I.G., and M. Wabl. (1983) Immunoglobulin heavy chain binding protein. Nature, 306:387-389.

121. Bole, D.G., L.M. Hendershot, and J.F. Kearney. (1986) Post-translational association of Immunoglobulin heavy chain binding protein with nascent heavy chains in nonsecreting and secreting hybridomas. J. Cell Biol.,102:1558-1566.

122. Gething, M.F., K. McCammon, and J. Sambrook. (1986) Expression of wild-type and mutant forms of influenza hemagglutinin: the role of folding in intracellular transport. Cell, 46:939-950.

123. Ellis, J. (1987). Proteins as molecular chaperones. Nature, 328:378-379.

124. Miyazaki, J.-I., E. Appella, and K. Ozato. (1986) Intracellular transport blockade caused by disruption of the disulfide bridge in the third external domain of major histocompatibility complex class I antigen. Proc. Natl. Acad. Sci. USA, 83:757-761.

125. Kreis, T.E., and H.F. Lodish. (1986) Oligomerization is essential for transport of vesicular stomatitis viral glycoprotein to the cell surface. Cell, 46:929-937.

126. Bergman, L.W., and W.M. Kuehl. (1979) Formation of an intrachain disulfide bond on nascent immunoglobulin light chains. J. Biol. Chem. 254:8869-8876.

127. Morgan, E.H., and T. Peters, Jr. (1985) The biosynthesis of rat transferrin: evidence for rapid glycosylation, disulfide bond formation, and tertiary folding. J. Biol. Chem., 260:14793-14801.

128. Freedman, R.B., and D.A. Hillson. (1980) In: The Enzymology of Post-translational Modification of Proteins. Freedman, R.B. and H.C. Hawkins (Eds.) Vol. 1, pp 157-212. Academic Press.

129. Freedman RB. (1984) Native disulfide bond formation in protein biosynthesis: evidence for the role of protein disulfide isomerase. Trends biochem. Sci. 9:438-441.

130. Creighton, T.E. (1984) Disulfide bond formation in proteins. In: Methods in Enzymology, Vol. 107. pp 305-329. Academic Press, Inc.

131. Issacs, J., and F. Binkley. (1977) Glutathione dependent control of protein disulfide-sulfhydryl content by subcellular fractions of hepatic tissue. Biochem.

Biophys. Acta., 497:192-204.

132. Ziegler, D.M., M.W. Duffel, and .L. Poulsen. (1980) Ciba Found. Symp., 72:191-204.

133. Rothman, J. (1981) The Golgi apparatus: two organelles in tandem. Science, 213:1212-1219.

134. Blobel, G., and B. Dobberstein. (1975) Transfer of proteins across membranes, II. Reconstitution of functional rough microsomes from heterologous components. J. Cell. Biol., 67:852-862.

135. Hubbard, S.C., and R.J. Ivatt. (1981) Synthesis and processing of asparagine-linked oligosaccharides. Annu. Rev. Biochem., 50:555-538.

136. Anfinsen, C.B. (1973) Principles that govern the folding of protein chains. Science, 181:223-233.

137. Creighton, T.E., D.A. Hillson, and R.B. Freedman. (1980) Catalysis by protein-disulfide isomerase of the unfolding and refolding of proteins with disulfide bonds. J. Mol. Biol. 142:43-62.

138. Koivu, J., R. Myllyla, T. Helaakaoski, T. Pihajaniemi, K. Tasanen, and K.I. Kivirikko. (1987) A single polypeptide acts both as the beta-subunit of prolyl 4-hydroxylase and as a protein disulfide-isomerase. J. Biol. Chem., 262:6447-6449.

139. Pihajaniemi, T., T. Helaakaoski, K. Tasanen, R. Myllyla, M.-J. Huhtala , J. Koivu, and K.I. Kivirikko. (1987) Molecular cloning of the beta-subunit of human prolyl 4-hydroxylase. This subunit and protein disulfide-isomerase are products of the same gene. EMBO J., 6:643-649.

140. Bergman, L.W., and W.M. Kuehl. (1979) Formation of intermolecular disulfide bonds on nascent immunoglobulin polypeptides. J. Biol. Chem. 254:5690-5694.

141. Carlin, B.E., J.C. Lawrence, J.M. Lindstrom, and J.P. Merlie. (1986) An acetylcholine receptor precursor alpha subunit that binds alpha-bungarotoxin but not alpha-tubocurate. Proc. Natl. Acad. Sci. USA., 83:498-502.

142. Carlin, B.E., J.C. Lawrence, J.M. Lindstrom, and J.P. Merlie. (1986) Inhibition of

acetylcholine receptor assembly by activity in primary cultures of embryonic rat muscle cells. J. Biol. Chem. 262:5180-5186.

143. Rudden, R.W., R.F. Krzesicki, S.E. Norton, J.S. Beebe, B.P. Peters, and F. Perini. (1987) Detection of a glycosylated, incompletely folded form of chorionic gonadotropin beta-subunit that is a precursor of hormone assembly in trophoblastic cells. J. Biol. Chem. 262:12533-12540.

144. Koivu, J., and R. Myllyla. (1987) Interchain disulfide bond formation in types I and II procollagen: evidence for a protein disulfide isomerase catalyzing bond formation. J. Biol. Chem., 262:6159-6164.

145. Lambert, N., and R.B. Freedman. (1983) Structural properties of homogeneous protein disulfide-isomerase from bovine liver purified by a rapid high-yielding procedure. Biochem. J., 213:225-234.

146. Doms, R.W., D.S. Kelly, A. Helenius, and W.E. Balch. (1987) Role for adenosine triphosphate in regulating the assembly and transport of vesicular stomatitis virus G protein trimers. J. Cell Biol., 105:1957-1969.

147. Land, H., L.F. Parada, and R.A. Weinberg. (1983) Cellular oncogenes and multi-step carcinogenesis. Science, 222:771-778.

148. Bishop, J.M. (1987) The molecular genetics of cancer. Science, 235:305-311.

149. Bishop, J.M. (1983) Cellular oncogenes and retroviruses. Annu. Rev. Biochem. 52:301-354.

150. Hara, H., and M. Ogawa. (1976) Erythropoietic precursors in mice with phenylhydrazine-induced anemia. Am. J. Hematol. 1:453-458.

151. Friend, C., M. C. Patuleia, and E. De Harven. (1966) Erythrocytic maturation in vitro of murine (Friend) virus-induced leukemic cells. Natl. Cancer Inst. Monogr. 22:505-519.

152. Schwartz, R. J., J. A. Haron, K. N. Rothblum, and A. Dugaiczyk. (1980) Regulation of muscle differentiation: cloning of sequences from alpha-actin messenger ribonucleic acid. Biochem 19:5883-5890.

153. Hofer, E., and J. E. Darnell, Jr. (1981) The primary transcription unit of the mouse ß-major globin gene. Cell 23:585-593.

154. Ellis, R. W., D. DeFeo, T. Y. Shih, M. A. Gonda, H. A. Young, N. Tsuchida, D. R. Lowy, and E. M. Scolnick. (1981) The p21 *src* genes of Harvey and Kirsten sarcoma viruses originate from divergent members of a family of normal vertebrate genes. Nature (London) 292:506-510.

155. Hall, A., C. J. Marshall, N. K. Spurr, and R. A. Weiss. (1983) Identification of transforming gene in two human sarcoma cell lines as a new member of the *ras* gene family located on chromosome one. Nature (London) 303:396-400.

156. Grace, L. C., E. J. Keath, S. P. Piccoli, and M. D. Cole. (1982) Novel *myc* oncogene RNA from abortive immunoglobulin-gene recombination in mouse plasmacytomas. Cell 31:443-452.

157. Klempnauer, K-H., T. J. Gonda, and J. M. Bishop. (1982) Nucleotide sequence of the retroviral leukemic gene v-*myb* and its cellular progenitor c-*myb*: the architecture of a transduced oncogene. Cell 31:453-463.

158. Oren, M., and A. J. Levine. (1983) Molecular cloning of a cDNA specific for the murine p53 cellular tumor antigen. Proc. Natl. Acad. Sci. USA 80:56-59.

159. Robert-Lezenes, J., F. Moreau-Gachelin, F. Wendling, P. Tambourin, and A. Tavitian. (1984) Expression of c-*ras* and c-*myc* oncogenes in murine erythroleukemias induced by Friend viruses. Leukem. Res. 8:975-984.

160. Nepveu, A., P. D. Fahrlander, J-Q Yang, and K. B. Marcu. (1985) Amplification and altered expression of the c-*myc* oncogene in A-MuLV-transformed fibroblasts. Nature (London) 317:440-443.

161. Mowat, M., A. Cheng, N. Kimura, A. Bernstein, and S. Benchimol. (1985) Rearrangements of the cellular p53 gene in erythroleukemic cells transformed by Friend virus. Nature (London) 314:633-636.

162. Chow, V., Y. Ben-David, A. Bernstein, S. Benchimol, and M. Mowat. (1987) Multistage Friend erythroleukemia: Independent orgin of tumor clones with normal or rearranged p53 cellular oncogene. J. Virol., 61:2777-2781.

163. Marks, P. A., and R. A. Rifkind. (1978) Erythroleukemic differentiation. Ann. Rev. Biochem. 47:419-448.

164. Kirsch, I. R., V. Bertness, J. Silver, and G. F. Hollis. (1986) Regulated expression of the c-*myb* and c-*myc* oncogenes during erythroid differentiation. J. Cell. Biochem. 32:11-21.

165. Lachman H. M., and A. I. Skoultchi. (1984) Expression of c-*myc* changes during differentiation of mouse erythroleukemia cells. Nature (London) 310:592-594.

166. Ramsay, R. G, K. Ikeda, R. A. Rifkind, and P. A. Marks. (1986) Changes in gene expression associated with induced differentiation of erythroleukemia: protooncogenes, globin genes, and cell division. Proc. Natl. Acad. Sci. USA 83:6849-6853.

167. Ruscetti, S. K., and E. M. Scolnick. (1983) Expression of a transformation-related protein (p53) in the malignant stage of Friend virus-induced diseases. J. Virol. 46:1022-1026.

168. Shen, D-W., F. X. Real, A. B. DeLeo, L. J. Old, P. A. Marks, and R. A. Rifkind. (1983) Protein p53 and inducer-mediated erythroleukemia cell commitment to terminal cell division. Proc. Natl. Acad. Sci. USA 80:5919-5922.

169. Sato, T., C. Friend, and E. de Harven. (1971) Ultrastructural changes in Friend erythroleukemia cells treated with dimethyl sulfoxide. Cancer Res. 31:1402-1417.

170. Coppola, J. A., and M. D. Cole. (1986) Constitutive c-*myc* oncogene expression blocks mouse erythroleukemia cell differentiation but not commitment. Nature (London) 320:760-763.

171. Dmitrovsky, E., W. M. Kuehl, G. F. Hollis, I. R. Kirsch, T. P. Bender, and S. Segal. (1986) Expression of a transfected human c-myc oncogene inhibits differentiation of a mouse erythroleukemia cell line. Nature (London) 322:748-750.

172. Tsuei, D., B. G.-T. Pogo, and C. Friend. (1980) Variations in properties of virus released from morphologically different cell lines transformed by Friend leukemia virus. Proc. Natl. Acad. Sci. USA 77:5769-5773.

173. Faletto, D. L., A. S. Arrow, and I. G. Macara. (1985) An early decrease in phosphatidylinositol turnover occurs on induction of Friend cell differentiation and precedes the decrease in c-*myc* expression. Cell 43:315-325.

174. Greenberg, M. E., L. A. Greene, and E. B. Ziff. (1985) Nerve growth factor and epidermal growth factor induce rapid transient changes in proto-oncogene transcription in PC12 cells. J. Biol. Chem. 260:14101-14110.

175. Kelly, K., B. H. Cochran, C. D. Stiles, and Philip Leder. (1983) Cell-specific regulation of the c-*myc* gene by lymphocyte mitogens and platelet-derived growth factor. Cell 35:603-610.

176. Moreau-Gachelin, F., J. Robert-Lezenes, F. Wendling, A. Tavitian, and P. Tambourin. (1985) Integration of spleen focus-forming virus proviruses in Friend tumor cells. J. Virol., 53:292-295.

177. Moreau-Gachelin, F., L. D'Auriol, J. Robert-Lezenes, F. Galibert, P. Tambourin, and A. Tavitian. (1986) Analysis of integrated proviral DNA sequences with an octadecanucleotide probe designed for specific identification of spleen-focus forming virus in the mouse genome. J. Virol. 57:349-352.

178. Moreau-Gachelin, F., A. Tavitian, and P. Tambourin. (1988) Spi-1 is a putative oncogene in virally induced murine erythroleukemias. Nature, 331:277-280.

179. Nusse, R., and H.E. Varmus. (1982) Many tumors induced by the mouse mammary tumor virus contain a provirus integrated in the same region of the host genome. Cell 31:99-109.

180. Peters, G., S. Brookes, R. Smith, and C. Dickson. (1983) Tumorigenesis by mouse mammary tumor virus : Evidence for a common region for provirus integration in mammary tumors. Cell, 33:369-377.

181. Peters, G., C. Kozak, and C, Dickerson. (1984) Mouse mammary tumor virus integration regions int-1 and int-2 map on different mouse chromosomes. Mol. Cell. Biol. 4:375-378.

182. Tsichlis, P.N., P.G. Strauss, and L.F. Hu. (1983) A common region for proviral DNA integration in MoMuLV-induced rat thymic lymphomas. Nature, 302:445-

448.

183. Tsichlis, P.N., P.G. Strauss, and M.A. Lohse. (1985) Concerted DNA rearrangements in Moloney murine leukemia virus-induced thymomas: a potential synergistic relationship in oncogenesis. J. Virol., 56:258-267.

184. Steffen, D. (1984) Provirses are adjacent to c-*myc* in some murine leukemia virus-induced lymphomas. Proc. Natl. Acad. Sci. USA., 81:2097-2101.

185. Hayward, W.S., B.G. Neel, and S.M. Astrin. (1981) Activation of a cellular *onc* gene by promoter insertion in ALV-induced lymphoid leukosis. Nature, 209:475-479.

186. Fung, Y.K.T., W.G. Lewis, H.J. Kung, and L.B. Crittenden. (1983) Activation of the cellular oncogene c-*erb* B by LTR insertion: molecular basis for induction of erythroblastosis by avian leukosis virus. Cell, 33:357-368.

187. Ruscetti, S.K., and L. Wolff. (1985) Biological and biochemical differences between variants of spleen focus-forming virus can be localized to a region containing the 3' end of the envelope gene. J. Virol., 56:717-722.

188. Payne, G.S., S.A. Courtneidge, L.B. Crittenden, A.M. Fadly, J.M. Bishop, and H.E. Varmus. (1981) Analysis of avian leukosis virus DNA and RNA in bursal tumors: Viral gene expression is not required for maintenance of the tumor state. Cell, 23:311-322.